STRUCTURE-FUNCTION RELATIONSHIPS OF THE PORE-FORMING SUBUNITS OF THE AMPA RECEPTOR AND THE AUXILIARY SUBUNIT STARGAZIN

By

YANINA LEVCHENKO-LAMBERT

Bachelor of Science in Biomedical Engineering
Oral Roberts University
Tulsa, OK
2004

Submitted to the Faculty of the
Graduate College of the
Oklahoma State University
in partial fulfillment of
the requirements for
the Degree of
DOCTOR OF PHILOSOPHY
July, 2009

STRUCTURE-FUNCTION RELATIONSHIPS OF THE PORE-FORMING SUBUNITS OF THE AMPA RECEPTOR AND THE AUXILIARY SUBUNIT STARGAZIN

Dissertation Approved:

Doris Patneau

Dissertation Adviser

Kenneth Miller

Gregory Sawyer

Dorothy Turetsky

Dr. A. Gordon Emslie

Dean of the Graduate College

ACKNOWLEDGMENTS

I would like to extend my sincere gratitude to Doris Patneau for her valuable guidance, mentorship and expertise. Thank you for sharing your lab with me and teaching me everything I know. I would also like to thank Dorothy Turetsky for her help and advise that was necessary for the completion of this dissertation project. Without her molecular biology expertise and sometimes harsh but constructive criticism I would not be a scientist I am now. I would also like to thank my committee for standing by me and guiding me all this time.

I would also like to thank my husband James for his never-ending love, support and encouragement.

TABLE OF CONTENTS

Chapter **Page**

Chapter **Page**

Chapter **Page**

Chapter **Page**

LIST OF TABLES

LIST OF FIGURES

Figure **Page**

Figure **Page**

LIST OF ABBREVIATIONS

ABP	AMPA receptor Binding protein
ALS	Amyotrophic lateral sclerosis
AMPA	α-amino-3-hydroxyl-5-methyl-4-isoxazole-propionate
ANOVA	Analysis of variance
ATP	Adenosine-5'-triphosphate
BAPTA	1,2-bis(o-aminophenoxy)ethane-N,N,N',N'-tetraacetic acid
CAMKII	Ca^{2+}/calmodulin-dependent protein kinase
CNIH-2	Cornichon analog II
CNIH-3	Cornichon analog III
CNQX	6-cyano-7-nitroquinoxaline-2,3-dione
CNS	Central nervous system
D1	Domain 1 of the extracellular portion of the AMPA receptor, forms a dimer interface with D1 of the adjacent subunits
D2	Domain 2 of the extracellular portion of the AMPA receptor
cDNA	Complementary Deoxyribonucleic acid
DNQX	6,7-Dinitroquinoxaline-2,3-dione
EPSP	excitatory postsynaptic potential
ER	Endoplasmic reticulum
FBS	Fetal bovine serum
GABA	γ-Aminobutyric acid
GLT-1	Glial high affinity glutamate transporter 1
GRIP	glutamate receptor interacting protein
GYKI 52466	1-(4-Aminophenyl)-4-methyl-7,8-methylenedioxy-5H-2,3-benzodiazepine hydrochloride
GYKI 53655	1-(4-aminophenyl)-3-methylcarbamyl-4-methyl-3,4-dihydro-7,8-methylenedioxy-5H-2,3-benzodiazepine
HEPES	4-(2-hydroxyethyl)-1-piperazineethanesulfonic acid
HEK293	Human embryonic cells 293
IDRA21	7-chloro-3-methyl-3,4-dihydro-2*H*-1,2,4-benzothiadiazine 1,1-dioxide
LTD	Long term depression
LTP	Long term potentiation
MEM	Minimum Essential Media
MP-20	Eye lens specific membrane protein 20
Ms	Millisecond
NBQX	2,3-dihydroxy-6-nitro-7-sulfamoyl-benzo[f]quinoxaline-2,3-dione
NMDA	N-methyl-D-aspartic acid

NSF	N-ethylmaleimide-sensitive fusion protein
NTD	N-terminal domain
OPTI MEM	Reduced Serum Media
pA	PicoAmperes
PDB	Protein data base
PDL	Poly-D-lysine
PDZ	Post synaptic density protein (PSD95), Drosophila disc large tumor suppressor (DlgA), and zonula occludens-1 protein (zo-1)
pEGFP	Red-shifted variant of wild-type green fluorescent protein
pF	PicoFarad
PICK1	Protein interacting with PRKCA 1
PKA	Protein kinase A
PKC	Protein kinase C
PMP-22	Peripheral myelin protein 22
PNQX	9-methyl-amino-6-nitro-hexahydro-benzo(F)quinoxalinedione
PSD-95	Post synaptic density protein 95 kDa
QBP	Glutamine-binding protein
RNA	Ribonucleic acid
RT-PCR	Reverse transcription polymerase chain reaction
SAP-97	Synapse associated protein 97
SAP-102	Synapse associated protein 102
SNAP	Synaptosome-associated protein
SOD-1	Superoxide dismutase 1, soluble
TARP	Transmembrane AMPA receptor regulatory protein
TCM	Trichlormethiazide
TM	Transmembrane region
UCSF	University of California, San Francisco
VGCC	Voltage-gated calcium channels

CHAPTER I

INTRODUCTION AND LITERATURE REVIEW

1.1. Introduction

Glutamate was proposed as a central nervous system synaptic transmitter in the 1950s because of its capability of causing convulsions and exciting central neurons (Hayashi, 1952; Curtis et al., 1959; Curtis et al., 1972). Despite this evidence, glutamate was not considered a specific transmitter, since it seemed to excite every neuron when tested and it was not accepted as an excitatory neurotransmitter until the late 1970s (Duggan and Johnston, 1970; Krnjevic, 1970; Martin et al., 1970). Glutamate is now recognized to be the major excitatory neurotransmitter in the vertebrate central nervous system. Glutamate receptors are expressed throughout the central nervous system as well as some peripheral tissues (Egebjerg et al., 1991). There are two major classes of glutamate receptors, metabotropic and ionotropic. Metabotropic glutamate receptors (mGluR1-mGluR8) signal via G-protein Galpha(*q/11*) or Galpha(*i*) signaling cascades (Inagaki et al., 1995; Weaver et al., 1996; Chenu et al., 1998; Patton et al., 1998), while ionotropic glutamate receptors are ligand-gated ion channels.

Three physiologically and pharmacologically distinct families of glutamate gated ion channels have been described and named after their selective agonists: N-methyl-D-aspartic acid (NMDA), α-amino-3-hydroxy-5-methyl-4-isoxazolepropioic acid (AMPA) and kainate. Among these, AMPA receptors mediate the majority of excitatory neurotransmission in the central nervous system. NMDA receptors are also primarily

found post-synaptically and play a major role in synaptic plasticity (Malenka and Bear, 2004). Kainate receptors play a lesser role in synaptic signaling and plasticity and they are primarily located pre-synaptically (Huettner, 1990).

NMDA receptors are tetramers of NMDAR1, NMDAR2A-D and NMDAR3A subunits with preferred stoichiometry of two NR1 and two NR2 subunits (Behe et al., 1995). AMPA receptors are tetramers of pore-forming subunits GluR1-4, encoded by four genes *GRIA1-4* respectively (Boulter et al., 1990; Keinanen et al., 1990), that co-assemble with auxiliary subunits of the transmembrane AMPA receptor regulatory protein family (TARPs) (Tomita et al., 2003) or cornichons (Schwenk et al., 2009). Kainate receptors form tetrameric assemblies consisting of KA1-2 and GluR5-7 subunits, encoded by five genes *GRIK1-5* respectively (Hollmann et al., 1989). Structural relatives of ionotropic glutamate receptors δ1 and δ2 receptors are encoded by 2 genes *GRID1-2* (Lomeli et al., 1993). Because δ1 and δ2 neither bind glutamate, nor form functional channels when expressed alone, their role in the CNS function remains unknown. NMDA, AMPA and kainate receptor subunits do not co-assemble together to form functional channels (Brose et al., 1994; Patneau et al., 1994).

1.2 Structure and function of the AMPA receptor pore-forming subunits

1.2.1 Identification and cloning.

Original studies on native AMPA receptors from rat primary neuronal cultures concentrated on characterizing the functional properties of the receptor. In these studies, AMPA receptors from distinct areas of the brain elicited currents in response to glutamate that were primarily carried by sodium and had low permeability to calcium (Olsen et al., 1987; Iino et al., 1990). Early experiments also observed a striking property

of AMPA receptors, rapid desensitization (1-10 ms) of glutamate evoked currents to a small steady-state level in the continuous presence of agonist (Trussell et al., 1988; Mayer and Vyklicky, 1989; Patneau and Mayer, 1991; Raman and Trussell, 1992). The affinity of AMOA receptor for to glutamate increased 19 fold as receptor entered the desensitized state from EC_{50} 361 µM to EC_{50} 19 µM (Patneau and Mayer, 1990).

The cloning of the AMPA receptor subunit GluR1 by Hollmann et. al. in 1989 opened new avenues for glutamate receptor research. This subunit was first identified as GluR-K1 with sequence homology to that of a previously identified kainate binding protein of the chick and frog (Hollmann et al., 1989). This cloned subunit was able to form functional channels when injected into *Xenopus Oocytes* and were gated by both glutamate and kainate. Interestingly, these homomeric channels were calcium permeable, which contradicted previous data from neuronal cultures, where the majority of AMPA receptors were calcium impermeable (Keinanen et al., 1990). Further investigation led to cloning of three more cDNAs encoding 900-amino acid AMPA receptor subunits with approximately 70 percent sequence homology termed GluR2 – 4 (Boulter et al., 1990; Keinanen et al., 1990).

Detailed electrophysiological analysis of recombinant AMPA receptors led to identification of two distinct rectification patterns that were coincidentally correlated with calcium permeability. Channels composed of GluR1, GluR3 or GluR4 subunits all showed a doubly rectifying pattern (i.e., the channels were unable to conduct current in an outward direction when the holding potential was positive) and were calcium permeable, while channels containing a GluR2 subunit showed simple outward rectification (i.e., the channels were able to conduct current in both directions, inward and

outward, when the driving force was changed accordingly) and had low calcium permeability. Sequence comparison revealed a post-transcriptionally modified site in the pore domain of GluR2 that was subjected to RNA editing (Verdoorn et al., 1991). This single Q/R amino acid exchange is responsible for the specific electrophysiological properties of GluR2 containing AMPA receptors, which include a linear current-voltage relationship, low calcium permeability and low single channel conductance (Swanson et al., 1996). Linear current-voltage relationship and low calcium permeability are dominant in heteromeric assemblies of AMPA receptors containing GluR2 (Hume et al., 1991; Verdoorn et al., 1991; Egebjerg and Heinemann, 1993).

The topology of glutamate receptors differs from that of other ligand-gated ion channels. AMPA receptors possess an extracellular N-terminus, intracellular C-terminus, three transmembrane (TM) domains, TM1, TM3 and TM4, and a channel lining re-entrant membrane segment TM2 (see Figure 1.1) (Hollmann et al., 1994; Bennett and Dingledine, 1995; Seal et al., 1995).

Detailed analysis of cDNAs encoding all four AMPA receptor subunits revealed a 115 base pair segment conserved throughout the AMPA receptor family, that encodes for 38 amino acid residues within a domain preceding transmembrane region 4 (TM4). This segment occurs in two alternative versions named "*flip*" and "*flop*", arising from alternative splicing (Sommer et al., 1990) (illustrated in Figure 1.1). The versions are very similar, with most nucleotide substitutions being silent changes in respect to protein sequence, differing in only 9 amino acids. These two alternative versions of the protein show a distinct pattern of expression in the brain and a different desensitization profile. *Flop* receptors desensitize more rapidly and profoundly than *flip* receptors, revealing the

importance of the *flip/flop* region as a regulatory point in molecular and functional properties of AMPA receptors (Sommer et al., 1990).

Analysis of the exon – intron organization of the RNA of AMPA receptors led to the discovery of differences in the C-terminus coding sequence arising from alternative splicing. C-terminal splice variants are found in GluR2 and GluR4 subunits that exist both in long and short C-terminus forms (illustrated in Figure 1.1) (Gallo et al., 1992; Kohler et al., 1993). Functional differences between short and long AMPA receptor splice variants have not been reported. The different length of the C-terminal tail, however, may play a role in binding different intracellular proteins, leading to a different pattern of receptor expression and membrane targeting (Osten et al., 1998).

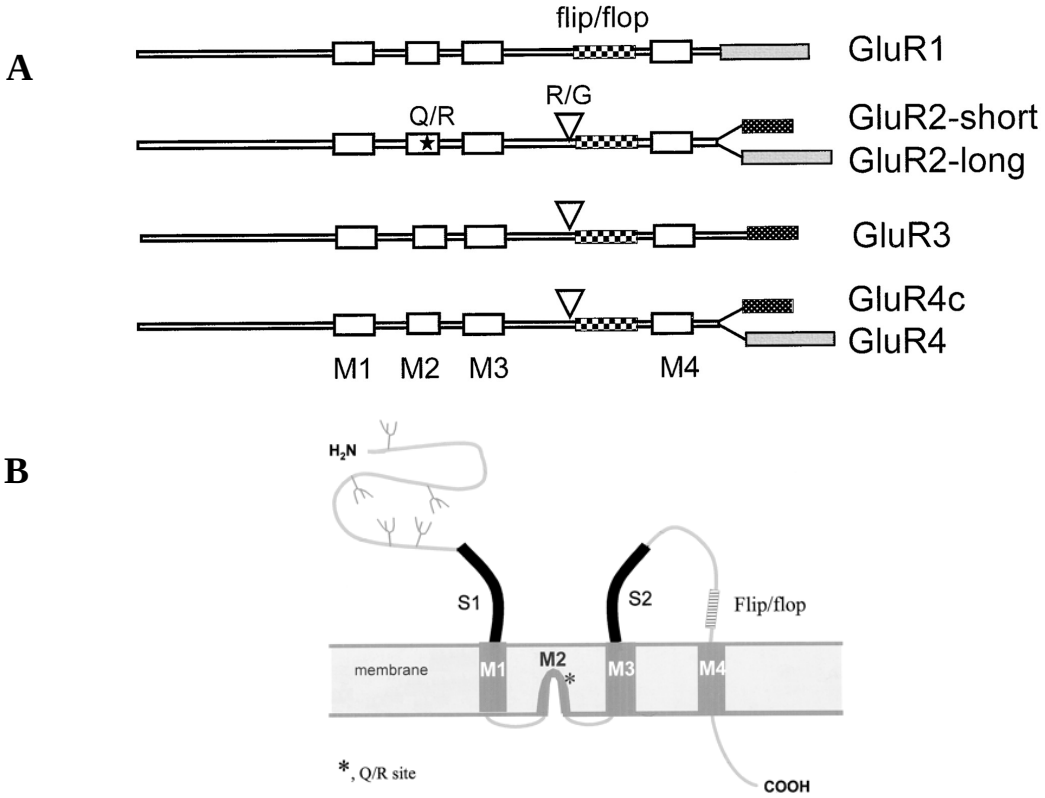

Figure 1.1: AMPA receptor splice variants, editing sites and topology. Schematic representation of the AMPA receptor protein sequence with alternative splicing and RNA editing sites (A) and Schematic illustration of AMPA receptor topology (B). From Dingledine et al., 1999. See text for details.

AMPA receptors are crucial for brain function and development and thus it is imperative to have mechanisms to control AMPA receptor functional properties, trafficking and expression. These control mechanisms include differential splicing and RNA editing to create a diversity of AMPA receptors with distinct kinetic, pharmacological and expression profiles, that are imperative for normal brain function.

1.2.2 Post-Translational Modification

The AMPA receptor protein undergoes post-translational modifications including N-linked glycosylation and phosphorylation at specific sites (Hollmann et al., 1994; Kawamoto et al., 1995; Roche et al., 1996; Mammen et al., 1997). The C-terminus of the AMPA receptor contains a number of consensus sites for phosphorylation, including phosphokinase A (PKA), calcium/calmodulin-dependent protein kinase II (CAMKII) and phosphokinase C (PKC) (Roche et al., 1994; Mammen et al., 1997).

N-linked glycosylation of AMPA receptors is imperative for both channel activity and their modulation by lectins. When glycosylation is prevented using tunicamycin, the molecular mass of GluR1 and GluR2 subunits is decreased by 4 kDa, indicating that AMPA receptors contain 4 to 6 *N*-glycosylation sites (Everts et al., 1997). The unglycosylated form of the receptor does not bind [^{3}H]AMPA (Kawamoto et al., 1995) and the maximal amplitude of kainate induced currents mediated by GluR1*flop* in HEK cells is reduced by fifty percent (Hollmann et al., 1994). These results demonstrate that N-linked glycosylation of AMPA receptors is important for the formation and maintenance of the mature receptor protein.

1.2.3 AMPA receptor pharmacology

AMPA receptor agonists are found in two major chemical classes based on homology of their structure to either AMPA or the willardiines. The class of AMPA receptor full agonists includes glutamate, AMPA and quisqualate, while kainate and willardiine derivatives are only partial agonists. In addition, several potent neurotoxins including domoic acid from dinoflagellates and beta-N-methylamino-L-alanine from cycad seeds are powerful AMPA receptor agonists. No agonists have been identified that exhibit selectivity for particular AMPA receptor subunit combinations.

AMPA receptor currents can be potentiated by positive allosteric modulators. Such modulators impede receptor desensitization and include benzodiathiazines such as cyclothiazide and IDRA21 (Yamada and Rothman, 1992; Patneau et al., 1993; Yamada and Tang, 1993; Thompson et al., 1995; Zivkovic et al., 1995), pyrrolidinones such as aniracetam (Ito et al., 1990; Isaacson and Nicoll, 1991; Vyklicky et al., 1991), and the AMPAkines such as BCP and BDP (Desai et al., 1995; Arai et al., 1996). These different classes of drugs have a similar effect of slowing the decay of excitatory post-synaptic potentials (EPSP), thereby increasing efficacy of glutamatergic synaptic transmission. These compounds are highly selective for AMPA receptors, although their effects are different with alternatively spliced flip/flop region in the M3-M4 loop domain (Cotton and Partin, 2000).

AMPA receptor antagonists have been synthesized and studied for their possible therapeutic benefit in ischemic stroke and excitotoxic disorders like ALS. Antagonists are divided into three categories: competitive antagonists that bind at the glutamate binding site; open channel blockers that block the ion pore; and non-competitive antagonists that

inhibit AMPA receptor function while binding at a site distinctly different from glutamate. The most effective competitive blockers of AMPA receptors were synthesized from compounds in quinoxalines and quinoxalinediones families, including CNQX, DNQX, NBQX and PNQX (Honore et al., 1988; Sheardown et al., 1990; Bigge et al., 1995).

AMPA receptor channel block by natural toxins, including argiotoxin and Joro spider toxin, and endogenous polyamines are dependent on the Q/R site editing of the M2 lining the ion channel pore. These small positively charged molecules are attracted to the negatively charged residues in the ion pore, while being repelled by the positively charged arginine present in GluR2 (Kawai et al., 1982; Magazanik et al., 1997; Williams, 1997).

AMPA receptor selective non-competitive antagonists include another class of drugs, 2,3-benzodiazepines (Buchan et al., 1993; Donevan and Rogawski, 1993; Zorumski et al., 1993; Fletcher and Lodge, 1996). In contrast to their 1,4 analogues, 2,3-benzodiazepine derivatives have no affinity for $GABA_A$ receptors (Zappala et al., 2001). GYKI 52466 (1-(4-aminophenyl)-4-methyl-7,8-methyl-enedioxy-5H-2,3-benzodiazepine) was initially shown to act as a muscle relaxant (Tarnawa et al., 1990). Subsequent experiments demonstrated that GYKI 52466 and the related GYKI 53655 (1-(4-aminophenyl)-3-methylcarbamyl-4-methyl-7,8-methylenedioxi-3,4-dihydro-5H-2,3-benzodiazepine) are highly selective, non-competitive antagonists of AMPA receptors, and as such could have potential uses as anticonvulsants (Rogawski, 1993).

1.2.4 Receptor stoichiometry and assembly.

Ionotropic glutamate receptors are multisubunit assemblies organized around a central ion conducting pore. Two studies in 1998 provided support for a tetrameric structure of the pore-forming subunits (Mano and Teichberg, 1998; Rosenmund et al., 1998). Rosenmund et. al. assumed that each of the subunits contains a functional binding site and that the number of binding sites is equal to the number of subunits in receptor assembly. Channel conductances observed as a result of agonist binding proceeded in a "staircase" fashion through 3 distinguishable conductance states (small = 5 pS, medium = 15 pS and large = 23 pS). By measuring the time the receptor spent in each conductance state, it was clear that the transition between the closed and smallest conductance state was twice as long as the transition between the small and medium or medium and large conductance states. This is in agreement with pharmacological studies indicating that two molecules of agonist must bind to open the channel (Patneau and Mayer, 1990).

Unlike nicotinic receptors, that assemble in predetermined fashion (Kubalek et al., 1987), AMPA receptor assembly is poorly understood and there is no obligatory subunit stoichiometry. However it has been shown that differential subunit assembly controls functional properties, trafficking (Barry and Ziff, 2002; Bredt and Nicoll, 2003) and synaptic targeting of native receptors (Gardner et al., 2001). This subunit composition also plays a crucial part in synaptic plasticity and efficacy (Malinow, 2003).

Early experiments in co-expression of GluR1 or GluR2 in edited (R) and unedited (Q) forms suggested that homomeric receptors assembled stochastically, while heteromeric receptors preferentially formed with a stoichiometry of two GluR1 and two GluR2 subunits, with identical subunits positioned on opposite sides of the channel pore (Stern-

Bach et al., 1994; Mansour et al., 2001). Further studies suggested that composition of AMPA receptors is not static but can be altered in response to certain stimuli. It is unclear which properties and/or modifications of AMPA receptors are crucial for the assembly process. Several possibilities have been described in the literature, including involvement of the GluR2 subunit, Q/R editing site and flip/flop cassette (Stern-Bach et al., 1994; Mansour et al., 2001; Greger et al., 2003; Brorson et al., 2004).

Several studies indicate that the N-terminal domain (NTD) of AMPA receptors is also involved in heteromeric receptor assembly (Leuschner and Hoch, 1999; Ayalon and Stern-Bach, 2001). The AMPA receptor NTD, which is composed of approximately 400 amino acids and is homologous to bacterial periplasmic protein (Jin et al., 2009), has been recently crystallized. Data suggest that dimerization of the NTDs has to occur before AMPA receptor dimers can form, therefore contributing to AMPA receptor assembly (Ayalon et al., 2005; Jin et al., 2009).

1.2.5 Ion pore structure.

AMPA receptor topology differs from that of the superfamily of the cys-loop ligand-gated ion channels, but is similar in structure to that of potassium channels. Based on this observation, early modeling of AMPA receptor gating was done on the basis of homology with potassium channels, which have a 4-fold symmetry in the pore with a rigid TM3 that does not move during gating. The narrowest part (the innermost part) of the AMPA receptor channel is lined by the residues that lie shortly after the turn of the alpha-helix in the TM2 re-entrant segment. The Q/R site is located downstream of the apex of the re-entrant loop, forming the selectivity filter of the channel (Seeburg et al., 2001). The outer part of the pore is lined by the residues from TM3 which contains a

motif conserved through all AMPA receptors – SYTANLAAF (Figure 1.2) (Sobolevsky et al., 2004).

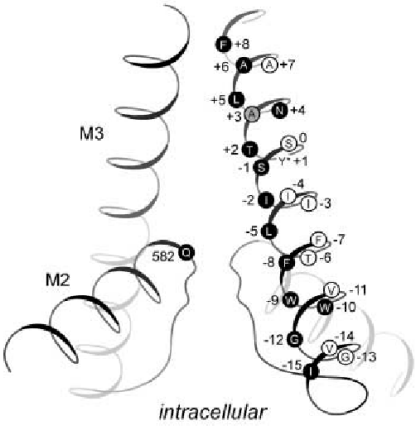

Figure 1.2: Graphical representation of the glutamate receptor ion pore. (From Sobolevsky, 2004)

Cysteine scanning mutagenesis in both TM3 and TM2 that line the ion pore identified an interesting fact. The segments of TM3 deep inside the pore as well as the corresponding segment on the extracellular face of the pore move simultaneously, suggesting that the entire TM3 segment of AMPA receptors moves during receptor gating. The outermost part of TM3 contributing to the channel operates in concert with the adjoining TM3 of another subunit in a dimer, thus following a 2-fold symmetry (Sobolevsky et al., 2004). Therefore, unlike potassium channels, the AMPA receptor has a highly movable TM3 and a 2-fold symmetry for the outer segment of the pore. It is unclear whether the innermost portion of the channel has a 2- or 4-fold symmetry.

1.3 Additional structure and gating mechanisms learned from the AMPA receptor crystal structure

1.3.1 Ligand-binding core

Sequence comparisons revealed that mammalian glutamate-gated ion channels have regions of weak sequence homology with the bacterial periplasmic amino acid binding protein (QBP). The structure of QBP has been solved and was known to include two lobes separated by a cleft. This structure suggested a "venus fly-trap" model in which glutamate binds and forces closure of the binding site around itself (Nakanishi et al., 1990).

In an attempt to identify the binding domain of glutamate receptors, several studies paved the way for future receptor crystallization. Performing exchange of portions of the AMPA receptor subunit GluR3 and the kainate receptor subunit GluR6, two segments of interest were identified (Stern-Bach et al., 1994). They were each approximately 150 amino acids long and were responsible for agonist pharmacology of these chimeric receptors. The first segment (S1) is adjacent and N-terminal to TM1, whereas the second segment (S2) consists of the extracellular loop between TM3 and TM4. Only simultaneous exchange of S1 and S2 converted the pharmacological profile of the recipient receptor to that of the donor receptor (Stern-Bach et al., 1994). A later investigation demonstrated that deletion of the first 400 amino acids of the N-terminal domain (NTD) and the C-terminal 90 amino acids from GluR6 left a membrane-bound core homomeric receptor that displayed normal [^{3}H]kainate binding properties (Keinanen et al., 1998). Based on this work, a subsequent study demonstrated that constructs containing GluR2 S1 and S2 domains joined by a short linker of 13 amino acids could be

expressed in insect and bacterial cells and were capable of binding agonist with affinities similar to that of native receptors (Arvola and Keinanen, 1996). These studies defined the ligand-binding core of glutamate receptors and confirmed homology of the ligand-binding core structure of the glutamate receptor to that of the QBP "venus fly-trap" model of agonist binding. These studies also facilitated crystallization of glutamate receptors.

Crystallization of any membrane-bound protein is complicated by its low concentration in the plasma membrane. Creation of the construct containing S1 and S2 domains joined by a short linker that was secreted from bacterial cells and could be purified and concentrated finally made crystallization of a crucial portion of an AMPA receptor possible. The high-resolution crystal structure (approximately 1.9 Å) of GluR2 S1-S2 "*flop*" protein bound to kainate was resolved via X-ray diffraction. The bilobed structure had a striking resemblance to QBP and possessed a clamshell-like shape with agonist bound in the cleft between the two halves of the clamshell (Figure 1.3) (Armstrong et al., 1998). Interestingly, some crystals formed dimers with their ligand binding domains facing outwards, conforming to a 2-fold symmetry model. This model implies that the ligand-binding domains of two subunits operate in concert (Armstrong and Gouaux, 2000; Sun et al., 2002).

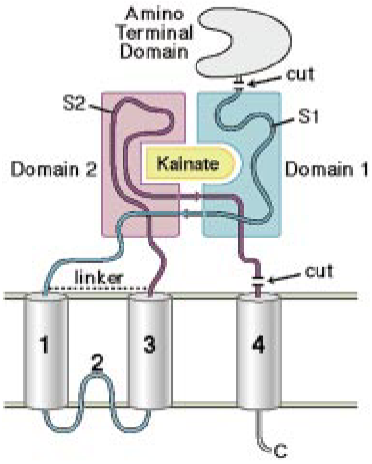

Figure 1.3: Schematic of the GluR2 subunit used to crystallize the ligand-binding domain of the protein (Armstrong et al., 1998)

According to the crystal structure, the S1-S2 protein has two domains arranged in the shape of a kidney with domains one and two mainly composed of S1 and S2 segments respectively. Helixes of the S1-S2 domains are lettered A – K while the loops are numbered 1 – 2. S1 crosses over S2 and ends in domain 2, while the distal portion of S2 contributes to domain 1 (Armstrong et al., 1998). The two domains are connected by two β strands each composed of 3 residues: Met496 – Leu498 and Lys730 – Tyr732. Proteolysis studies of S1-S2 bound to glutamate identified regions important for ligand binding. Regions resistant to proteolysis Gly499 – Pro507 and Pro632 – Lys641 are crucial to agonist binding and when deleted abolish agonist binding altogether. Regions susceptible to proteolysis Gln508 – Glu524, Glu627 – Ser631 and Gly776 – Asn791 do not participate in agonist binding and when deleted have no effect on agonist binding (Chen et al., 1998). The crevice for kainate and glutamate binding is formed between S1 and S2 by four helixes D, F, H and I (illustrated in Figure 1.4). Two residues, Glu402 and Tyr686, are crucial for agonist binding but rather than directly participating in kainate binding, instead help hold the clamshell in the closed conformation (Armstrong et al.,

1998). Kainate induces an intermediate degree of clamshell closure as compared to the opened and closed conformations of QBP.

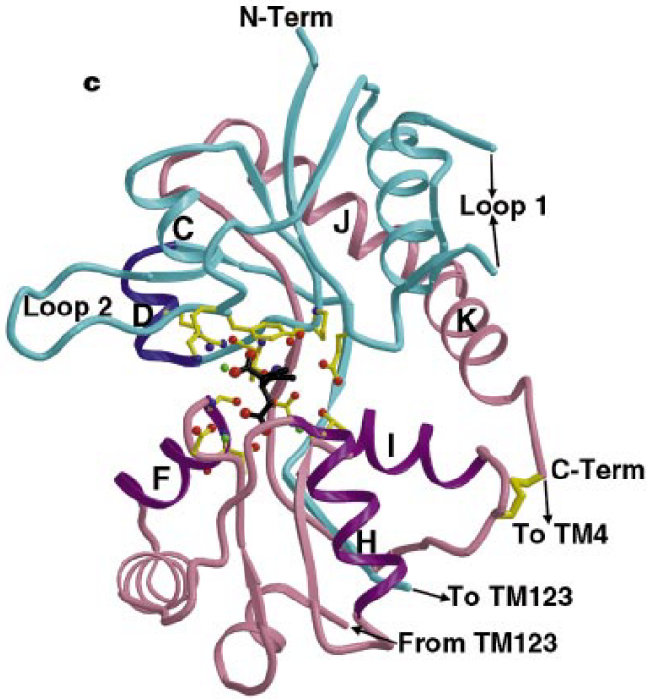

Figure 1.4: Helices D, F, H and I comprising the clamshell binding domain of GluR2 S1S2 domains (Armstrong et al., 1998)

Further crystal structure studies revealed that the full agonists glutamate, AMPA and quisqualate bring the domains of the ligand binding core approximately 21 degrees closer together compared to the open (apo) configuration. This is in contrast to the partial agonist kainate, which induces only 12 degrees of domain closure compared to the apo state because of its physical interaction with residues Tyr450 and Leu650, producing steric hindrance that prevents full domain closure (Armstrong and Gouaux, 2000). Mutation of Tyr450 to smaller residues yields a non-functional ligand binding core, while mutation of Leu650 to a threonine inverts the relative potency of AMPA and kainate, making kainate 10-fold more efficacious while making AMPA a partial agonist (Armstrong et al., 2003). These studies indicate that the glutamate receptor ligand-

binding domain can adopt a range of conformations dependent on the specific ligand bound, and that the conformational change determines whether a ligand is a full agonist, partial agonist or antagonist.

The conformational changes following agonist binding in AMPA receptors are complex, involving both channel opening and desensitization. A study of GluR4 S1-S2 protein bound to glutamate indicates that the process of ligand binding consists of two steps: docking and locking (Mamonova et al., 2008). Docking occurs as a glutamate molecule binds to domain 1 of S1-S2 adjacent to residues Glu402 and Tyr450. Following docking the protein undergoes locking, that leads to formation of a high affinity stable protein complex. The locking process involves formation of a hydrogen bond network between the agonist and the side chain of Thr480 and Glu705 as well as interaction and bonding of residues Glu402 and Tyr686. The locking process is thought to initiate channel gating, however it is hard to correlate these processes, because the S1-S2 crystal lacks the linker regions and actual ion channel (Abele et al., 2000).

1.3.2 Partial agonist action

Partial agonists are useful tools for studying the gating mechanism of the AMPA receptor. Historically, two models for gating of ligand-gated ion channel have been proposed. The two-state model (concerted transition) proposed that receptors exist in equilibrium between resting and active conformations (Monod et al., 1965). This model suggests that differences in agonist efficacy result from different relative affinities of agonist for resting and active conformation of the receptor. The multistate model (induced fit) suggests instead that the receptor can exist in multiple conformational states

and those ligands that best fit the receptor binding pocket produce the greatest extent of activation (Koshland, 1958; Koshland et al., 1966).

Structural work on AMPA receptors suggested that domain closure, as a result of ligand binding, leads to opening of the ion channel and those agonists with better fit promoted greater closure of the ligand binding core. Further, variations in the extent of domain closure, as a result of agonist steric occlusion, correlated with the efficacy for activation of channel gating (Armstrong and Gouaux, 2000; Jin and Gouaux, 2003). In the case of competitive antagonists, a crystal structure of GluR2 with CNQX shows only a slight domain closure, a movement that is presumably not enough to open the ion channel (Armstrong and Gouaux, 2000). Further structural work by the same group elucidated principles of partial agonist action in AMPA receptor using a L650T mutation, that increases kainate apparent affinity 46-fold while lowering AMPA efficacy to that of a partial agonist. After crystallization of the construct it was apparent that domain closure of L650T with kainate bound increased to 15 degrees as compared to Apo state. This was an increase of 3 degrees compared to wild type receptor with kainate bound. However when the L650T mutant was crystallized with AMPA, the partial agonist in this case, the degree of domain closure was comparable to that of a wild type receptor with AMPA or glutamate bound – 21 degrees, indicating that, although AMPA was able to elicit full domain closure, it was unable to fully gate the channel (Armstrong et al., 2003). Recent crystallographic studies with GluR2 S1-S2 indicate that binding of the partial agonists not only prevent full cleft closure, but also induce a twist in the protein (Bjerrum and Biggin, 2008). Thus, the gating mechanism of the AMPA receptor is better described by multistate model and may involve several conformational changes different from those

with full agonist bound, including graded ligand binding domain closure, protein twisting as well as some other unknown mechanisms.

1.3.3 Mechanism of Desensitization

One important feature of AMPA receptors is their rapid and profound desensitization in the continued presence of agonist. Figure 1.5 illustrates responses from homomeric GluR1 receptors expressed in HEK293 cells in the presence of glutamate, kainate and glutamate + trichlormethiazide (TCM), a positive allosteric modulator of AMPA receptors that blocks desensitization.

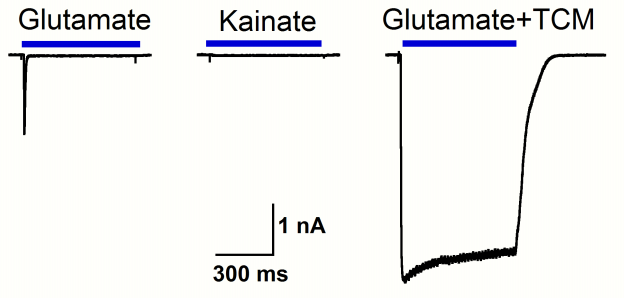

Figure 1.5: GluR1 responses to glutamate, kainate and combination of glutamate and trichlormethiazide. Blue bar indicates the duration of drug application.

The mechanism of AMPA receptor desensitization, as shown in the response to glutamate above, seems to involve multiple conformational changes in AMPA receptor extracellular domains. Combined studies involving site-directed mutagenesis of domain 1 and crystallization revealed a complex series of protein interactions between domains 1 of adjacent subunits in the dimer. For example, mutation of GluR3*flip* L507Y (equivalent to L483Y in GluR2) blocks receptor desensitization by creating an additional salt bridge between domains 1 of the dimer (Stern-Bach et al., 1998; Sun et al., 2002). The importance of maintaining contacts within the dimer interface is further supported by evidence that the positive modulator cyclothiazide, which blocks desensitization, binds at

the dimer interface (illustrated in Figure 1.6), interacting with both domains of the AMPA receptor, thus stabilizing the open conformation (Jin et al., 2005). Site directed mutagenesis indicates that two critical residues of GluR3 Ser750 on helix J and Ser493 are exposed on the dimer interface of the protein and are imperative in cyclothiazide binding and conferring its effect on receptor desensitization (Partin, 2001). Mutations that promote desensitization appear to act by introducing steric hindrance within the dimer interface, thus destabilizing dimer interactions, while mutations that stabilize the dimer interface appear to slow the onset of desensitization (Partin et al., 1994; Sun et al., 2002; Horning and Mayer, 2004).

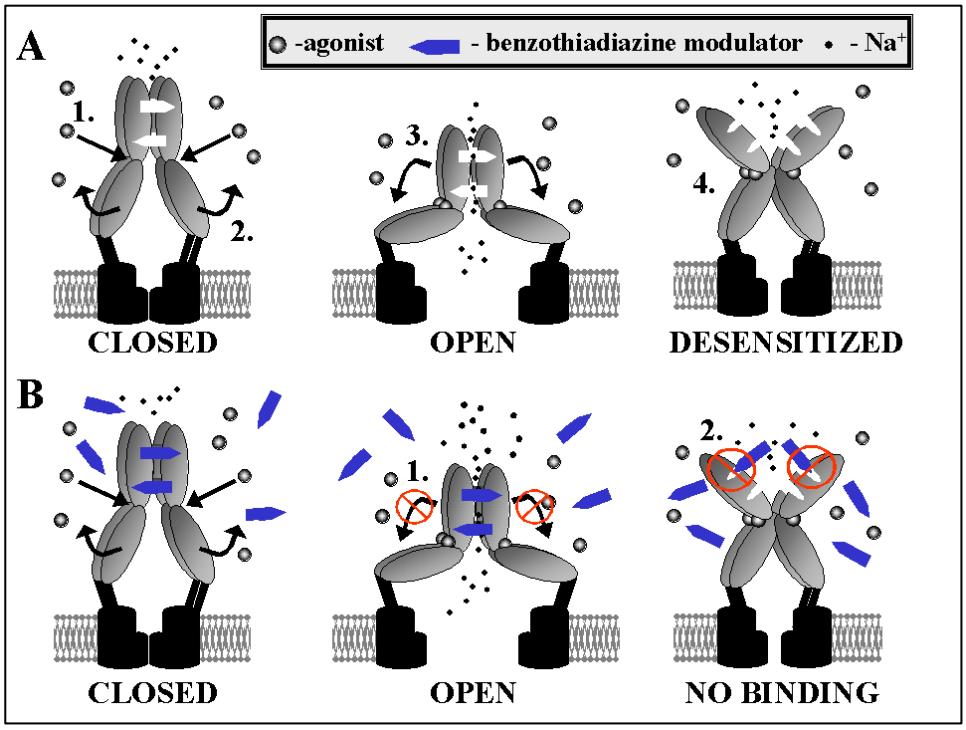

Figure 1.6: Mechanism of AMPA receptor desensitization onset and the action of the benzothiadiazine modulator. The binding of the neurotransmitter by the ligand-binding cores initiates channel opening and desensitization (A). Binding of the positive allosteric modulators across the intra-dimer interface blocks desensitization (B).

Taken together, the current model of channel gating and desensitization involves several conformational rearrangements (illustrated in Figure 1.6). Upon agonist binding

the clamshell closes trapping the agonist in the cleft between domains 1 and 2. The energy of the agonist binding is translated into the channel opening. Simultaneously with channel opening, the receptor enters the desensitized state that is accompanied by the breaking of the protein interactions between helices J and D of opposing subunits in the dimer (helices are illustrated in Figure 1.7). It is presumed that the dissociation of domains relieves the stress on the linkers connecting S1 and S2 to the TMs and channel pore that opens the channel, allowing the receptor to enter into a non-conducting or a very low conducting state without dissociation of agonist (Sun et al., 2002).

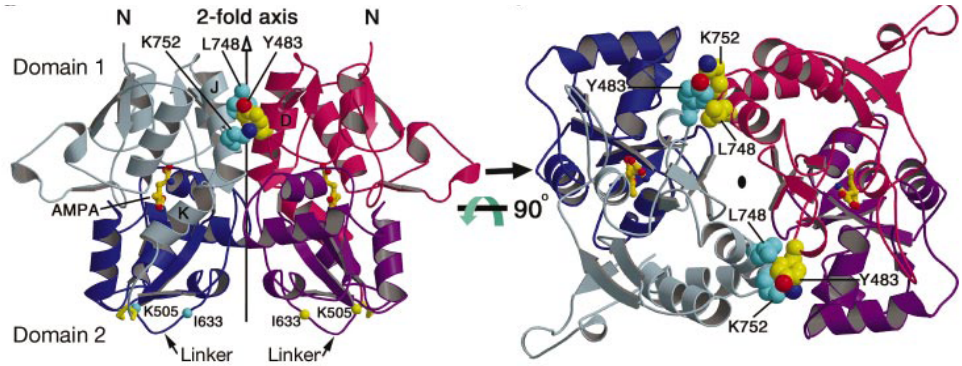

Figure 1.7: Schematic representation – side view (left) and top view (right), of AMPA receptor dimer interface, based on a crystal structure of L483Y in GluR2 with AMPA bound.

Multiple protein interactions between the subunits in the dimer, including salt bridges, hydrogen bonds and Van der Wall's interactions contribute to the stability of the dimer interface (Sun et al., 2002; Horning and Mayer, 2004). Two salt bridges spanning across the dimer interface connect domain 1 of each subunit. They are formed by residues E486 (helix D) and K493 (helix D) in domain 1 of the adjacent subunit of a dimer. Mutation of these residues to alanine destabilizes the dimer interface, increasing the rate of desensitization 41 fold for K493A and 10 fold for E486A. A vast network of hydrogen bonds supports the dimer interface, formed by residues E486 (helix D), K493 (helix D), N747 (helix J) and E755 (helix J), connecting helix D of one subunit with helix J of the

other. Mutation of these residues to alanine destabilized the dimer interface, increasing the desensitization rate 19 fold for the N747A mutant. Residues I481, L483, K493 in helix D and L751, K752, L748 in helix J form contacts via van der Waal's interactions (illustrated in Figure 1.8). Mutations of these residues significantly destabilize the dimer interface. For example in mutations I481A and L751A, responses to glutamate were not detected until application of cyclothiazide, indicating that these mutations severely compromised the dimer interface, while substitution L748A produced a mutant with 12 fold faster desensitization kinetics. Surprisingly both mutations L483A and K752A produced a receptor with a slower onset of desensitization. This result would indicate that these residues actually produce steric hindrance within the dimer interface and their truncation to alanine results in a more stable dimer interface (Horning and Mayer, 2004).

Interactions observed between two dimers occur at the lateral dimer interface and are much less profound than those between two subunits in a dimer (Sun et al., 2002). Structures involved in these interactions include side chains from loop 1 in domain 1 and helices F, G and K in domain 2 (Figure 1.8).

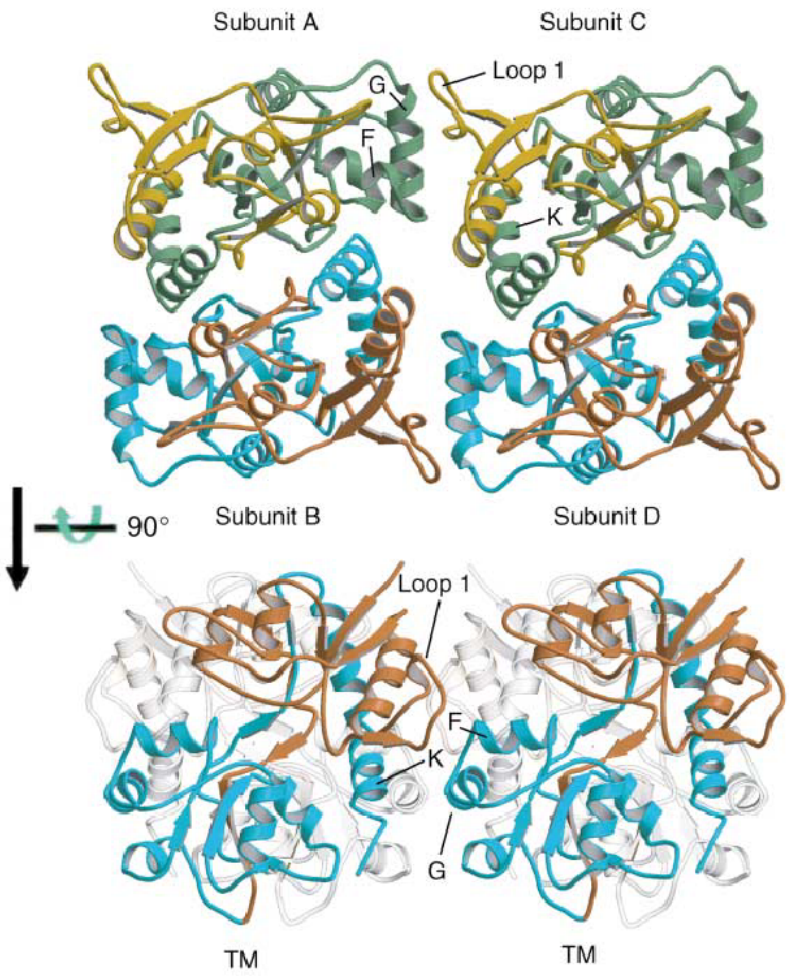

Figure 1.8: Schematic representation of an AMPA receptor tetramer, based on a crystal structure of N754D mutant. Subunits A and B as well as C and D form dimers. Top view of the tetramer is illustrated on the top portion of the figure and side view is illustrated on the bottom (from (Horning and Mayer, 2004).

The amino acids that form the interaction sites are highly conserved in all AMPA receptors. Residues N411 and E419 of loop 1 participate in the lateral dimer interactions. Mutation of these residues to alanine has no effect on desensitization of the AMPA receptor, while deletion of the entire loop 1 produces a misfolded non-functional protein. Residue D668 of helix G participates in a hydrogen bond within the lateral dimer interface, and its mutation to alanine also has no effect on desensitization. These results suggest that the lateral dimer interface does not play a significant role in the mechanism

controlling onset of desensitization unlike the interface between subunits in a dimer that seems to be crucial in this mechanism (Horning and Mayer, 2004).

The mechanism of AMPA receptor desensitization is only understood for the extracellular portion of the protein because the crystal structure for the complete AMPA receptor is unknown. It is interesting to note, however, that although the desensitized state is the most stable in native channels; it has never been crystallized, indicating that its stabilization requires portions of the protein that are absent from the crystal structure. Although multiple mutations on the dimer interface affected the rate of desensitization onset, none seemed to affect the rate of recovery from desensitization, indicating that the mechanism for recovery from desensitization lies outside of the dimer interface. Therefore many aspects of desensitization mechanism remain unknown.

1.4 AMPA receptor associated proteins

AMPA receptor anchoring at the synapse involves a number of proteins that all seem important in retaining the ion channel at the synaptic surface (illustrated in Figure 1.9). Among the intracellular proteins that regulate AMPA receptor targeting and clustering are several proteins containing PDZ (Post synaptic density protein, Drosophila disc large tumor suppressor and Zonula occludens-1 protein) domains. Several lines of research indicate that phosphorylation of these domains at different kinase consensus sites plays a role in the activity-dependent synaptic plasticity and AMPA receptor internalization. Proteins from this family that interact with AMPA receptors include PSD-95, glutamate receptor-interacting protein (GRIP), protein interacting with C kinase 1 (PICK1) and AMPA receptor-binding protein (ABP) (Dong et al., 1997; Srivastava et al., 1998; Xia et al., 1999; Fukata et al., 2005; Silverman et al., 2007).

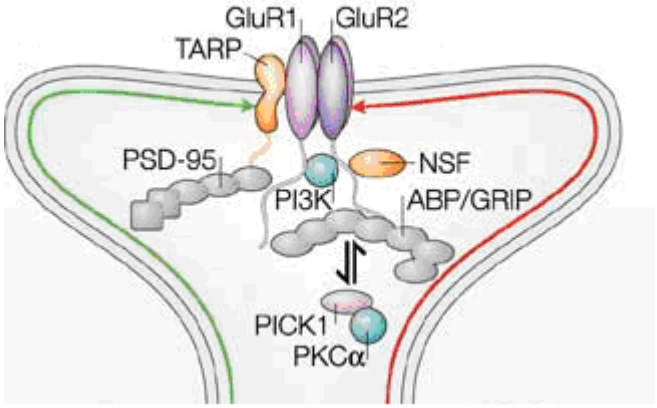

Figure 1.9: A schematic of AMPA receptor scaffolding at the post-synaptic membrane (Collingridge et al., 2004)

GluR2 AMPA receptor subunit C-terminal peptide was shown to interact and colocalize with an ATPase N-ethylmaleimide-sensitive fusion protein (NSF) and alpha- and beta-soluble NSF attachment proteins (SNAPs) (A. Nishimune et al., 1998; P. Osten et al., 1998). NSF specifically interacts with GluR2 and GluR4c, but not any other AMPA receptor subunits, demonstrating that this interaction can mediate an important step in trafficking of AMPA receptors with specific composition (Song et al., 1998).

1.4.1 AMPA receptor auxiliary subunits – transmembrane AMPA receptor regulatory proteins (TARPs).

A spontaneous mutation in a mouse that presented with ataxic gait, upward head-elevating movements and episodes of epileptic spike-wave discharges identified at Jackson Laboratories revolutionized the AMPA receptor field (Letts et al., 1998). The mouse was named stargazer and the protein responsible for the phenotype was named stargazin, also referred to as γ2 by homology with the voltage gated calcium channel γ1 subunit (Letts, 2005). Several other γ subunits were subsequently cloned and now include γ 1 - γ 8 (Klugbauer et al., 2000; Burgess et al., 2001; Moss et al., 2002). Because the

stargazer mutation altered calcium entry in neurons and thus caused the seizure phenotype, it was originally thought that stargazin mediated its effect via modulation of calcium channels (Letts et al., 1998). Further studies determined that stargazin was predominantly expressed in cerebellar granule cells and the stargazer phenotype was caused by the lack of functional AMPA receptors. This finding implicated stargazin's role in normal AMPA receptor function instead of voltage gated calcium channels, as previously thought (Chen et al., 2000).

The first set of studies concentrated on the function of stargazin in synaptic targeting of AMPA receptors. Stargazin has a C-terminal PDZ-binding domain, essential for binding to post synaptic density 95 (PSD-95) and PDZ domain-containing proteins SAP97, SAP102 and nPIST: property crucial for delivery of AMPA receptors to synapses and anchoring them in place (Chen et al., 2000; Ives et al., 2004). This mechanism of delivery is regulated via PKA phosphorylation at Thr321 in the C-terminal tail of stargazin. As the site becomes increasingly phosphorylated the association of stargazin with PSD-95 is decreased dramatically, thus regulating the number of AMPA receptor – stargazin complexes in the post-synaptic membrane (Chetkovich et al., 2002; Choi et al., 2002). Interaction of stargazin with PSD-95 is believed to control the number of AMPA receptors in the post-synaptic membrane (Schnell et al., 2002).

Wide distribution of AMPA receptors in the brain led to a hypothesis that proteins homologous to stargazin might be expressed throughout the brain and may influence AMPA receptor function. Homology cloning identified total of eight γ subunits γ1- γ8, which possess four trans-membrane domains with both N- and C-termini on the intracellular side of the cell and are homologous to the claudin family of proteins and cell

adhesion molecules essential in forming epithelial tight junctions (Morita et al., 1999). Stargazin (γ2) related proteins, that include γ3, γ4 and γ8, have been grouped into Class I transmembrane AMPA receptor regulatory (TARP) subunits based on homology and their effects on function of all AMPA receptors, while closely related γ5 and γ7 are classified as Class II TARPs and are specific to GluR2 (Tomita et al., 2005a; Turetsky et al., 2005; Kato et al., 2007; Korber et al., 2007; Kato et al., 2008). γ1 and γ6 have been shown to associate with and have effects on voltage-gated calcium channels (VGCC) (Arikkath et al., 2003). Figure 1.10 represents a phylogenic tree showing a relationship between γ subunits and related proteins (taken from Tomita 2003).

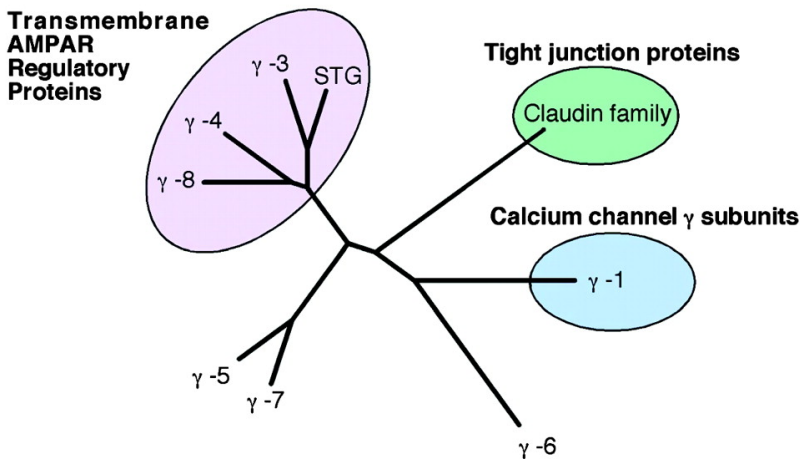

Figure 1.10: Schematic representation of the phylogenetic relationship between different γ subunits and their related proteins (from Tomita 2003).

All of the proteins in the γ subunit family have a conserved consensus site for C-linked mannosylation (GLWXXR). It is currently unknown if this site is mannosylated in any of the γ subunits, the only confirmed mannosylation was present in one of the distantly related tetraspanin proteins - membrane protein 20 (MP20) and played a role in the export of the protein from the ER and its association with other proteins (Ervin et al., 2005). Although most of the γ subunits carry a consensus sites for N-linked glycosylation

(NXTX), the role of this glycosylation in the function of the protein remains unknown. To date only γ1 has been definitively shown to be glycosylated and removal of this glycosylation did not affect association with VGCC (Arikkath et al., 2003).

Effects of all TARPs on glutamate receptor family are exclusive to AMPA receptors (Chen et al., 2003). TARPS are physically associated with the majority of AMPA receptors in the brain, leading to the conclusion that they are AMPA receptor's auxiliary subunits (Vandenberghe et al., 2005a, b). This physical association of AMPA receptors with TARPs plays a role in receptor trafficking, where TARPs behave as ER chaperones, ensuring the correct folding and delivery of the protein to the membrane (Vandenberghe et al., 2005b). The C-terminus of stargazin contains a conserved motif that that binds to PDZ domains of post-synaptic proteins such as PSD-95, thus stabilizing AMPA receptors at the membrane (Chen et al., 2000). In addition to trafficking and anchoring functions, TARPs play a role in positive allosteric modulation of AMPA receptor function by reducing receptor desensitization in response to glutamate, slowing receptor deactivation, potentiating kainate responses, attenuating internal polyamine block and increasing receptor trafficking and rate of channel opening (Priel et al., 2005; Tomita et al., 2005b; Turetsky et al., 2005; Soto et al., 2007). Homomeric and heteromeric AMPA receptors expressed in heterologous expression systems have a weak non-desensitizing response to kainate. However when co-expressed with TARPs the responses are potentiated 200-fold (Turetsky et al., 2005).The effect of stargazin on the responses to kainate is mediated by an effect distinct from its effect on glutamate desensitization (Turetsky et al., 2005). Different domains of stargazin have been implicated in above modulatory functions of the AMPA receptor (Figure 1.11).

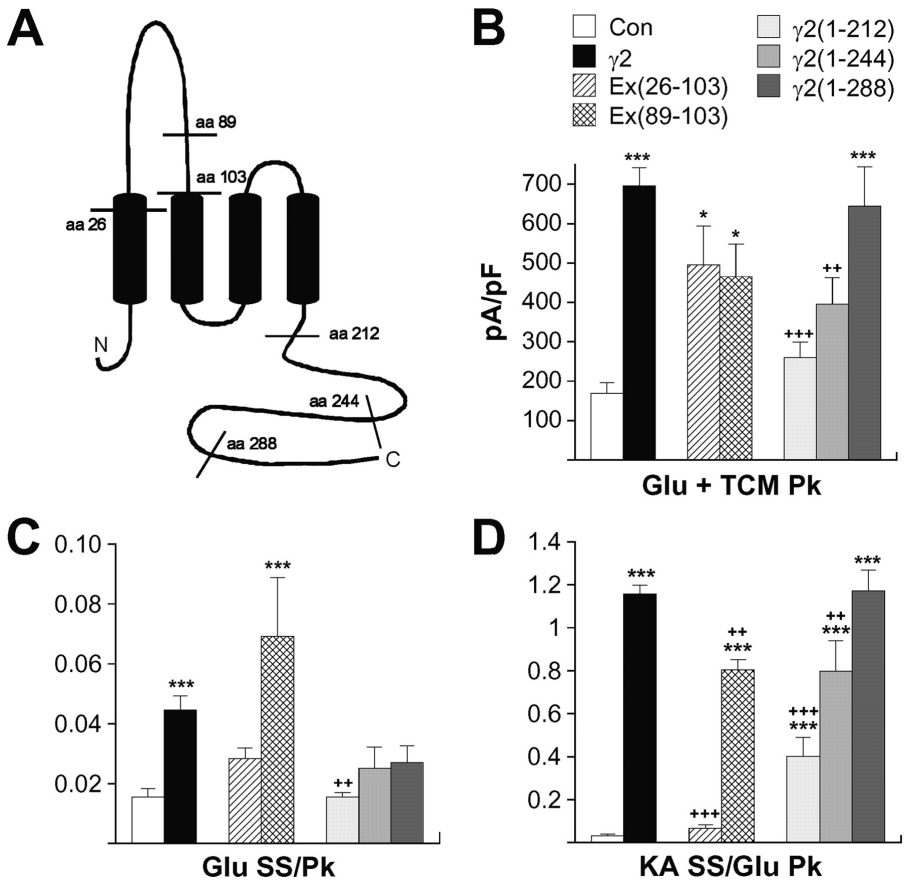

Figure 1.11. Both intracellular and extracellular regions of γ2 mediate functional changes in AMPA receptor properties. **A**, Schematic depiction of the transmembrane topology of γ2. Amino acids demarcating boundaries for the chimeras and the C-terminal truncations are noted. Current density (**B**), normalized glutamate steady-state currents (**C**), and normalized kainate currents (**D**) in HEK293 cells transfected with GluR1 alone or GluR1 plus γ2, γ2(Δ26-103)/ γ5(ins26-99), γ2(Δ89-103)/ γ5(ins85-99), γ2(1-212), γ2(1-244), or γ2(1-288) are shown. The error bars in **B-D** represent the mean ± SEM (n = 9-46). $^{*}p < 0.05$, $^{**}p < 0.01$, $^{***}p < 0.001$, significant difference relative to the corresponding control; $^{+}p < 0.05$, $^{++}p < 0.01$, $^{+++}p < 0.001$, significant difference from γ2 condition. Glu, Glutamate; Con, control; KA, kainate; SS, steady state; Pk, peak. Figure taken from (Turetsky et al., 2005).

Chimeric exchanges of the first two-thirds of stargazin's extracellular loop Ex(26-103) generated a protein with decreased effects on AMPA receptor desensitization, kainate efficacy and slightly but significantly decreased trafficking. While the smaller exchange Ex(89-103) presented with only a slight decrease in kainate efficacy, indicating that most of the stargazin's function on AMPA receptor desensitization and kainate efficacy is located in the first two-thirds of the first extracellular loop. The largest

truncation of the C-terminal tail γ2(1-212) of stargazin presented with complete loss of trafficking and decreased effects on AMPA receptor desensitization and kainate efficacy (Figure 1.11). While the smaller truncations γ2(1-244) and γ2(1-288) presented with gradual increases in trafficking and kainate efficacy, suggesting that the entire C-terminal tail of stargazin is important for trafficking and kainate efficacy. In summary, the first extracellular loop of stargazin is involved in modulating AMPA receptor desensitization, kainate efficacy and trafficking, while the intracellular C-terminal tail of stargazin mostly modulates trafficking (Turetsky et al., 2005). The C-terminal cytoplasmic tail of stargazin also has a signal sequence that promotes sorting and trafficking of AMPA receptor to the cell surface (Bedoukian et al., 2008). Recent studies indicate that the intracellular N-terminus and loop of stargazin may also contribute to AMPA receptor gating (Milstein and Nicoll, 2009)

Association of AMPA receptor with TARPs alters receptor pharmacological properties in response to positive modulators, competitive and non-competitive antagonists (Cokic and Stein, 2008; Soto et al., 2009). For example, the AMPA receptor positive modulator cyclothiazide displays a preference for *flip* rather than *flop* isoforms of the receptor. Co-expression of AMPA receptor with TARPs attenuates this preference, making both splice variants almost equally sensitive to cyclothiazide (Tomita et al., 2006). TARPs also modulate the ligand efficacy of AMPA receptors. In the absence of TARPs, quinoxalinedione compounds such as 6-cyano-7-nitroquinoxaline-2,3-dione (CNQX) are AMPA receptor antagonists. A crystal structure of GluR2 with CNQX bound reveals that CNQX induces a slight domain closure (<1 degree), a movement that is not enough to open the ion channel. However, when AMPA receptors are co-expressed

with TARPs, CNQX becomes a partial agonist. This result may indicate that TARPs act by strengthening a coupling mechanism between the ligand-binding core and the ion pore (Menuz et al., 2007). Co-expression of stargazin also increases efficacy and apparent affinity of the AMPA receptor to non-competitive antagonists GYKI 52466 and GYKI 53655, shifting the dose inhibition response curve to the left (Cokic and Stein, 2008). Taken together, these studies emphasize the significance of TARPs as AMPA receptor auxiliary subunits. It is now widely accepted that TARPs are crucial components of neuronal AMPA receptors and different TARP isoforms are important determinants of the properties of excitatory post-synaptic potentials (EPSPs) of various synapses (Fukata et al., 2005; Tomita et al., 2005a; Turetsky et al., 2005; Cho et al., 2007). Their co-expression in the brain plays an important functional role in the development and wiring of the nervous system (Dakoji et al., 2003; Tomita et al., 2005b; Deng et al., 2006).

1.4.2 Auxiliary Subunit - Cornichon

Recent studies using proteomic analysis of native AMPA receptor complexes identified cornichon homolog 2 (CNIH-2) and cornichon homolog 3 (CNIH-3) to be specifically associated with AMPA receptors (Schwenk et al., 2009). Cornichon proteins are only present in AMPA receptor complexes without TARPs. CNIH-2 and CNIH-3 have topology distinct from TARPs with an intracellular N-terminus, 3 transmembrane domains and extracellular C-terminus. Previous experimental evidence has shown their involvement in polarization of the embryo in *Drosophila* and ER protein export in yeast (Bokel et al., 2006; Castillon et al., 2009). Consistent with their role in trafficking cornichon proteins increased surface expression of homomeric GluR1*flop* 10-fold in a *Xenopus* Oocyte expression system. In addition to trafficking, cornichons also appear to

modulate AMPA receptor channel gating. Based on these observations, cornichon proteins are now considered, along with TARPs, as AMPA receptor auxiliary subunits (Schwenk et al., 2009).

1.5 Significance

AMPA receptors have been implicated in the synaptic changes underlying animal models of learning and memory, including long-term potentiation (LTP) (Anderson and Lomo, 1966; Shi et al., 1999) and long-term depression (LTD) (Barrionuevo et al., 1980; Christofi et al., 1993). In both cases, the synaptic changes that occur in response to stimuli result in an increase (LTP) or decrease (LTD) of the number of AMPA receptors at the synapse (Shi et al., 1999). In addition to regulation of AMPA receptor number, pore-forming subunit composition of AMPA receptors (Zhu et al., 2000), including the addition of different auxiliary subunits (Fukaya et al., 2006; Bats et al., 2007), has also been implicated in synaptic plasticity. These processes have also been implicated not only in memory formation but also normal development of the brain (Kirkwood et al., 1995) and involve different mechanisms at different stages of organism development (Yasuda et al., 2003).

Western society has long been plagued by increased incidence of cardiovascular disease. According to the American Heart Association, one in every four Americans will develop cardiovascular disease, accounting for 40% of all death in the USA. With development of modern medicine, the survival rate during heart attacks has increased dramatically. However, patients surviving these episodes can be left with insurmountable cognitive and motor disabilities caused by exitotoxic events in the CNS. During ischemic conditions in the brain following a heart attack or a stroke, production of neuronal ATP is

decreased, leading to elevated vesicular release of glutamate and impaired uptake of the neurotransmitter. This abnormal glutamate release and uptake contribute to the over-excitation of post-synaptic neurons: activation of AMPA receptors that leads to membrane depolarization and increased calcium influx through NMDA receptors. Elevated intracellular calcium causes a series of events that lead to cell death, termed excitotoxicity (Choi, 1988). In vivo evidence from animal models indicates that use of AMPA receptor competitive antagonists during ischemic events reduces the size of ischemic lesions (Sheardown et al., 1990), while use of AMPA receptor non-competitive antagonists may be protective against AMPA receptor mediated excitotoxicity (May and Robison, 1993). Such therapies in human patients suffering from strokes and heart attacks could be used to minimize neuronal damage in the CNS, thus increasing the quality of life for survivors.

AMPA receptors are thought to mediate neuronal damage in amyotrophic lateral sclerosis (ALS) and epilepsy (Pollard et al., 1993). Deficits in synaptic transmission underlie the dementia in Alzheimer's disease, and blocking AMPA receptor desensitization may be beneficial in treatment of dementia symptoms. In models of inflammatory and neuropathic pain, up-regulation of glutamate receptors contributes to nociceptive behaviors (Carlton and Coggeshall, 1999). Thus, blocking glutamate receptors has anti-nociceptive effects (Hunter and Singh, 1994).

ALS is caused by degeneration of motor neurons and in 10% of the cases it is caused by sporadic mutations in superoxide dismutase 1 (SOD1) (Rosen et al., 1993). Motor neuron degeneration in the other 90% of the case remains unclear and three different non-exclusive mechanisms are supported by experimental evidence. The first suggests that

over activation of calcium permeable glutamate receptors in response to increased release of glutamate contribute to this degeneration (Yin et al., 1995). The second one proposes that motor neurons are selectively vulnerable to excitotoxic events because of their high density of AMPA receptors (Vandenberghe et al., 2000). The third one relies on the fact that some of the ALS patients carry mutations in the glutamate transporter GLT-1, suggesting that pathogenesis of ALS is in part a result of decreased glutamate re-uptake and the resulting prolonged activation of AMPA (Meyer et al., 1995; Rothstein et al., 1995).

Epilepsy is a common disorder, resulting in synchronous activity in the brain, affecting approximately 50 million people worldwide. There are multiple causes of epilepsy, approximately 10% are caused by mutations in voltage-gated or ligand-gated ion channels (Yamakawa et al., 1995; Wallace et al., 1998; Catterall et al., 2008). In some cases, mutations of a voltage-gated sodium channel result in a longer channel open time and prolonged glutamate release from the pre-synaptic terminal. AMPA receptors have been shown to play a role in the cell death after seizures and increased influx of calcium through calcium permeable glutamate receptors has also been shown to contribute to this process (Pollard et al., 1993).

In Alzheimer's disease, amyloid beta peptides are accumulated in the matrix surrounding neurons causing dementia. The recent literature indicates that synaptic AMPA receptors are down regulated in the early stages of the disease (Armstrong et al., 1994) and that the cognitive defects observed in the process of the disease are actually a result of synaptic failure, not neuronal cell death (Selkoe, 2002). Therefore use of

nootropic drugs, like aniracetam or AMPAkines, that reduce AMPA receptor desensitization may help reduce the rate of synaptic failures.

With increasing knowledge of the role of AMPA receptors in the above disorders, more treatment options can be developed and ultimately more lives can be saved or dysfunction ameliorated. Understanding AMPA receptor desensitization better might provide insight into rational drug design for pore-forming subunits. Also, because TARPS have such a profound effect on AMPA receptor desensitization and pharmacology, they may provide a new target for rational drug design. The medical as well as scientific field could benefit greatly from the research unlocking mysteries underlying AMPA receptor physiology, its role in synaptic plasticity and pathological conditions.

CHAPTER II

RESEARCH DESIGN AND METHODS

2.1 Site directed mutagenesis

In order to prepare constructs utilized in this project, mutations were introduced into the GluR1 AMPA receptor protein (AMPA receptor clones were a gift from Dr. P. H. Seeburg; Max Planck Institute for Medical Research, Heidelberg, Germany) as well as TARPS γ2 (cloned from adult rat cerebellum) and γ5 (cloned from adult rat forebrain), using the ProSTAR Ultra HF RT-PCR system (Stratagene, La Jolla, CA). The QuickChange II XL site-directed mutagenesis kit from Stratagene is optimized for site-directed mutagenesis of double-stranded plasmids with large inserts (the plasmid is 10 kb and GluR1 is 5 kb). This kit utilizes thermal cycling to denature the parental DNA template, anneal the primers introducing the mutations and extend the primers with *PfuUltra* DNA polymerase. Digestion of the parental DNA plasmid with DpnI endonuclease follows thermal cycling (DpnI Endonuclease is specific for methylated and hemimethylated DNA, therefore it will only digest the parental strands). DNA was transformed into XL10-Gold ultracompetent bacterial cells and individual colonies were selected after plating on agar containing antibiotic. To insure that no collateral mutations were introduced during mutagenesis, mini-prepped DNA was sequenced at the Recombinant DNA/Protein resource facility at Oklahoma State University, Stillwater, OK. We sequenced both strands of the plasmid DNA in opposite directions and the sequence normally runs approximately 1200 base pairs. The total length of GluR1 is

approximately 2700 base pairs, and because the sequence overlaps from the beginning of S1 to the end of S1 we usually sequence approximately 75% of the receptor. The ligand-binding domain and transmembrane domains forming the channel are always present in our sequence. DNA is then maxi-prepped using a Qiagen kit and stored at 4^{o}C. All mutations are done in collaboration with Dr. Turetsky's laboratory.

2.2 HEK293 tissue culture

For expression of recombinant AMPA receptors, human embryonic kidney cells (HEK293) cells from American Type Culture Collection (Manassas, VA) were grown at 37 degrees C in a humidified 5% CO_2 incubator. 90% MEM plus Earle's salt (Invitrogen) and 10% Fetal bovine serum (FBS) (Invitrogen) was used as medium for cell culture. Cells were passaged in 25^{2}cm flasks. Once they reached 70% confluency they were plated on 35 mm dishes for transfection and/or passaged. Cells were typically used up to passages 15-17 before being discarded.

2.3 Transient transfections

Because the surface of the plastic and the surface of the cells are negatively charged, 35 mm dishes were coated with Poly-D Lysine (PDL) that is positively charged to ensure proper attachment of HEK293 cells. After the cells growing in the flasks reached 70% confluency, we plated them on the coated 35 mm dishes at 2000 cells per dish. 24 hours later, cells were transfected using Lipofectamine reagent from Invitrogen. For each 35 mm dish to be transfected, 2 µg of Qiagen purified DNA was diluted in 100 µl of OPTI MEM (Invitrogen) and was combined with 8 µl of Lipofectamine reagent diluted in 100 µl of OPTI MEM (use of OPTI MEM is recommended by Invitrogen for transient transfections). This mixture was incubated for 20 minutes at room temperature. 800 µl of

OPTI MEM was added to the transfection mixture to bring transfection volume to 1 ml. Cells were washed 3 times with 3 ml of OPTI MEM to remove all traces of serum, since serum interferes with transfection. The last wash was replaced with transfection solution. Cells were returned to the incubator for 3 hours. Following incubation, cells were washed 3 times with 3 ml of MEM to remove traces of DNA and lipofectamine, and were fed with complete culture medium supplemented with 50 μM of the competitive antagonist NBQX (Tocris) to block activation of expressed AMPA receptors and to prevent excitotoxicity. Electrophysiological experiments were performed 36-40 hours later.

DNA was transfected at a ratio of 1:1 for GluR1 and γ2. pEGFP DNA (Clontech, Palo Alto, CA) was included in transfection for identification of transfected cells in electrophysiological experiments. To avoid DNA toxicity during transfection, we always maintained a constant amount of DNA in each dish, 2 μg. In the past experiments in our laboratory we utilized heteromeric receptors as well as transfection with multiple auxiliary subunits, where, for example, we used 0.55 μg of GluR1, 0.55 μg of GluR2 (or PSD-95), 0.55 μg of stargazin and trace amounts of pEGFP. In order to keep our older and newer data compatible, we continued using the same amount of DNA in this set of experiments, while only using homomeric GluR1 and stargazin DNA in transfection. Therefore for transfections presented in this dissertation, we used 0.55 μg of GluR1, 0.55 μg of stargazin and 0.9 μg of pEGFP.

2.4 Electrophysiology

Whole-cell patch clamp recordings were performed at room temperature with cells voltage clamped at -60 mV. Recording electrodes are pulled from borosilicate glass (World Precision Instruments, CA) using a PE-30 puller (Sutter instruments) and fire-

polished on a Narishege microforge. Resistance in series with the cell usually was 2-7 MΩ and was compensated using an Axopatch 200A patch-clamp amplifier (Molecular Devices, Foster City, CA). Recorded data was filtered at 1-3 kHz, sampled at 2-10 kHz and recorded using pClamp10 (Molecular Devices) operating on a Dell computer.

Extracellular recording solution contained (in mM) 145 NaCl, 5.4 KCl, 1 $MgCl_2$, 1.8 $CaCl_2$, 5 HEPES, 5.5 glucose and 0.01 mg/ml phenol red, osmolarity was adjusted to 300mOsm and pH adjusted with sodium hydroxide to 7.3. During the experiment, the recording chamber was continually perfused by bath containing extracellular recording solution and 500 μM of the rapidly reversible antagonist kynurenic acid (Tocris) to protect cells from excitotoxicity and pre-exposure to agonists. Patch pipettes were filled with intracellular solution containing (in mM) 135 CsCl, 10 CsF, 2 $MgCl_2$, 0.5 $CaCl_2$, 5 Cs_4BAPTA, 10 HEPES, 2 Na_2ATP (all reagents obtained from Sigma) with osmolarity adjusted to 295 mOsm and pH adjusted with cesium hydroxide to 7.2. Cesium was used instead of potassium in the intracellular solution in order to block potassium channels present in the HEK293 cells.

Rapid agonist application was achieved using a glass flowpipe array (12 parallel barrels, each 400 μm in diameter) placed near a voltage-clamped cell. The first set of experiments described in Chapter 3 utilized a pump-forced perfusion (Minipuls3; Gilson Medical Electric, Middleton, WI) through three-way solenoid valves (Isolatch; General Valve, Fairfield, NJ). This system achieved solution exchange around a small cell within 5–10 ms. The remainder of the experiments described in chapters 4, 5 and 6 used a gravity-fed perfusion system, with 10 ml syringes filled with solutions elevated approximately 6 feet above the recoding platform. Solution application was controlled

with Lee minisolenoid valves (World Precision Instruments, CA). The data achieved by these different methods of perfusion appeared comparable because the decay rates of the glutamate peaks were undistinguishable. Nonetheless, we only used experimentally matched controls with every set of experiments. For both perfusion systems, valve opening and closing was coordinated with flowpipe movement using the Warner Instruments (Hamden, CT) SF-77B fast-step Perfusion system.

A standard protocol for examining AMPA receptor glutamate kinetics, responses to full and partial agonists as well as positive and negative modulators was used. The actual sequence of drug applications was optimized for cell survival, because repeated applications of TCM cause cell death. Because most of the run-down occurs in the first three application of agonist we initially subjected cells to three 600 ms applications of 3 mM glutamate that were followed by applications of 3 mM glutamate + 30 μM GYKI 52466 (negative allosteric modulator of AMPA receptors), 1.5 mM AMPA, 600 μM kainate, 3 mM glutamate + 500 μM TCM (positive allosteric modulator of AMPA receptors) and glutamate again in order to calculate recovery. The very last step in the sequence was a 3 step protocol that subjected a cell to a 500 ms application of glutamate, followed by a 7 second application of TCM (500 μM) plus glutamate (3 mM), followed by a 7 second application of glutamate (3 mM) alone. Applications of drugs were preceded and followed by a wash in control solution. In steps where the modulators were applied, the cells were first pre-treated with a modulator alone. Each agonist was applied twice to ensure the recorded traces were repeatable.

Every two months, the valves were tested for optimal performance. This was done by using HEK293 cells transfected with a mutant GluR1 construct A518S/Y519P/

S784G/A789G that had faster than normal desensitization kinetics. The valves were matched in 6 pairs with less than 5% difference in peak responses of A518S/Y519P/ S784G/A789G mutant construct in response to 3 mM glutamate applications.

2.5 Data Analysis

Peak and steady state currents of single representative agonist-evoked responses were measured using Clampfit 10 (Molecular Devices, Foster City, CA). To minimize the variability introduced by different cell passages, transfections and valves the data sets were grouped with their corresponding controls based on the date they were recorded. Cells that did not recover to 70% of the original glutamate peak were excluded from the data set. In addition to cells that did not recover, cells that had peak currents over 10 nA or under 50 pA were also excluded from the data set. Cells with peak currents over 10 nA are subject to greater current leak during voltage-clamp, while the accuracy of recordings from cells with peak currents under 50 pA was affected by electrical “noise” of the setup (10-20 pA).

2.5.1 Measurement of steady-state responses and percent desensitization.

In response to agonist binding, the AMPA receptor ion channel opens and the peak current can be observed on electrophysiological recording, but, as the receptor enters the desensitized state, the peak current rapidly decays to a steady-state level. It is currently unclear what precisely contributes to steady-state current, whether it is merely a summation of the currents flowing across the membrane as receptors cycle between open and desensitized states, or if the current flowing through a low-conducting desensitized state also contributes. Mean steady-state was measured relative to baseline before agonist application using Clampfit10 software within a 150 – 200 ms epoch. The extent of

steady-state desensitization was calculated relative to maximal current in the presence of TCM (1- Glutamate steady-state/Glutamate + TCM Peak)*100%. Two kinetic parameters were also used to characterize AMPA receptor desensitization, the rate at which the receptor enters and recovers from desensitization.

2.5.2 Measurement of desensitization kinetics

The rate of desensitization onset was measured as an exponential fit of the decay from glutamate peak to steady-state in the continued presence of 3 mM glutamate. The Chebyshev function used for fitting was generated by Clampfit10 software.

The rate of recovery from desensitization was assessed using a 3 step protocol. Benzothiadiazine modulators that block AMPA receptor desensitization (cyclothiazide and trichlormethiazide (TCM) cannot bind AMPA receptors in the desensitized state (Sun et al., 2002). Therefore this limited binding of benzothiadiazines can be demonstrated electrophysiologically by its dramatically slowed association with the receptor in the presence of glutamate. The rate of TCM on-rate is proportional to the rate at which AMPA receptors recover from desensitization (illustrated in Figure 2.1). The two-exponential Chebyshev function used for fitting the rate of recovery from desensitization was also generated by Clampfit10 software. The slow component of the exponential fit was usually the larger component and because both components decrease in constructs co-expressed with stargazin, the slow component was illustrated as representative.

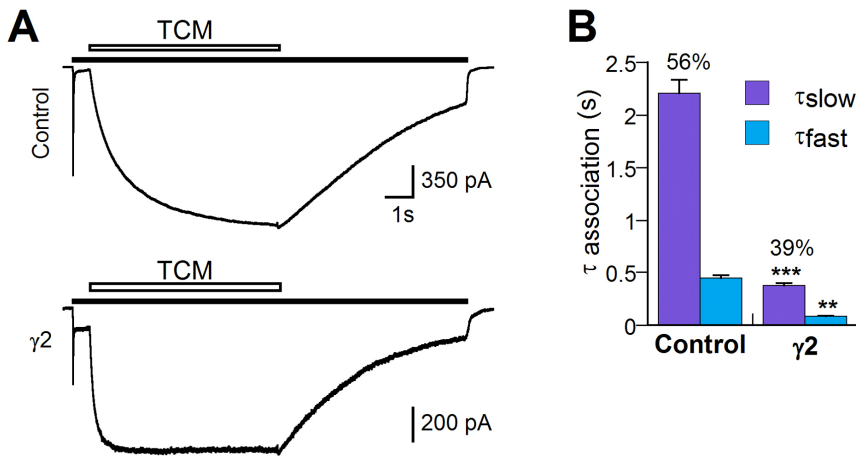

Figure 2.1: Stargazin speeds binding of positive allosteric modulators. (A) Responses to a 3 step-protocol from hippocampal neurons transfected with GFP (above) or γ2+GFP (below) show the association kinetics of TCM (500 μM) in the presence of glutamate (3 mM) (B). Onset kinetics were fit with the sum of two exponentials (% contribution of τ slow is shown). Bars represent mean ± SEM (control n = 19, γ2 n = 17). Asterisks indicate a significant difference between γ2 and the corresponding control (** P<0.01, *** P<0.001); (Turetsky et al., 2005).

2.5.3 Measurement of trafficking

The whole cell current is directly proportional to the number of AMPA receptors on the surface, therefore the maximal current density of AMPA receptors expressed at the cell surface was obtained by dividing the peak current obtained by co-application of 3 mM glutamate and 500 μM trichlormethiazide (to block receptor desensitization) by the whole cell capacitance (pA/pF). Although cyclothiazide is the most widely used drug to block AMPA receptor desensitization, we used its analog trichlormethiazide because it has much faster association and dissociation kinetics while having the same effect on blocking AMPA receptor desensitization as cyclothiazide. This functional measure of AMPA receptor trafficking was validated with surface biotinylation experiments (Turetsky et al., 2005)

2.6 Statistical Analysis

Peak and steady state currents of the single representative agonist-evoked responses were measured using Clampfit 10 (Molecular Devices, Foster City, CA). Statistics were preformed using a SigmaStat 3.1 software package (Systat Software Inc, 2004). For comparison of two groups, unpaired Student's T-test was used. For comparison of multiple groups, the data was evaluated using a One-Way ANOVA with Student-Neuman-Keuls post-hoc tests. The level of significance was set to $P<0.05$ while the power of the performed test was above 0.8 for all analyses presented in this dissertation. Bar graphs presented in the results sections were expressed as mean ± SEM unless reported otherwise.

CHAPTER III

MECHANISM UNDERLYING THE EFFECT OF STARGAZIN ON AMPA RECEPTOR DESENSITIZATION

3.1 Introduction

In response to agonist binding the AMPA receptor ion channel opens and the peak current can be observed in electrophysiological recording, but, as the receptor enters the desensitized state, the peak current rapidly decays to a steady-state level. Co-expression of AMPA receptors with TARPs results in a desensitization profile that dramatically differs from that of pore-forming subunits expressed alone. TARPs modulate AMPA receptor functional properties by decreasing the amount of steady-state desensitization (Turetsky et al., 2005), increasing the efficacy of the agonist and slowing the rate of channel deactivation (Priel et al., 2005). Three plausible mechanisms have been proposed to explain stargazin's effect on AMPA receptor steady-state desensitization.

The first mechanism, proposed by Priel and colleagues, suggested stargazin acts to stabilize the dimer interface, and thus slows the onset of desensitization. They found that stargazin changes the EC_{50} of glutamate in homomeric GluR3 receptors (from 18.5 ± 0.5 µM without stargazin to 5.0 ± 0.3 µM with stargazin), while being unable to do so in the L507Y mutant construct, which already exhibits increased agonist efficacy (from 18.5 ± 0.5 µM in GluR3 to 4.3 ± 0.1 µM in L507Y). The authors assumed that the effects of stargazin on AMPA receptor agonist efficacy, deactivation and desensitization are caused by the same mechanism and, because effects of stargazin were occluded by the L507Y

mutation, that stargazin must act by the same mechanism as the L507Y mutation, i.e. by stabilizing the dimer interface (Priel et al., 2005). However, because the experiments were done in the *Xenopus Oocyte* expression system, where rapid desensitization kinetics cannot be observed, and in the presence of positive allosteric modulator cyclothiazide, their data are difficult to interpret.

The second mechanism, proposed by our laboratory, suggests that stargazin decreases steady-state desensitization by destabilizing the desensitized state. Benzothiadiazines like cyclothiazide and trichlormethiazide (TCM) cannot bind AMPA receptors in the desensitized state (Sun et al., 2002). This limited binding of benzothiadiazines can be demonstrated elecrophysiologically by its dramatically slowed association with the receptor in the presence of glutamate. Co-expression with TARPs speeds binding of the positive allosteric modulator TCM to AMPA receptors in the presence of glutamate, thus suggesting that the rate of recovery from the desensitized state is increased (Turetsky et al., 2005).

The third proposed mechanism relies on single channel evidence indicating that co-expression with stargazin increases relative frequency of large conductance openings and causes a two-fold increase in duration of bursts without an actual change in the length of individual openings. Zhang et al. suggest that the effects of stargazin on desensitization are secondary to its effects on gating kinetics (Zhang et al., 2006). Although, the effects of stargazin on gating kinetics in neurons are apparent, they are not mutually exclusive with stargazin's effect on the rate of recovery from desensitization.

To elucidate the mechanism of TARP modulatory action on AMPA receptor desensitization, we utilized the effects of mutations known to affect protein interactions

in the dimer interface (helices D and J) and examined the effects of γ2 on desensitization kinetics in these mutants. Figure 3.1 illustrates the crystal structure of the GluR2 dimer with helices J and D delineating the dimer interface (Horning and Mayer, 2004).

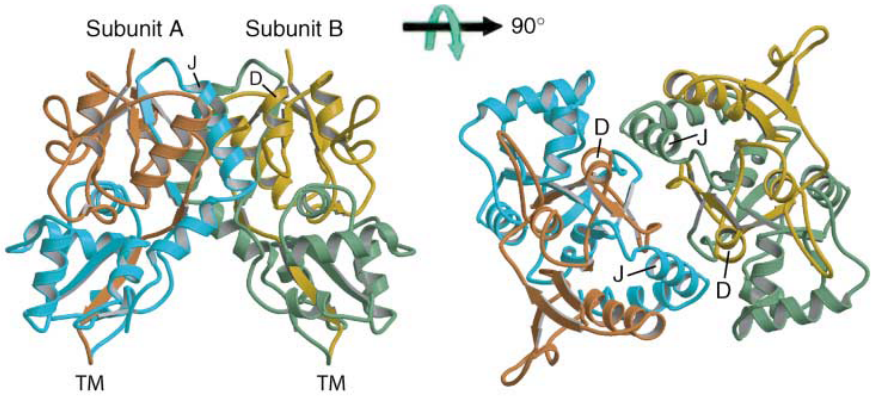

Figure 3.1: Schematic representation of the GluR2 flop crystal structure. Left: side view of the intra dimer interface; Right: top-down view of the dimer (from Horning and Mayer 2004).

In GluR2 residues L483 (in helix D) and K752 (in helix J) introduce steric hindrance within the network of bonds that stabilize the dimer interface. Removing the steric hindrance by truncating these residues to alanines results in a more stable dimer interface and thus slower onset of desensitization (Horning and Mayer, 2004), while mutating L483 to tyrosine creates an additional salt bridge between adjacent subunits and completely blocks desensitization (Stern-Bach et al., 1998; Sun et al., 2002). Residues E486 and K493 (in helix D) and N747 and E755 (in helix J) participate in a network of hydrogen bonds supporting stability of the dimer interface connecting helix D of one subunit with helix J of another. Truncation of any of these residues to alanine results in a less stable dimer interface and increased rate of desensitization onset. Interestingly, none of the mutations on the dimer interface had an affect on AMPA receptor recovery from desensitization (Horning and Mayer, 2004).

Although most of the crystallographic work has been done in the GluR2 subunit, homomeric GluR2 receptors do not occur endogenously and are difficult to work with in

electrophysiological experiments due to their low conductance. In contrast homomeric GluR1*flip* subunits produce robust responses and are endogenously expressed. Thus we made some of the corresponding mutations in GluR1. Table 3.1 lists mutations that had intermediate desensitization phenotypes and were chosen for the electrophysiological experiments outlined below.

Table 3.1: Residues on the AMPA receptor intra-dimer interface having an intermediate effect on receptor desensitization

Mutation (GluR2)	Mutation (GluR1)	Interaction partner	Location	Effect on Desensitization Rate in GluR2	Reference
L483Y*	L479Y	L748, L751	helix D	prevents desensitization	(Stern-Bach et al., 1998) *
L483A	L479A	L748, L751	helix D	3-fold decrease	(Horning and Mayer, 2004)
E486A	E482A	K493, F491, N747	helix D	46-fold increase	(Horning and Mayer, 2004)
N747D	N743D	E486	helix J	19-fold increase	(Horning and Mayer, 2004)
K752A	K748A	helix D	helix J	4.7-fold decrease	(Horning and Mayer, 2004)

* L507Y mutation was originally done in GluR3

3.2 Statement of hypothesis

Because stargazin modulates AMPA receptor desensitization by controlling the rate of recovery from desensitization, stargazin's effects should be additive with constructs carrying mutations of the residues on the dimer interface controlling the rate of desensitization onset.

3.3 Results and Discussion

To elucidate the mechanism responsible for the effect of TARPs on AMPA receptor desensitization, mutations listed in Table 3.1 were made in a GluR1 background and expressed as homomers with and without stargazin. Whole cell patch clamp recordings were performed to identify the effects of these mutations on AMPA receptor.

First we assayed the effects of the mutations on AMPA receptor expression. All of the constructs produced robust currents, indicating that mutated constructs were processed by the ER machinery and expressed as functional proteins on the plasma membrane (in fact the L479A construct had significantly higher current density when compared to a control). Although, in all cases, the mutated GluR1 constructs co-expressed with stargazin showed significantly increased trafficking, the fold effect of stargazin on trafficking of different constructs was not the same (Figure 3.2)

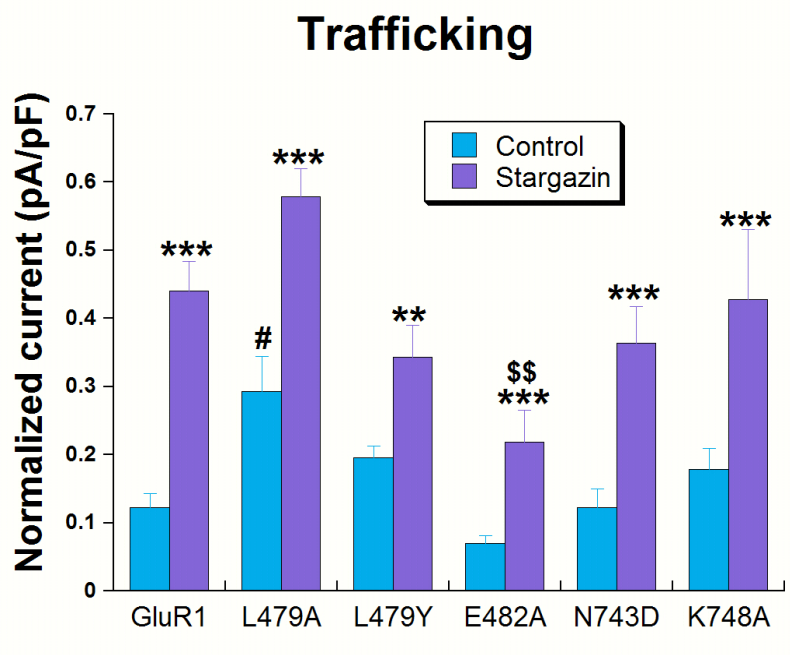

Figure 3.2: Stargazin increases trafficking of mutations that participate in the stability of the intra-dimer interface. As a functional measure of trafficking, peak currents for glutamate + TCM application were divided by whole cell capacitance to yield current density (pA/pF). Bar graphs represent means ± SEM, n=9-18. * indicates statistical difference within a construct, # indicates statistical significance as compared to GluR1, $ indicates significance as compared to GluR1γ2. (* P<0.05; ** P<0.01; ***P<0.001)

3.3.1 The effects of stargazin and mutations stabilizing the intra-dimer interface on AMPA receptor desensitization.

In our attempt to elucidate the mechanism of stargazin's action on AMPA receptor desensitization, we examined desensitization properties of mutants listed in Table 3. The

decay of the glutamate peak was fit with exponential function to determine the rate of desensitization onset for these constructs. Because the rate of desensitization onset and the degree of steady-state desensitization are not necessarily correlated for all dimer interface mutants, (Horning and Mayer, 2004) we also characterized percent desensitization relative to maximal current in the presence of Glutamate + TCM (% desensitization = (1-Glutamate Steady-State / Glutamate + TCM Peak)*100%).

Because previous results from the *Xenopus* Oocyte expression system suggested that stargazin's functional effects on L507Y mutant were occluded by the mutation, we transferred this mutation to a GluR1 background (L479Y) and examined its desensitization properties in HEK 293 cells. In agreement with Priel et. al., our data indicate that the only effect of stargazin in this mutant is increased trafficking (Figure 3.3).

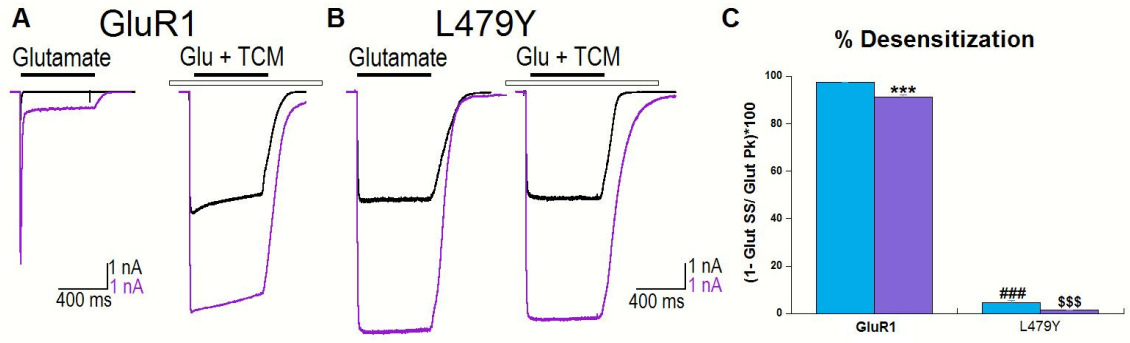

Figure 3.3: Co-expression of L479Y mutant with stargazin does not further decrease AMPA receptor desensitization. Representative traces of responces to glutamate and glutamate + TCM in GluR1 (A) and L479Y (B) expressed with (lavender) and without (black) stargazin. Black solid line indicates the duration of glutamate application, while the open box indicates the duration of TCM application. The scale bars indicate whole-cell current amplitude and time in milliseconds. Percent desensitization of glutamate traces (C). Bar graph represent means ± SEM, n = 9-12. * indicates statistical difference within a construct, # indicates statistical significance as compared to GluR1, $ indicates statistical significance as compared to GluR1 co-expressed with stargazin (*P<0.05; **P<0.01; ***P<0.001).

However, because mutation of residue L479 to tyrosine essentially locks the dimer interface by introducing a salt bridge, it prevents the receptor from ever entering the desensitized state. Thus this mutation is not useful in elucidating the mechanism of stargazin's action on AMPA receptor desensitization.

We next examined the previously described L479A, a mutation with a less severe desensitization phenotype. Interestingly, unlike in GluR2, this mutation in GluR1 was indistinguishable from control (Figure 3.4 C, I, J, and K). Such discrepancy is probably caused by the innate differences between GluR1 and GluR2 subunits.

Mutation of K748 to alanine resulted in a construct that behaved similarly to its GluR2 counterpart. Steady-state desensitization of K748A was significantly reduced and the rate of desensitization onset was significantly slower when compared to control GluR1, indicating that mutation of this residue stabilized the dimer interface (Figure 3.4 I and J).

Mutation E482A was previously shown to cause an increase in the rate of desensitization onset in GluR2 (Horning and Mayer, 2004). However, when we examined this mutation in GluR1, it had an opposite effect on desensitization properties. This construct had a significantly slowed rate of desensitization onset and decreased steady-state desensitization (Figure 3.4 I and J). This inconsistency probably also arose from differences between the GluR1 and GluR2 protein structure.

In agreement with Horning et. al., we did not observe changes in the kinetics of recovery from desensitization in any of the above described mutations, indicating that their main effect was on the onset of desensitization (Figure 3.4K).

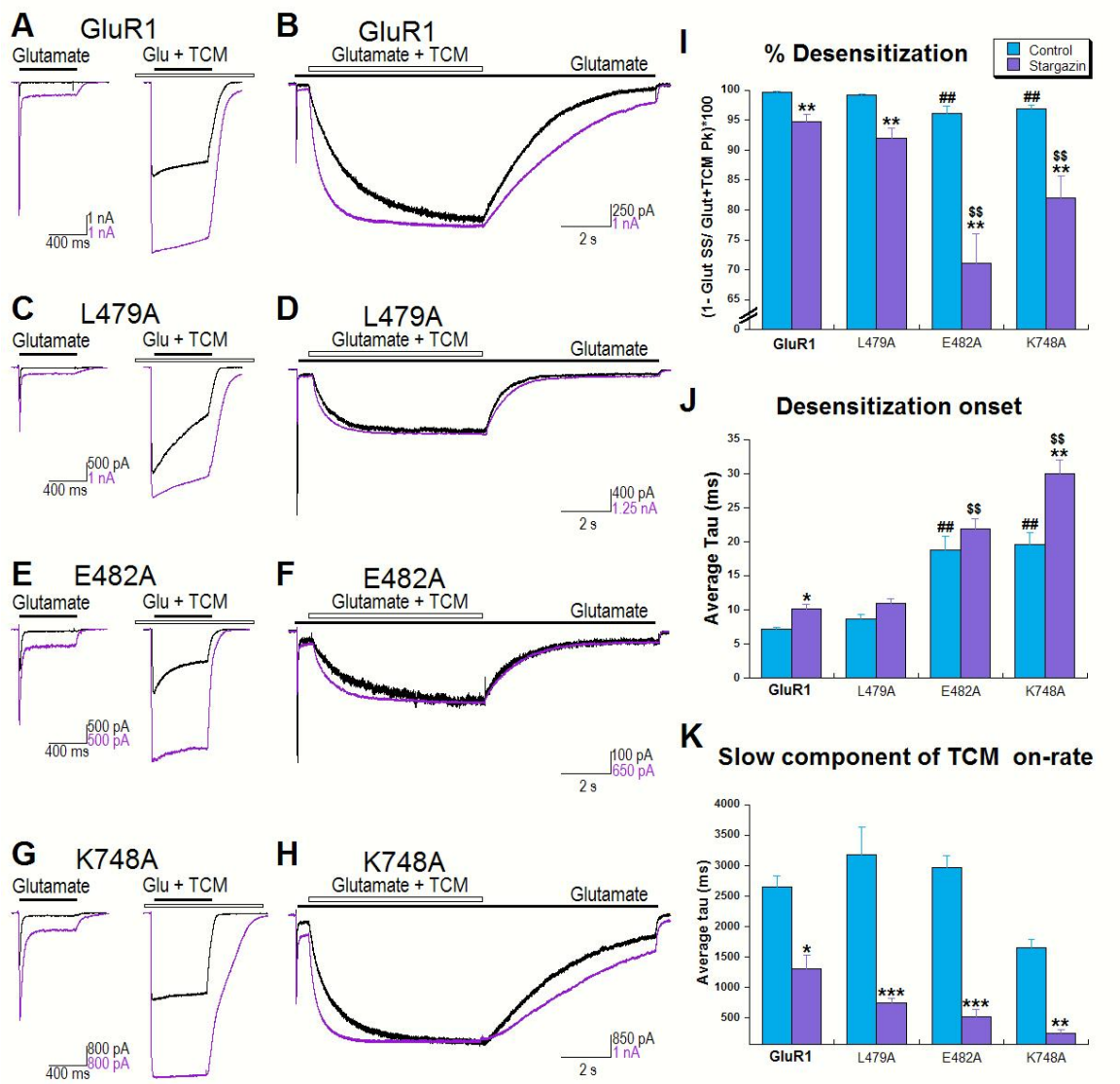

Figure 3.4: Effects of stargazin on desensitization in mutations that stabilize the dimer interface are additive. Representative traces for glutamate in the presence and absence of TCM for GluR1 (A), L479A (C), E482A (E) and K748A (G) expressed with (lavender) and without (black) stargazin. Traces to a 3 step protocol demonstrate relative recovery from desensitization of GluR1 (B), L479A (D), E482A (F) and K748A (H) expressed alone (black) or with stargazin (lavender). Percent desensitization is measured relative to glutamate + TCM peak (I). The time constant of desensitization onset was determined by fitting a decay of glutamate peak with a single exponential function (J). The time constant of recovery from desensitization is represented by the slow component of a two exponential fit of the TCM on-rate in the presence of glutamate (K). Bar graphs represent means ± SEM, n = 9-18. * indicates statistical difference within a construct, # indicates statistical significance as compared to GluR1, $ indicates significance as compared to GluR1γ2. (* P<0.05; ** P<0.01; ***P<0.001).

Interestingly, the mutations on helix D, L479A and E482A, had an unexpected effect on negative cooperativity between glutamate and trichlormethiazide as shown in the traces of these constructs (Figure 3.4 C and E). As more glutamate binds the ability of TCM to block desensitization in these mutants was reduced. Because part of the binding site for TCM is located on the dimer interface and is coordinated by the residues on the β strand 7, downstream of helix D, it is possible that the mutations of the residues in helix D alter the conformation or exert tension on the β strand 7 during glutamate binding, thus decreasing the affinity for TCM.

To determine whether the desensitization effects of the mutations that stabilize the dimer interface are additive or occlude the effects of stargazin, all mutant receptors were expressed with γ2 and their desensitization profiles were examined. If stargazin were to act by stabilizing protein interactions of the dimer interface, then the effects of stargazin on mutations that do the same should be occluded. However if stargazin acts by making the desensitized state less favorable, then the effects of stargazin should be additive with the effects produced by mutations stabilizing the dimer interface.

Steady-state desensitization of all three mutant constructs illustrated in Figure 3.4 was significantly reduced when expressed with stargazin (Figure 3.4 I). The rate of recovery from desensitization was also significantly faster in all mutations as well as control GluR1 (Figure 3.4 K). This result is consistent with our previous data, indicating that stargazin speeds the binding of positive allosteric modulators in the presence of glutamate (Turetsky et al., 2005). Thus, stargazin's effects on steady-state desensitization and rate of recovery from desensitization in mutations that stabilize the dimer interface were at

least additive and possibly synergistic (compare % desensitization for E482A and K748A relative to control GluR1).

3.3.2 Stargazin's effects on steady-state desensitization in a mutant construct destabilizing the intra-dimer interface are occluded.

We next examined the effects of a mutation that destabilizes the dimer interface, N743D. Peak responses to glutamate in this mutation were very small, suggesting that the receptor entered the desensitized state before the channel could open or the desensitized state was favored at rest (Figure 3.5 C).

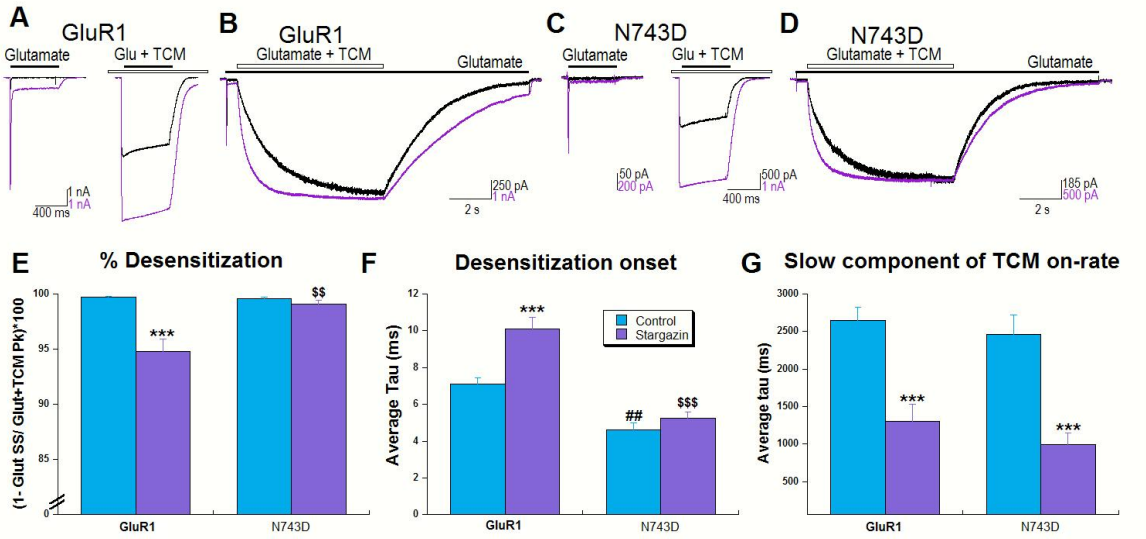

Figure 3.5: Effects of stargazin on steady-state desensitization in a mutation that destabilizes the dimer interface are occluded. Representative traces for glutamate in the presence and absence of TCM for GluR1 (A), N743D (C) expressed with (lavender) and without (black) stargazin. Traces to a 3 step protocol demonstrating the recovery from desensitization of GluR1 (B), N743D (D), expressed alone (black) or with stargazin (lavender). Percent desensitization is measured relative to glutamate + TCM peak (E). The time constant of desensitization onset was determined by fitting a decay of glutamate peak with a single exponential function (F). The time constant of recovery from desensitization is represented by the slow component of a two exponential fit of the TCM on-rate in the presence of glutamate (G). Bar graphs represent means ± SEM, n = 9-18. * indicates statistical difference within a construct, # indicates statistical significance as compared to GluR1, $ indicates significance as compared to GluR1γ2. (** $P<0.01$; ***$P<0.001$).

Steady-state desensitization of the N743D mutant was comparable to control GluR1 (Figure 3.5 E) while the rate of desensitization onset was significantly faster than a control (Figure 3.5 F). However, recovery from desensitization in the N743D mutant was comparable to control GluR1, supporting the evidence that mutations on the dimer interface affect only the onset of desensitization, but not recovery from desensitization (Figure 3.5 D and G).

To elucidate the mechanism of stargazin's action on AMPA receptor desensitization, the N743D mutant was co-expressed with stargazin and its desensitization profile was characterized. If stargazin were to act by stabilizing protein interactions on the dimer interface then it would be expected that stargazin would reduce desensitization of this mutant. However, if stargazin were to act by a different mechanism, then it would not be able to overcome the instability of the dimer interface.

When co-expressed with stargazin, currents of N743D mutant looked very different from the mutations that stabilize the dimer interface. Although neither the steady-state desensitization of N743D nor the kinetics of desensitization onset were affected by co-expression with stargazin (Figure 3.5 E and F), the peak response to glutamate was increased, suggesting that stargazin reduces the number of receptors desensitized at rest. Interestingly, stargazin had a full effect on speeding the recovery from desensitization in N743D mutant (Figure 3.5 D and G).

3.4 Summary of the results

Our exploration of the mechanism of stargazin's action on AMPA receptor desensitization revealed several interesting aspects about the mechanism of stargazin's effect on AMPA receptor desensitization:

- Stargazin’s effects on steady-state desensitization are additive and possibly synergistic with the mutations that participate in the stabilization of the dimer interface.
- Stargazin’s effects on steady-state desensitization are occluded by the mutation that destabilizes the dimer interface.
- Stagazin’s effect on the recovery from desensitization is independent from the mechanism controlling desensitization onset.

CHAPTER IV

IDENTIFICATION OF EXTRACELLULAR AMPA RECEPTOR DOMAINS CRUCIAL FOR TRANSDUCING EFFECTS OF STARGAZIN ON DESENSITIZATION AND KAINATE EFFICACY

4.1 Introduction

The areas of the AMPA receptor that associate with or transduce functional effects of TARPs have not been identified. Experiments with chimeras of γ2 and γ5 identified two domains important for different aspects of stargazin function: the first extracellular loop, responsible for stargazin's effects on desensitization and kainate efficacy, and the C-terminal cytoplasmic tail, responsible for receptor trafficking (Tomita et al., 2005a). Studies from our laboratory indicate that the function of these two domains is not quite so clear cut, with deletion of the C-terminal cytoplasmic tail also affecting desensitization and kainate efficacy, and changes in the first extracellular loop also impacting trafficking (Turetsky et al., 2005). Our work suggests that the AMPA receptor and stargazin are capable of association even when most of the C-terminal cytoplasmic tail is truncated or when the first extracellular loop is completely exchanged with that of γ5 (Turetsky et al., 2005), indicating that there are at least two points of association (extracellular and intracellular) between the AMPA receptor and stargazin, and that both of these contacts are necessary for full function.

In past experiments to determine the mechanism of AMPA receptor desensitization, the crystal structure of the ligand-binding domain was used to identify residues that may

play a role in the interactions between helices on the dimer interface (Sun et al., 2002), while further experiments mutated these residues to elucidate and confirm the mechanism of AMPA receptor desensitization (Horning and Mayer, 2004). In our effort to locate the domains of the AMPA receptor responsible for associating with TARPs we used a similar approach to guide our selection of residues for subsequent mutagenesis.

Because effects of stargazin on AMPA receptor functional properties are predominantly associated with the first extracellular loop, we would predict that breaking the extracellular association would result in loss of the majority of stargazin's effects on AMPA receptor desensitization and kainate efficacy, while still preserving trafficking. Other areas of the AMPA receptor may not directly associate with stargazin, but instead transduce stargazin's effects and when mutated could also affect kainate efficacy and/or desensitization. Thus we would expect that a construct with almost complete loss of stargazin's effect on kainate efficacy and desensitization as a candidate association point, while a construct with a smaller reduction in functional effects of stargazin as an efficacy site.

Figure 4.1 illustrates a top-down view of the tetrameric GluR2 ligand-binding domain crystal structure. The intra-dimer interface interactions, discussed in detail in Chapter III, are responsible for the stabilization of the interface and control the rate of desensitization onset (delineated by red ovals in Figure 4.1), while residues forming interactions between two dimers on the lateral dimer interface (delineated by green oval in Figure 4.1) did not affect the rate of desensitization onset (Horning and Mayer, 2004). The areas of the receptor that form the lateral inter-dimer interface and lateral faces of the receptor include loops 1 and 2 and helices B, G and K. Because of how the AMPA receptor tetramer

assembles, the same residues that participate in the interactions on the lateral inter-dimer interface are also present on the exposed lateral faces of the tetramer (delineated by green brackets in Figure 4.1). The outer faces of the receptor, which include helix H, are always exposed and are capable of interacting with other proteins (delineated by blue brackets in Figure 4.1).

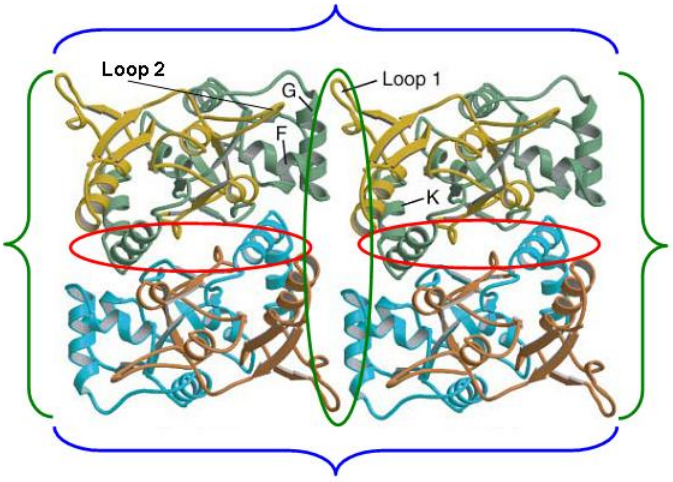

Figure 4.1: Schematic representation of top-down view of AMPA receptor tetramer based on the GluR2 crystal structure. Red ovals indicate the location of the intra-dimer interface, green oval indicates the location of the lateral inter-dimer interface, green bracket delineates location of the exposed lateral face, blue bracket delineates location of the outer face of the AMPA receptor (Horning and Mayer, 2004).

We assumed that residues in the AMPA receptor associating with stargazin do not participate in subunit interactions within the tetramer, and further that the regions of the receptor most likely to associate with stargazin are on the lateral and outer faces of the receptor. Figure 4.2 indicates the exposed residues of a single subunit. Note the location of loops 1 and 2 and helices B, G, K and H.

Because stargazin does not associate with kainate receptors (Chen et al., 2003), we used homology to further refine areas of interest, selecting residues that were conserved among AMPA receptors but not between AMPA and kainate receptors. Table 4.1 lists the residues that fit these criteria.

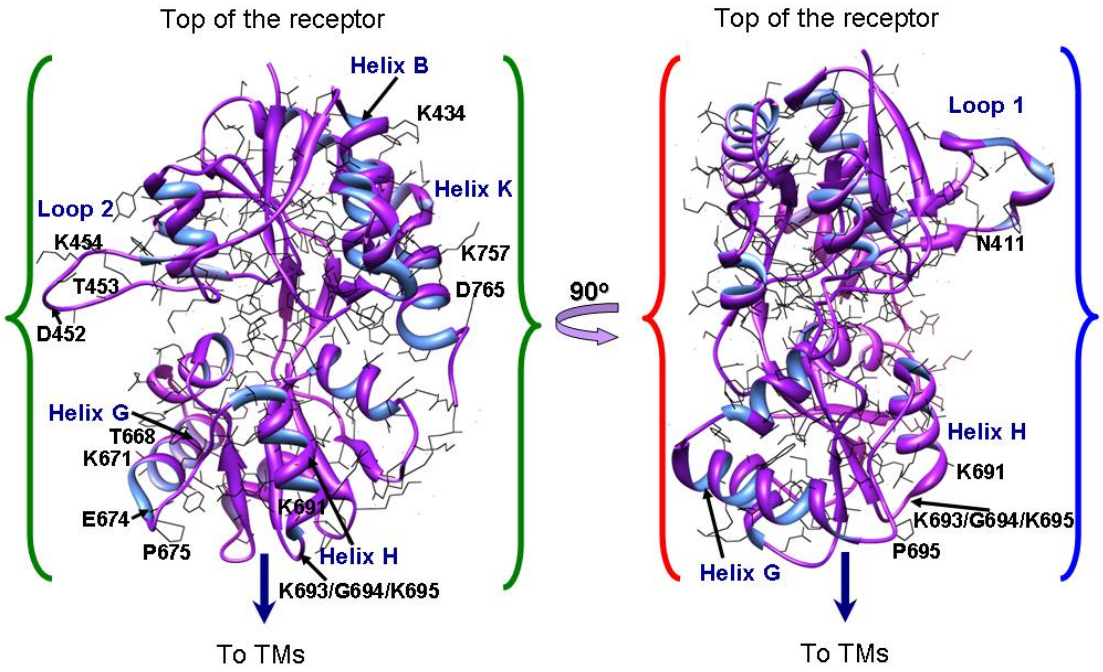

Figure 4.2: GluR2 single subunit ligand-binding domain crystal structure. **LEFT** - Side view of the subunit, with the dimer interface pointing into the page and the outer face of the subunit pointing out of the page; green brackets indicate faces of possible lateral inter-dimer interface/the lateral face of the receptor. **RIGHT** - Side view of the subunit, red bracket delineates intra-dimer interface, blue bracket indicates the outer face of the receptor, and possible lateral dimer interface/the lateral face of the receptor is pointing in and out of the page. Figure was made with the use of Chimera modeling software (UCSF) with the crystal structure from protein data base (PDB # 1FW0).

Table 4.1: Mutations in GluR1 receptor ligand-binding domain

Construct	Location	N	% Desensitization		τ recovery		Kainate efficacy	
			alone	+ γ2	alone	+ γ2	alone	+ γ2
K434T	Helix B	8	99.28	99.15$$$	4631.8###	1865.8***$$	0.0081	0.341***$$
T668A	Helix G	9	99.47	90.90***	1550.2	470.2***	0.0028	0.612***
K671S	Helix G	9	99.25	94.81***	2225.5	707.1***	0.0065	0.593***
E674R/P675Q	Helix G	9	99.11	99.25$$$	3664.6###	3156.4$$$	0.0209	0.297***$$$
K691T	Helix H	12	99.39	96.61***	1332.2	730.9***	0.0039	0.545***
del(K693/G694) /K695D	Downstream of helix H	10	99.65	99.56$$$	3452.1###	2996.1$$$	0.0058	0.184**$$$
K693G/K695D	Downstream of helix H	8	99.55	97.89$$$	1742.8	1909.1$$$	0.0083	0.367***$$$
K757M	Helix K	14	99.17	93.98***	2379.9##	705.5***	0.0034	0.399***$$
D765G	Helix K	14	99.74	96.83**	2699.8###	774.9***	0.0030	0.464***$
GluR1		**38**	**99.31**	**93.93*** **	**1746.9**	**569.5*** **	**0.0040**	**0.572*** **

Table 4.1: Table illustrates location and phenotypes of the mutations expressed with and without stargazin in GluR1 background. N indicates the number of cells in each data set. % Desensitization is measured as (1 – glutamate steady-state / glutamate +TCM peak)*100%. The rate of recovery from desensitization is represented by the slow component of a two exponential fit of the TCM on-rate. Kainate efficacy is measured by normalizing kainate current to Glutamate + TCM peak. # indicates statistical significance compares to GluR1 alone, * indicates statistical difference within each construct, $ indicates statistical significance compared to GluR1 co-expressed with stargazin (* P<0.05; ** P<0.01; ***P<0.001).

4.2 Statement of purpose

In order to identify possible areas of association between the AMPA receptor and stargazin, we mutated amino acids whose side chains were pointing out of the protein and that were conserved among AMPA receptors, but not in kainate receptors, and examined them using electrophysiological techniques.

4.3 Results and Discussion

Because mutations in the pore-forming subunits of the AMPA receptor might affect receptor function on their own, mutant constructs were expressed alone and with stargazin and evaluated using electrophysiological methods. An initial mutation on loop 1, N411D, was done in the GluR2Q background and did not have a different phenotype than control GluR2 with or without stargazin (data not shown).

4.3.1 Mutation of residues in helix G reduce the effects of stargazin on AMPA receptor functional properties.

Examination of the GluR2 crystal structure places helix G on the lower portion of the lateral face of the crystal. We mutated polar amino acids threonine 668 and lysine 671 that point out and away from the helix (Figure 4.2), to corresponding GluR6 residues alanine (A) and serine (S), respectively. In addition, polar glutamate residue (E) in position 674 is located on the exposed surface of the helix and is followed by proline (P) 675 that introduces a bend in the protein structure, thus ending helix G. Interestingly, this proline residue is conserved in all AMPA receptors but not in kainate receptors, where a glutamine residue takes its place, indicating that the position of helix G in kainate receptors differs from that of AMPA receptors. Because kainate receptors do not

associate with stargazin, we mutated residues E674 and P675 to their corresponding residues in GluR6 arginine (R) and glutamine (Q), respectively, in a single construct.

The helix G constructs were functional and trafficked robustly with the exception of the double mutant E674R/P675Q, which had significantly lower trafficking when compared to control GluR1 (Figure 4.3). When co-expressed with stargazin, all constructs had significantly increased trafficking, suggesting that the association between GluR1 and stargazin responsible for trafficking was maintained. Stargazin's effect on steady-state desensitization was intact with the exception of the E674R/ P675Q construct, where % desensitization was not affected, indicating that the functional effects of stargazin that control AMPA receptor desensitization were lost in this mutant (Figure 4.3 C and F and Table 4.1). Because stargazin's main effect on desensitization lays in the kinetics of the recovery from desensitization, we examined the kinetics of TCM on-rate in the presence of glutamate. Interestingly, the E674R/ P675Q construct expressed alone had a significantly slower rate of TCM on-rate in the presence of glutamate, indicating that the mutation affected the rate of recovery from desensitization, while T668A and K671S constructs had rates that were comparable to control GluR1 (Figure 4.3 D and G). When co-expressed with stargazin, the rates of TCM binding in the presence of glutamate in T668A and K671S construct were significantly decreased, indicating that stargazin's effect on recovery from desensitization is intact. Intriguingly, stargazin was unable to decrease the rate of recovery from desensitization in the E674R/P675Q mutant construct, indicating that its effect on desensitization was lost (Figure 4.3 D and G). Stargazin significantly potentiated kainate currents in all three constructs. However, kainate

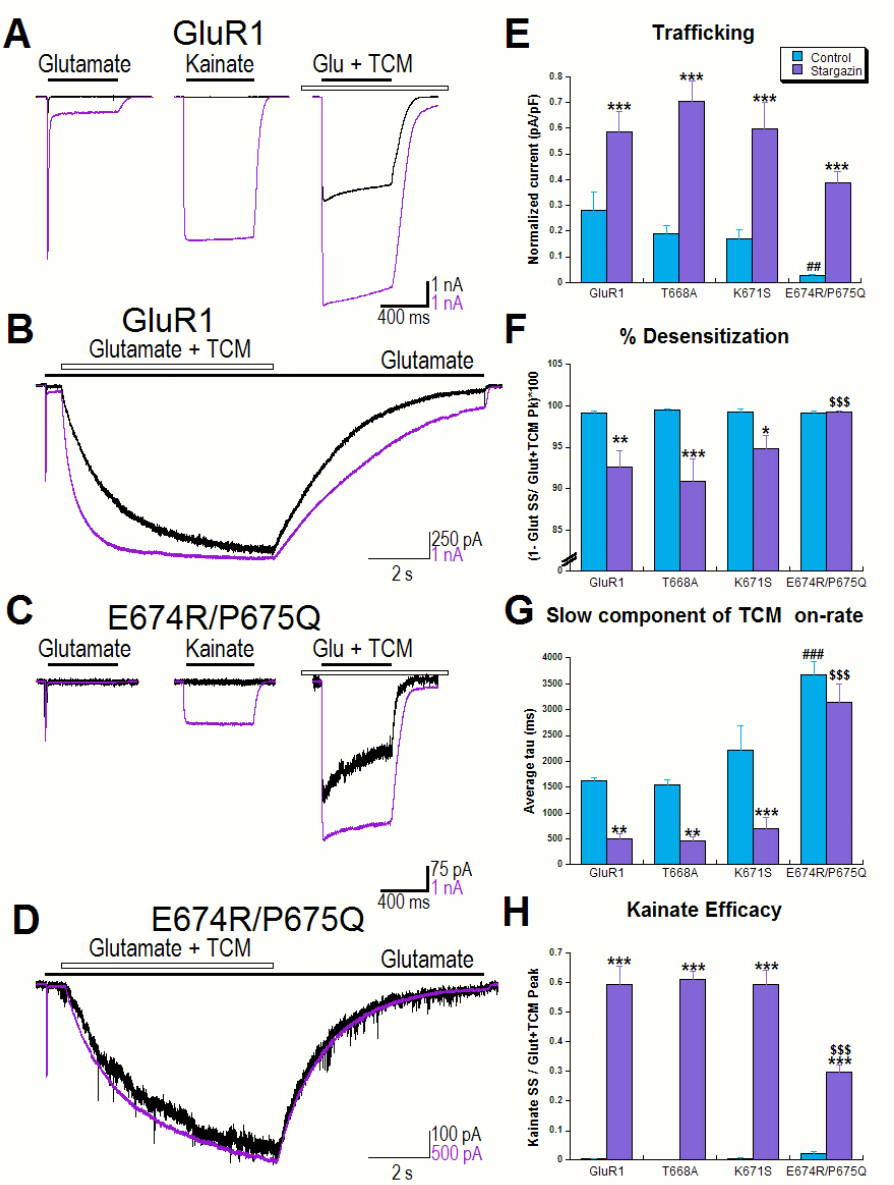

Figure 4.3: Residues in helix G are responsible for transducing functional effects of stargazin in GluR1. Representative traces for constructs alone (black) and co-expressed with stargazin (lavender) in response to glutamate and kainate in the presence and absence of TCM for GluR1 (A) and E674R/P675Q (C); and in response to a 3 step protocol for GluR1 (B) and E674R/P675Q (D). Summary of the results of trafficking as measured by whole cell currents to application of Glutamate + TCM normalized to whole cell capacitance (E); Percent desensitization is measured relative to glutamate + TCM peak (F); The time constant of recovery from desensitization is represented by the slow component of a two exponential fit of the TCM on-rate in the presence of glutamate (G) and Kainate efficacy as measured by normalizing the kainate current to Glutamate + TCM peak (H) are represented by bar graphs illustrating means ± SEM, n = 7-10. * indicates statistical difference within each constructs, # indicates statistical difference compared to GluR1 expressed alone, $ indicates significance as compared to GluR1γ2. (* P<0.05; ** P<0.01; ***P<0.001).

potentiation was markedly reduced in the E674R/P675Q, indicating that some of stargazin's effect on kainate efficacy was also lost (Figure 4.3 C and H).

Overall these results indicate that residues T668 and K671 in helix G are not important for association with, or transducing the effects of stargazin. Mutation of residues E674 and P675 to their corresponding GluR6 residues, however, substantially reduced the effects of stargazin on AMPA receptor desensitization and kainate efficacy. Because the mutation E674R/P675Q introduces structural changes to the protein by removing proline at the end of helix G, it may create tension that affects not just helix G but also helix H. The conservative interpretation of these results is that the mutation E674R/P675Q changes the conformation of helix G and H, thus leading to loss or substantial weakening of association with stargazin.

4.3.2 Residues downstream of helix H participate in association with stargazin.

Helix H is located on the lowermost portion of the outer face of the crystal. Several polar lysine residues are located at the bottom of the helix and are pointing out of the protein, where they could interact with stargazin.

Residue K691 on helix H (Figure 4.2) was mutated to the corresponding GluR6 residue threonine. Interestingly, while comparing the sequence alignment of GluR1 and GluR6 immediately downstream of helix H, we noticed that GluR6 was missing two residues present in AMPA receptors, K693 and G694, while the immediately following residue K695 in AMPA receptors was substituted by aspartate (D) in GluR6. To resolve this problem two constructs were made, first with deletion of K693 and G694 plus a substitution of residue K695 to aspartate to mimic GluR6 spacing (del(K693/G694)/K695D), and second with a double mutation of K693A and K695D,

preserving G694 to maintain GluR1 spacing (K693A/K695D). These resulting mutations have different length and thus put different amounts of tension on the areas downstream of helix H.

All resulting constructs were functional, however both del(K693/G694)/K695R and K693A/K695D trafficked significantly less than control GluR1. Stargazin, however, was able to significantly potentiate trafficking of all three constructs, indicating that the association responsible for trafficking was maintained. Although trafficking of del(K693/G694)/K695R and K693A/K695D co-expressed with stargazin was significantly reduced when compared to GluR1 co-expressed with stargazin, the trafficking was potentiated 2.8- and 10-fold respectively, compared to 2.5-fold for control GluR1 (Figure 4.4 A, C and E). Both steady-state desensitization and the rate of recovery from desensitization of the K691T construct co-expressed with stargazin were comparable to control GluR1 co-expressed with stargazin. Co-expression with stargazin in del(K693/G694)/K695R and K693A/K695D constructs did not yield a decrease in steady-state desensitization or the rate of recovery from desensitization, indicating that stargazin's ability to affect desensitization in these mutants was lost (Figure 4.4 B, D and F).

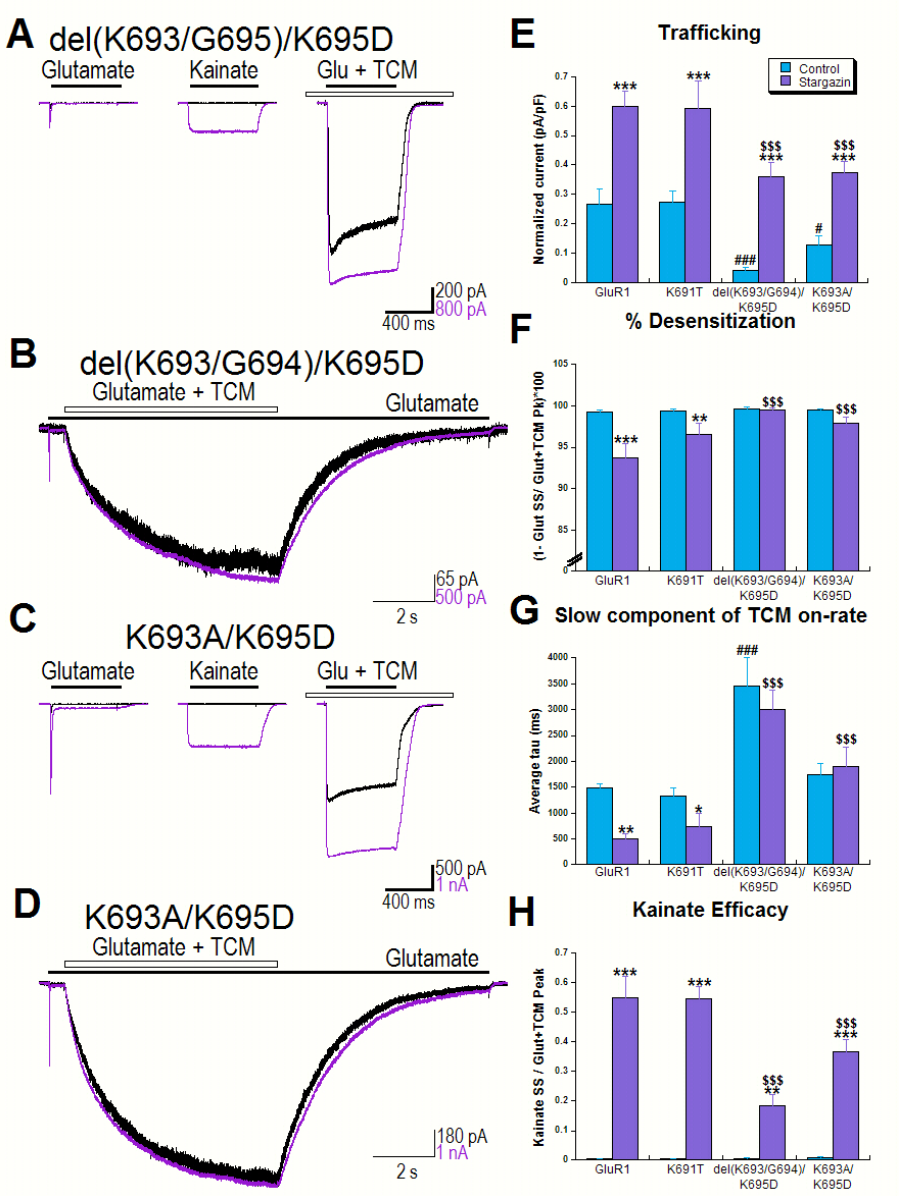

Figure 4.4: Mutation of residues in and downstream from helix H reduces functional effects of stargazin in GluR1. Representative traces for constructs alone (black) and co-expressed with stargazin (lavender) in response to glutamate and kainate in the presence and absence of TCM for del(K693/G694)/K695D (A) and K693A/K695D (C); in response to a 3 step protocol for del(K693/G694)/K695D (B) and K693A/K695D (D). Summary of the results of trafficking as measured by whole cell currents to application of Glutamate + TCM normalized to whole cell capacitance (E); Percent desensitization is measured relative to glutamate + TCM peak (F); The time constant of recovery from desensitization is represented by the slow component of a two exponential fit of the TCM on-rate in the presence of glutamate (G) and Kainate efficacy as measured by normalizing the kainate current to Glutamate + TCM peak (H) are represented by bar graphs illustrating means ± SEM, n = 8-10. * indicates statistical difference within each constructs, # indicates statistical difference compared to GluR1 expressed alone, $ indicates significance as compared to GluR1γ2. (* P<0.05; ** P<0.01; ***P<0.001).

Interestingly, del(K693/G694)/K695D mutant expressed alone had a slowed rate of TCM binding in the presence of glutamate, indicating that this construct was slower to recover from desensitization (Figure 4.4 B, and F). Stargazin was able to fully potentiate kainate current in the K691T construct, while being only partially effective in potentiating kainate currents of del(K693/G694)/K695D and K693A/K695D (Figure 4.4 A, C and H).

Overall these data indicate that lysine residues downstream of helix H participate in association with stargazin, while the exposed lysine 691 on helix H does not. Because of the different spacing introduced in the construct del(K693/G694)/K695D, it would be hard to interpret the effects caused by this mutation if taken alone. However, the results with construct K693A/K695D which preserves the spacing of GluR1, indicate that these residues are likely an association point between the AMPA receptor and stargazin.

4.3.3 Residues in helices K and B on the lateral dimer interface/lateral face of the receptor are important in transducing the effect of stargazin on AMPA receptor function.

Helices K and B lie on the lateral dimer interface/the lateral face of the receptor (illustrated in Figure 4.2). Because helix K is fully exposed and contains several polar residues that point out of the protein, we considered it a good candidate for association with stargazin. Helix B is located higher up on the lateral face of the crystal and has exposed residues in its upper portions. After observation of the GluR2 crystal structure, we selected three polar residues, K434, K757 and D765, that were pointing out of the protein, and were not participating in the dimer interaction and mutated them to their

corresponding GluR6 residues, threonine (T), methionine (M) and glycine (G), respectively.

Although resulting constructs were functional, K434T and K757M trafficked significantly less than control GluR1. Co-expression with stargazin resulted in significantly increased trafficking for all three constructs, indicating that the association responsible for trafficking was maintained (Figure 4.5 E). In contrast to stargazin's full effect on steady-state desensitization of both constructs in helix K (K757M and D765G), it was unable to decrease steady-state desensitization of the helix B mutant, K434T (Figure 4.5 F). Strikingly, while examining the rate of recovery from desensitization, we observed a significantly slower rate of recovery from desensitization in all three constructs, with K434T being almost 3-fold slower than control GluR1 (Figure 4.5 G). Previous experiments on the intra-dimer interface elucidated the mechanism involved in desensitization onset, but searches there or in loop 1 and helix G failed to discover any residues that affected the rate of recovery from desensitization (Horning and Mayer, 2004). Here we show that 3 residues on the lateral dimer interface affect the rate of recovery from desensitization when mutated to their corresponding residues in GluR6. When co-expressed with stargazin, the rate of recovery from desensitization was significantly faster in all three constructs (Figure 4.5 G). It is of interest to note that although stargazin was unable to decrease steady-state desensitization of K434T, it was still able to significantly speed its rate of recovery from desensitization, although not to control levels.

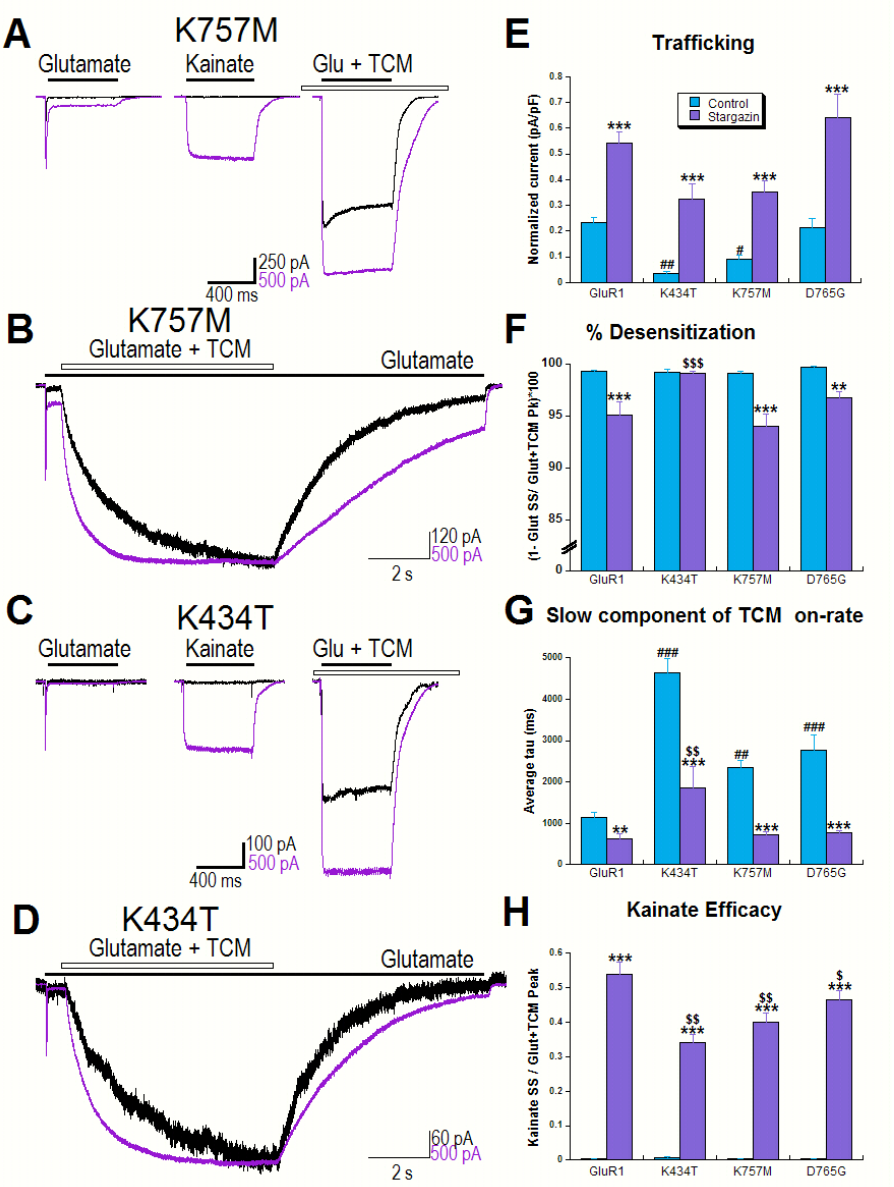

Figure 4.5: Mutation of residues in helices B and K reduces functional effects of stargazin in GluR1. Representative traces for constructs alone (black) and co-expressed with stargazin (lavender) in response to glutamate and kainate in the presence and absence of TCM for K757M (A) and D765G (C); in response to a 3 step protocol for K757M (B) and D765G (D). Summary of the results of trafficking as measured by whole cell currents to application of Glutamate + TCM normalized to whole cell capacitance (E); Percent desensitization is measured relative to glutamate + TCM peak (F); The time constant for recovery from desensitization is represented by the slow component of a two exponential fit of the TCM on-rate in the presence of glutamate (G) and Kainate efficacy as measured by normalizing the kainate current to Glutamate + TCM peak (H) are represented by bar graphs illustrating means ± SEM, n = 7-10. * indicates statistical difference within each constructs, # indicates statistical difference compared to GluR1 expressed alone, $ indicates significance as compared to GluR1γ2. (* P<0.05; ** P<0.01; ***P<0.001).

In contrast, stargazin was able to speed the recovery from desensitization to the levels of control GluR1 co-expressed with stargazin for the helix K mutations, indicating that it was able to fully rescue the desensitization deficits brought on by these mutations. Stargazin's effect on kainate efficacy, however, was decreased significantly, but not substantially, in all three constructs, (Figure 4.5 H).

Based on the results that stargazin was able to speed the recovery from desensitization in all three constructs, potentiate kainate efficacy and decrease steady-state desensitization in constructs in helix K, we suggest that residues in helices B and K do not directly associate with stargazin, but rather participate in the transduction of its effects on AMPA receptor function.

4.4 Summary of the results

In our attempt to identify areas of the AMPA receptor that associate with stargazin, we identified residues and helices on the exposed faces of the ligand-binding domain crystal that might participate in physical association with stargazin and/or transduce its effects on AMPA receptor function:

- The profound nature of stargazin deficits introduced by mutation of residues downstream of Helix H indicates that this area is a candidate association site for AMPA receptor pore-forming subunit with auxiliary subunit stargazin.
- Mutations of polar residues K434T, K757M and D765G in helices B and K on the lateral dimer interface/the lateral face of the receptor result in constructs with slowed rate of recovery from desensitization.

- Partial loss of effects of stargazin on mutant constructs in helices B and K suggest these residues participate in the transduction of stargazin's effects on AMPA receptor function.
- Changing the conformation of the loop downstream of helix G affects the association with stargazin, possibly by rearrangement of residues downstream of helix H.
- Introducing GluR6 spacing downstream of helix H slows the rate of recovery from desensitization.

CHAPTER V

AREAS OUTSIDE OF THE LIGAND-BINDING DOMAIN ARE IMPORTANT FOR RECOVERY FROM DESENSITIZATION AND STARGAZIN'S FUNCTIONAL EFFECTS ON THE AMPA RECEPTOR

5.1 Introduction

Chapter IV describes a set of experiments that focused on the identification of the regions in the AMPA receptor ligand-binding domain (available in crystal structure) that may play a role in association with TARPs. Results of these experiments identified an area of the AMPA receptor downstream of helix H, located on the lowermost portion of the outer face of the crystal that could possibly interact with the stargazin molecule. In addition, previous work suggested that there may also be an intracellular association (Tomita et al., 2005a; Turetsky et al., 2005). Based on these data we suspect that there are additional association sites in the AMPA receptor that are located outside the crystallized portion of the receptor.

While the ligand-binding domain of the AMPA receptor has been crystallized, the crystal structure of the majority of the receptor remains unresolved. Receptors lacking the N-terminal domain (in GluR1 amino acids 1-401) when co-expressed with stargazin, show a complete reduction in steady-state desensitization, an increase in kainate efficacy and an increase in receptor trafficking, indicating that this domain is not necessary for association with stargazin (Turetsky et al., 2005). The N-terminal domain is known to play a role in preferential AMPA receptor assembly (Ayalon and Stern-Bach, 2001), but

its other functions remain unknown. The conformation of the linker regions connecting the ligand-binding domain with the ion pore is also unknown. Interestingly, the M3 linker shares the most conservation between all AMPA and kainate receptors, while the M1 linker and the M4 linker are conserved among AMPA receptors but differ in kainate receptors. Two previously described mutations in the AMPA receptor M3 linker, A636T (*lurcher*) and R624E, significantly decrease AMPA receptor desensitization (Taverna et al., 2000; Klein and Howe, 2004; Yelshansky et al., 2004; Schmid et al., 2007). The GluR1 *lurcher* mutation increases the affinity of the receptor for glutamate and decreases steady-state desensitization (Klein and Howe, 2004), while in the R624E mutant construct the onset of desensitization is slowed (from 3.2 ± 0.2 msec in GluR1 to 5.8 ± 0.3 msec in R624E) without any effect on the rate of recovery from desensitization (Yelshansky et al., 2004).

The AMPA receptor C-terminal cytoplasmic tail plays an important role in receptor trafficking and its possible interactions with stargazin are the focus of work of several other labs (Chen et al., 2003; Tomita et al., 2004). In contrast, the intracellular loops of the AMPA receptor have received little attention in the research literature and both their conformation and their role in AMPA receptor channel physiology and function remain unknown. Interestingly, the second intracellular loop is conserved between AMPA receptors and kainate receptors, with only three conservative substitutions, while the first intracellular loop differs greatly even between AMPA receptors.

Previous research indicates that the majority of the function of stargazin on AMPA receptor desensitization and kainate efficacy is concentrated on the extracellular side of the molecule, while the majority of trafficking function is located intracellularly (Tomita

et al., 2005a; Turetsky et al., 2005). Recently, stargazin's intracellular N-terminus, intracellular loop and C-terminus were implicated in AMPA receptor trafficking and gating (Milstein and Nicoll, 2009). Our results with truncations of the C-terminal cytoplasmic tail of stargazin suggest that losing the intracellular association not only diminishes receptor trafficking, but also reduces stargazin's effect on AMPA receptor desensitization and kainate efficacy (See Figure 1.12). Overall these results suggest that multiple associations between the AMPA receptor and stargazin might exist on both intracellular and extracellular portions. Based on our observation with Ex(26-103) (Turetsky et al., 2005), we would predict that mutations on the AMPA receptor that break an extracellular association site would have profound loss of effect on receptor desensitization and kainate efficacy and mild to moderate loss of effect on trafficking (for details see Figure 1.10). Similarly, based on our observations deleting most of stargazin's C-terminal cytoplasmic tail (delta212), we would predict that mutations on the AMPA receptor that break an intracellular association site would have more severe trafficking deficits and only moderate loss of effects on receptor desensitization and kainate efficacy. However, there are probably areas of the AMPA receptor outside the ligand-binding domain that do not directly associate with stargazin, but instead transduce its effects. These areas, when mutated, may also present with decreased effects of stargazin on either kainate efficacy or desensitization.

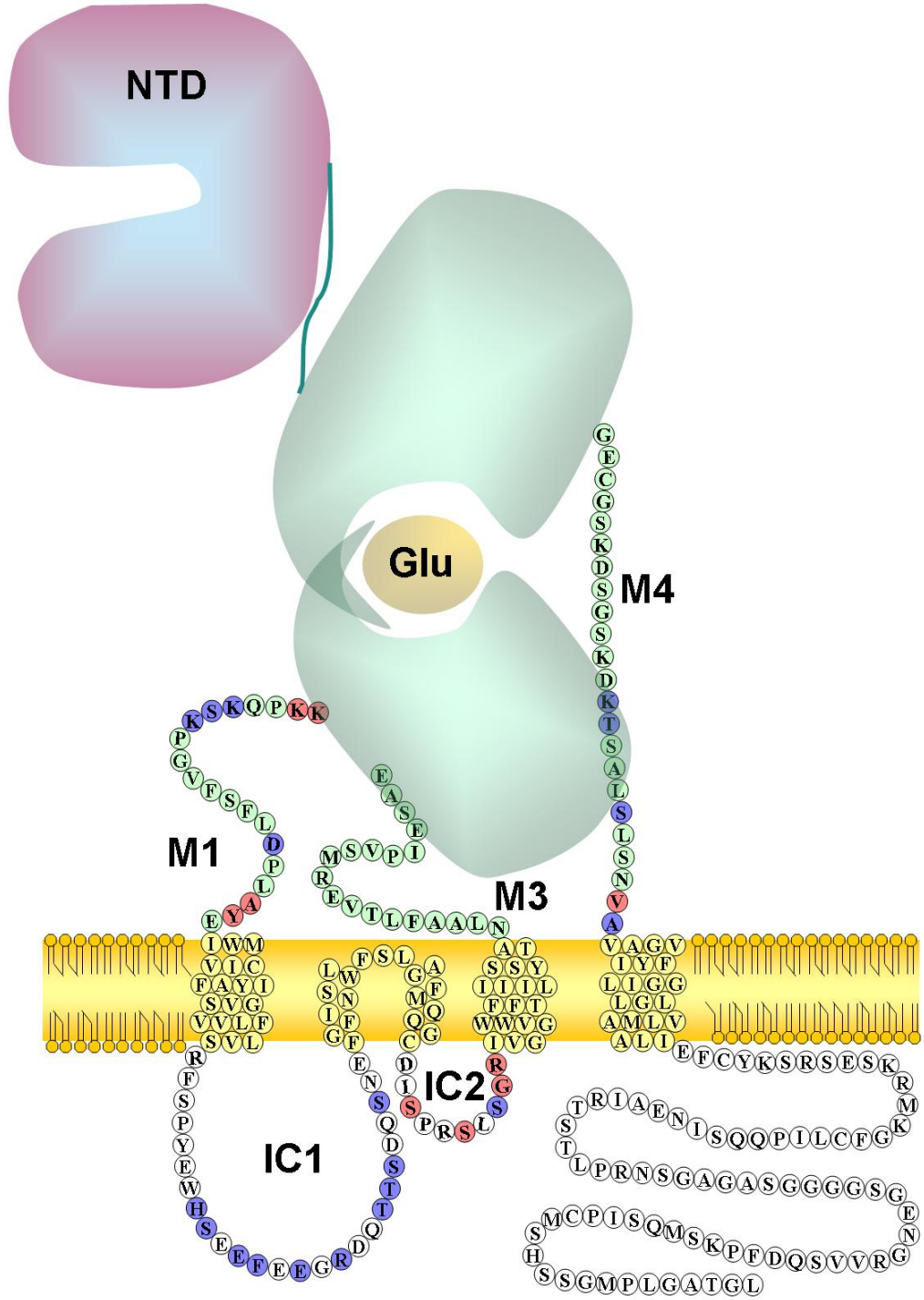

Figure 5.1: GluR1 schematic illustrating residues that were mutated and examined for desensitization changes. GluR1 subunit showing the ligand-binding domain, M1, M3, M4 linkers, intracellular loops 1 and 2, C-terminal cytoplasmic tail and transmembrane regions. Dark blue circles indicate mutations that had no effect on desensitization, and red circles indicate mutations that affect GluR1 desensitization.

Interestingly, even though the desensitized state is the most stable in the presence of agonist in the endogenous receptor, this state is the hardest to crystallize, suggesting that regions absent from the crystal structure (linker regions, transmembrane segments or the intracellular loops) are important in stabilizing the desensitized state (Mayer, 2005; Armstrong et al., 2006). It is, therefore, not surprising that in our attempt to locate regions of association between the AMPA receptor and stargazin in linker regions M1 and M4 as well as intracellular loops 1 and 2, we identified residues that play a role in recovery from desensitization. The summary of all mutations is illustrated in Figure 5.1 and presented in Table 5.1.

5.2 Statement of purpose

The purpose of the study was to identify residues in the non-crystallized portion of the AMPA receptor that are important for association with stargazin.

5.3 Results and Discussion

Mutations listed in Table 5.1 and illustrated in Figure 5.1 were made on the GluR1 background. Residues selected for mutagenesis were conserved among AMPA receptors but not in kainate receptors. A number of mutations had no distinguishable desensitization phenotype with or without stargazin (mutations not highlighted in Table 5.1) and they are not discussed in the data presentation below.

Table 5.1: Mutations outside of the AMPA receptor ligand-binding domain

Construct	Location	N	% Desensitization		τ recovery		Kainate efficacy	
			alone	+ γ2	alone	+ γ2	alone	+ γ2
K501A/K502A	S1-M1	12	99.84	99.19$	2449.3###	1250.9***$$$	0.0011	0.359 ***$$$
K505G/S506T/K507N	S1-M1	12	99.03	95.61**	1671.6	1091.2***	0.0032	0.596***
D515N	S1-M1	12	99.55	96.77**	2297.2	993.7***	0.0046	0.558***
A518S/Y519P@	S1-M1	17	97.43##	77.63***$$$	1363.6	453.5***	0.0141#	0.691***
S549N	IC loop 1	4	99.31	90.71**	2539.1	967.1***	0.0026	0.599 ***
F552P	IC loop 1	6	99.28	96.82**	2584.7	599.8***	0.0045	0.539***
E554N	IC loop 1	6	99.71	94.29**	3077.3	576.6***	0.0034	0.582***
T559V	IC loop 1	6	99.36	92.65***	1934.2	432.1***	0.0024	0.777***
T560V	IC loop 1	5	99.11	92.07***	2060.7	459.9***	0.0040	0.567***
S561A	IC loop 1	11	99.45	96.81*	1699.4	839.6***	0.0025	0.534***
S564A	IC loop 1	10	99.54	97.02*	2007.1	819.9***	0.0056	0.501***
S588M	IC loop 2	13	99.65	97.27**$$$	3027.8###	883.9***	0.0036	0.359**$$
S591A	IC loop 2	12	99.53	97.39*$$$	1874.2##	869.6***	0.0044	0.434***$
S593A	IC loop 2	5	99.01	94.21***	1876.5	498.7***	0.0044	0.556***
G594T	IC loop 2	13	99.73	98.58**$$$	2806.8###	1035.9***	0.0037	0.587***
R595A	IC loop 2	Construct was non-functional						
K779A/D780A	S2-M4	8	98.18#	92.55***	1543.9	624.6***	0.0141	0.675***
S784G/A789G@	S2-M4	8	99.69	98.82*$	1615.1	1286.5$$$	0.0074	0.311***$$$
V788I@	S2-M4	16	98.51	85.97***$$	1478.2	522.9***	0.0200##	0.626***
GluR1		**38**	**99.31**	**93.93*****	**1746.9**	**569.5*****	**0.0040**	**0.572*****

@ Mutations originally reported in Balannik et al. (2005) as potential binding sites for negative allosteric modulators
# indicates statistical significance compared to GluR1 alone, * indicates statistical difference within each construct, $ indicates statistical significance compared to GluR1 co-expressed with stargazin (* P<0.05; ** P<0.01; ***P<0.001).

5.3.1 Mutation of residues in the M1 and M4 linker regions create constructs with altered desensitization profiles

Of the seven mutations in linker regions M1 and M4, three were previously identified by Balannik et al., (2005) as possible sites of 2,3-benzodiazepine binding (A518S/Y519P, S784G/A789G and V788I). These mutations met the criteria of conservation between AMPA receptors and were used for the experiments presented below. Our previous examination of the lower portion of the AMPA receptor crystal structure revealed two lysine residues (K501 and K502) at the very beginning of the M1 linker. Although the crystal structure in this area was distorted due to introduction of the artificial sequence connecting linkers M1 and M3, these residues appeared exposed and able to interact with other proteins. Therefore, we mutated them to alanines for the purpose of these experiments.

All the linker constructs trafficked well (Table 5.1 and Figure 5.2 I). Three mutant constructs had obvious alterations in their desensitization phenotypes: K501A/K502A, A518S/Y519P and V788I. Mutant constructs A518S/Y519P in M1 linker and V788I in M4 linker had a larger steady-state and a significantly decreased percent desensitization, indicating that these mutations in regions immediately adjacent to the membrane had similar phenotypes (Figure 5.2 G and J). Interestingly, the kinetics of desensitization (onset and recovery) in these two mutant constructs was not affected, suggesting that the increased steady-state of these constructs reflects a change in channel gating or conductance rather than desensitization (Figure 5.2 K, and data not shown). In support of this interpretation, these two mutations also significantly increased kainate efficacy, which is affected by channel conductance (Figure 5.2 L).

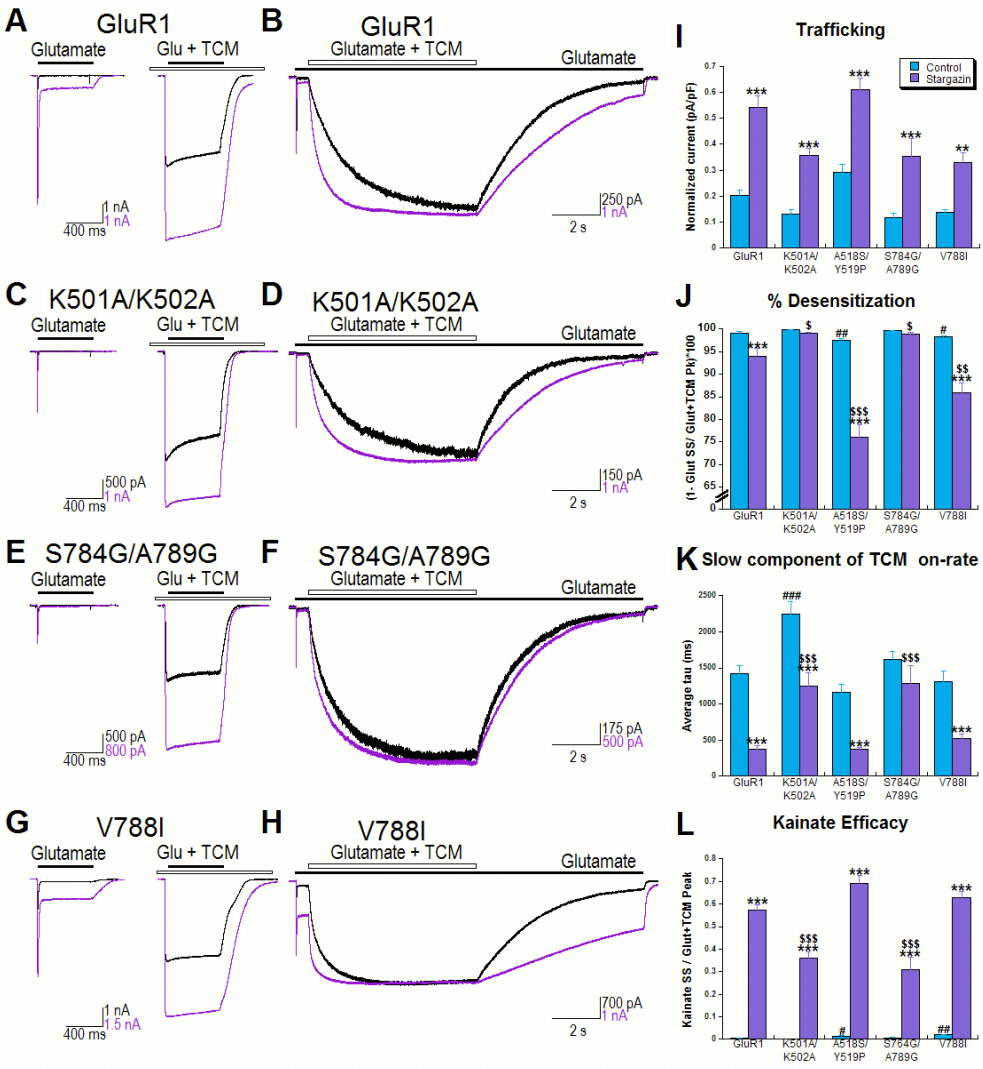

Figure 5.2: Mutations in the M1 and M4 linker regions affect AMPA receptor desensitization. Representative traces for constructs alone (black) and co-expressed with stargazin (lavender) in response to glutamate in the presence and absence of TCM for GluR1 (A), K501A/K502A (C), S784G/A789G (E) and V788I (G). Traces to a 3 step protocol demonstrate recovery from desensitization of GluR1 (B), K501A/K502A (D), S784G/A789G (F) and V788I (H) expressed alone (black) or with stargazin (lavender). Summary of the results of trafficking as measured by whole cell currents to application of Glutamate + TCM normalized to whole cell capacitance (I); Percent desensitization is measured relative to glutamate + TCM peak (J); The time constant of recovery from the desensitization is represented by the slow component of a two exponential fit of the TCM on-rate in the presence of glutamate (K) and Kainate efficacy as measured by normalizing the kainate current to Glutamate + TCM peak (L) are represented by bar graphs illustrating means ± SEM, n = 8-38. * indicates statistical difference within each constructs, # indicates statistical difference compared to GluR1 expressed alone, $ indicates significance as compared to GluR1γ2. (* P<0.05; ** P<0.01; ***P<0.001).

Mutation K501A/K502A had a slightly higher percent desensitization than control, but the result was not significantly different (Figure 5.2 C and J). However, the rate of recovery from desensitization in this construct was significantly slowed compared to control GluR1 (Figure 5.2 D and K). Interestingly, this mutation looked similar to that we have previously observed on helix B (see chapter IV for details), where the main effect of the mutation was on the rate of recovery from desensitization and co-expression with stargazin had reduced effects on stead-state desensitization and kainate efficacy (see below).

5.3.2 Stargazin's effect on constructs carrying mutations in M1 and M4 linkers differs depending on the construct.

To identify the role that stargazin plays in AMPA receptor desensitization, all the constructs described in Table 5.1 were co-expressed with stargazin. Stargazin was able to potentiate trafficking of all four constructs, indicating that the association responsible for trafficking is maintained (Figure 5.2 I). In mutations that decrease the amount of desensitization, (e.g., A518S/Y519P and V788I), stargazin was able to further decrease % desensitization (Figure 5.2 G and J), as well as speed recovery from desensitization (Figure 5.2 G and K), and increase kainate efficacy (Figure 5.2 L). Stargazin's effects on desensitization were at least additive, and maybe synergistic, with these mutations that decreased steady-state desensitization, indicating that they did not affect the ability of stargazin to associate with the AMPA receptor.

Mutations K501A/K502A and S784G/A789G had a surprising result. Stargazin was unable to increase glutamate steady-state current in these constructs (Figure 5.2 C, E and J).

Although stargazin did significantly speed the rate of recovery from desensitization in K501A/K502A, it was not equivalent to the level of GluR1 co-expressed with stargazin. However, stargazin was unable to speed the rate of recovery from desensitization in S784G/A789G mutant construct (Figure 5.2 D, F and K). Co-expression with stargazin in both K501A/K502A and S784G/A789G also resulted in significantly reduced kainate efficacy when compared to GluR1 co-expressed with stargazin (Figure 5.2 L). Overall these results indicate that stargazin was unable to elicit its full effect on mutant constructs K501A/K502A and S784G/A789G, while having no problems doing so for A518S/Y519P and V788I. Because mutant construct S784G/A789G had the most profound phenotype when co-expressed with stargazin, where stargazin had no effect on % desensitization or rate of recovery from desensitization, and a diminished effect on kainate efficacy, we suggest that these residues are candidates for an association point with stargazin. The K501A/K502A mutant construct, when co-expressed with stargazin, had a less profound phenotype suggesting that these residues are most likely participating in transduction of stargazin's effects on the AMPA receptor.

5.3.3 Constructs carrying mutations in intracellular loop 2 of the AMPA receptor exhibit a phenotype with slowed recovery from desensitization.

Previous results from our laboratory indicated that the C-terminal cytoplasmic tail of stargazin was partially responsible for AMPA receptor trafficking, desensitization and kainate efficacy (Turetsky et al., 2005), while more recent research indicates that stargazin's intracellular loop and N-terminus also play a role in AMPA receptor function (Milstein and Nicoll, 2009). In our attempt to identify intracellular regions of the AMPA receptor important for stargazin association, we mutated residues that were conserved

among AMPA receptors, but not kainate receptors, in the first and second intracellular loops of GluR1. Multiple mutations made in the first extracellular loop of the AMPA receptor yielded no significant findings (see table 5.1 for details). In contrast, mutations in the 2nd intracellular loop had clear desensitization phenotypes. Three of the mutations in the 2nd intracellular loop: S588M, S591A and G594T trafficked significantly less than control GluR1 (Figure 5.3 I). All constructs exhibited normal % desensitization (Figure 5.3 J) and rate of desensitization onset (data not shown). However, the rates of recovery from desensitization in these mutants were significantly increased (Figure 5.3 D, F, H and K), indicating that mutations of AMPA residues to kainate residues in the 2nd intracellular loop promote a kainate-like desensitization phenotype (i.e., slower recovery from desensitization). Interestingly, mutation of residue R595 to either alanine or serine (the naturally occurring mutation in GluR3 that leads to mental retardation (Wu et al., 2007)) resulted in a construct that was not functional, indicating that this residue is crucial for AMPA receptor channel function. Although G594T was functional when expressed homomerically, mutations of G594 to phenylalanine or lysine also resulted in non-functional receptors. Of all the mutations that we prepared for this dissertation only a single other mutation (cysteine at position 760) resulted in a non-functional receptor. The rarity of this occurrence suggests to us that the effects of G594T on AMPA receptor function are at least partially due to its proximity to R595.

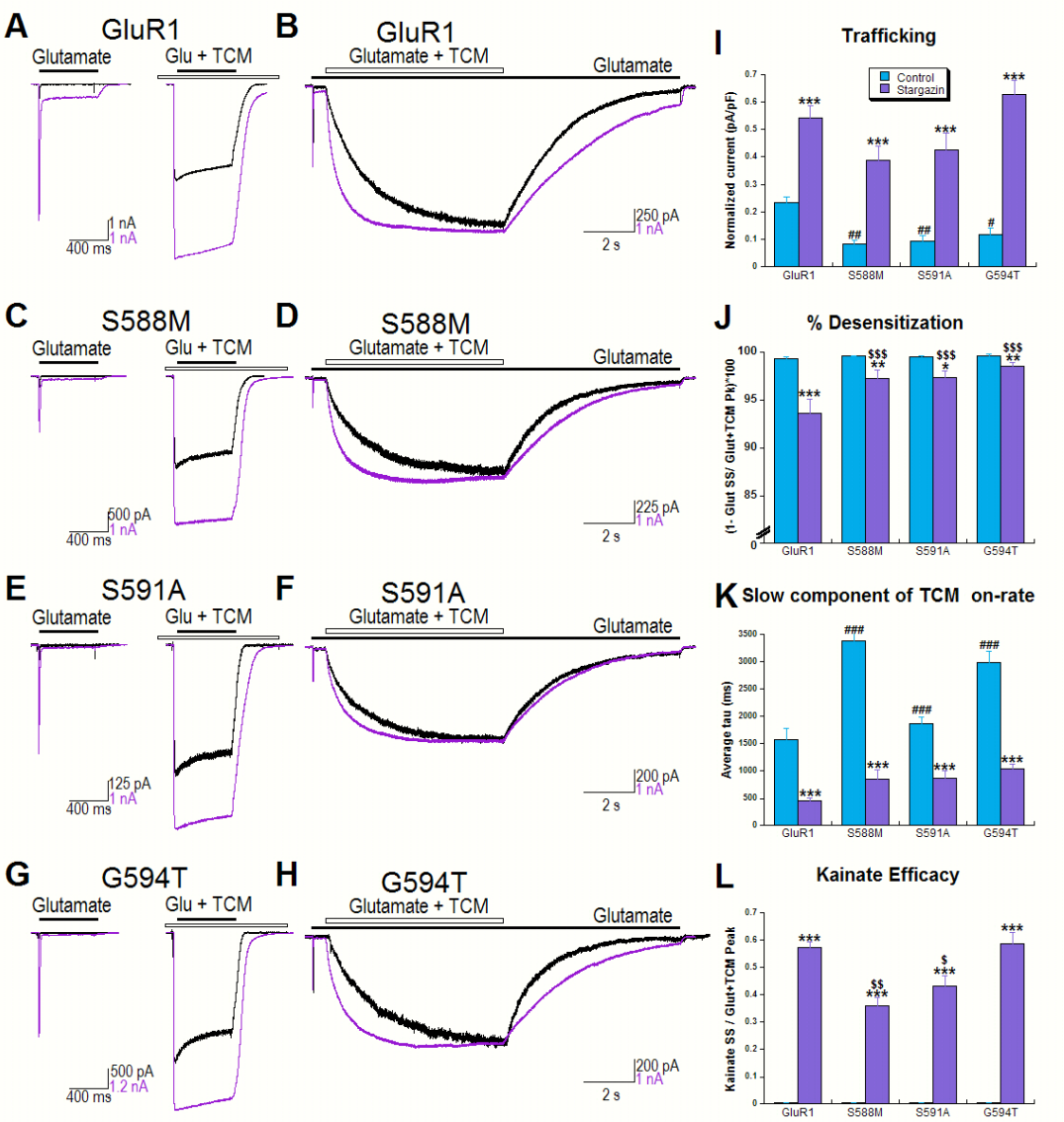

Figure 5.3: Mutations in the 2nd intracellular loop affect AMPA receptor desensitization. Representative traces for constructs alone (black) and co-expressed with stargazin (lavender) in response to glutamate in the presence and absence of TCM for GluR1 (A), S588M (C), S591A (E) and G594T (G). Traces to a 3 step protocol demonstrate recovery from desensitization of GluR1 (B), S588M (D), S591A (F) and G594T (H) expressed alone (black) or with stargazin (lavender). Summary of the results of trafficking as measured by whole cell currents to application of Glutamate + TCM normalized to whole cell capacitance (I); Percent desensitization is measured relative to glutamate + TCM peak (J); The time constant of recovery from desensitization is represented by the slow component of a two exponential fit of the TCM on-rate in the presence of glutamate (K) and Kainate efficacy as measured by normalizing the kainate current to Glutamate + TCM peak (L) are represented by bar graphs illustrating means ± SEM, n = 12-38. * indicates statistical difference within each constructs, # indicates statistical difference compared to GluR1 expressed alone, $ indicates significance as compared to GluR1γ2. (* P<0.05; ** P<0.01; ***P<0.001).

5.3.4 Mutations in the 2nd intracellular loop of GluR1 reduce stargazin's effect on AMPA receptor desensitization and kainate efficacy.

In order to elucidate areas of the AMPA receptor important for association with stargazin, we co-expressed constructs carrying mutations in the intracellular loop 2 with stargazin. Stargazin was able to significantly potentiate trafficking of all mutant constructs, indicating that the association that is important for trafficking is preserved (Figure 5.3 I). Although stargazin was able to increase the steady-state current and thus decrease the % desensitization in all constructs carrying mutations in intracellular loop 2, it was significantly less efficacious at doing so as compared to control GluR1 (Figure 5.3 C, E, G and J). However, stargazin was able to elicit its full effect on the rate of recovery from desensitization in these mutants (Figure 5.3 D, F, H and K). Kainate efficacy was significantly increased by co-expression with stargazin in all three constructs; however, the degree to which differed between mutant constructs (Figure 5.3 L). Interestingly, both S588M and S591A co-expressed with stargazin had significantly reduced kainate efficacy compared to control stargazin, indicating that stargazin was unable to elicit its full effect on kainate efficacy in these mutants. Because of the partial loss of effect on % desensitization and kainate efficacy, with preserved trafficking and speeding of recovery from desensitization, we propose S588 and S591 as candidate sites of interaction with the intracellular portions of stargazin responsible for modulation of receptor gating (Milstein and Nicoll, 2009).

5.4 Summary of results

In our quest to find areas of the AMPA receptor that participate in association with stargazin we have uncovered some unexpected results:

- Residues S784 and A789 located in the M4 linker of GluR1 are candidates for association with stargazin.
- Residues S588 and S591 located in the 2nd intracellular loop of GluR1 may also play a role in associating with the intracellular portions of stargazin.
- Mutation of residues K501/K502 in the M1 linker and S588, S591 in the 2nd intracellular loop of the AMPA receptor result in constructs with a slowed rate of recovery from desensitization.
- Mutations immediately adjacent to the membrane in linkers M1 or M4 (A518S/Y519P and V788I) produced AMPA receptors with decreased steady-state desensitization, but normal onset and recovery kinetics, suggesting these residues are important for receptor gating. Stargazin was able to exert its full effect on these mutant AMPA receptors.
- Partial loss of effects of stargazin on desensitization and kainate efficacy in the K501A/K502A mutation, located in the M1 linker, suggest these residues participate in the transduction of stargazin's effects on the AMPA receptor.
- The association between the AMPA receptor and stargazin responsible for trafficking was preserved in all of the mutant constructs described.

CHAPTER VI

IDENTIFICATION OF RESIDUES IN STARGAZIN THAT MEDIATE EFFECTS ON AMPA RECEPTOR DESENSITIZATION AND KAINATE EFFICACY

6.1 Introduction

TARPs have been shown to have multiple effects on AMPA receptor trafficking and function. Originally, TARPS were implicated in increasing AMPA receptor trafficking and targeting AMPA receptors to the synapse (Chen et al., 2000). Subsequently, TARPS were shown to affect the biophysical properties of the AMPA receptor, reducing agonist-evoked receptor desensitization, slowing receptor deactivation, potentiating kainate responses and increasing relative frequency of large conductance openings (Priel et al., 2005; Tomita et al., 2005b; Turetsky et al., 2005; Zhang et al., 2006). Stargazin also increases the binding rate for positive allosteric modulators in the presence of agonist. Because these modulators only bind to AMPA receptors in the non-desensitized state, this suggests that TARPs speed AMPA receptor recovery from desensitization.

Original chimeric exchanges between γ2 and γ5 identified the first extracellular domain of stargazin as important for stargazin's effect on AMPA receptor desensitization and kainate efficacy and the C-terminal cytoplasmic tail important for receptor trafficking (Tomita et al., 2005b). Work from our laboratory suggested that this dissociation of stargazin effects is not complete and that the extracellular loop 1 of stargazin also has a role in trafficking of the AMPA receptor, while the C-terminal cytoplasmic tail has a role in kainate efficacy and desensitization (Turetsky et al., 2005). Although major domains

of stargazin that mediate AMPA receptor trafficking and function have been recognized, the mechanism of stargazin's action, as well as specific residues that mediate this mechanism and specific points of association between stargazin and the AMPA receptor, remains unknown.

Based on previous experiments from our laboratory (Figure 1.11 and 6.1), we utilized chimeric exchanges in the first extracellular domain between the canonical TARP γ2 and γ5, which was originally thought to have no function in AMPA receptors (Figure 6.1 A). The largest exchange between stargazin and γ5, Ex (26-103), which exchanged almost all of the first extracellular loop, generated a chimeric protein that lost most of its ability to potentiate kainate efficacy and decrease AMPA receptor desensitization, while also having significantly decreased trafficking (Figure 6.1 B, C and D). Exchange of the distal portion of the extracellular loop Ex (89-103) produced a protein that was not significantly different from stargazin in its effects on AMPA receptor desensitization and kainate efficacy (Figure 6.1 C and D), while chimeric exchange Ex (61-103) (data not shown) resulted in a protein that lost its ability to elicit its effects on AMPA receptor desensitization, kainate efficacy and trafficking. Therefore we assumed that this construct was not functional.

Upon close inspection of the protein sequence of all TARPs we noted that Class I TARPs (γ2, γ3, γ4 and γ8) had a total of four cysteines in the first extracellular loop in positions 40, 67, 68 and 77, while the members of Class II TARPs (γ5 and γ7) had only two cysteines in positions 67 and 77. Interestingly, two cysteines in positions 67 and 77 were conserved even among non-TARPs γ1 and γ6 (for details see figure 6.2). Based on these observations we hypothesized that the first extracellular loop of stargazin might

undergo disulfide bonding and that the correct number of cysteines was crucial for proper protein structure. The non-functional Ex (61-103) had three cysteines in the first extracellular loop, with phenylalanine at position 68. Mutating F68 to a cysteine restored the TARP pattern of four cysteines and created a functional construct. The new construct Ex (61-103)/F68C had normal trafficking and desensitization but kainate efficacy was reduced approximately 60% relative to stargazin (Figure 6.1).

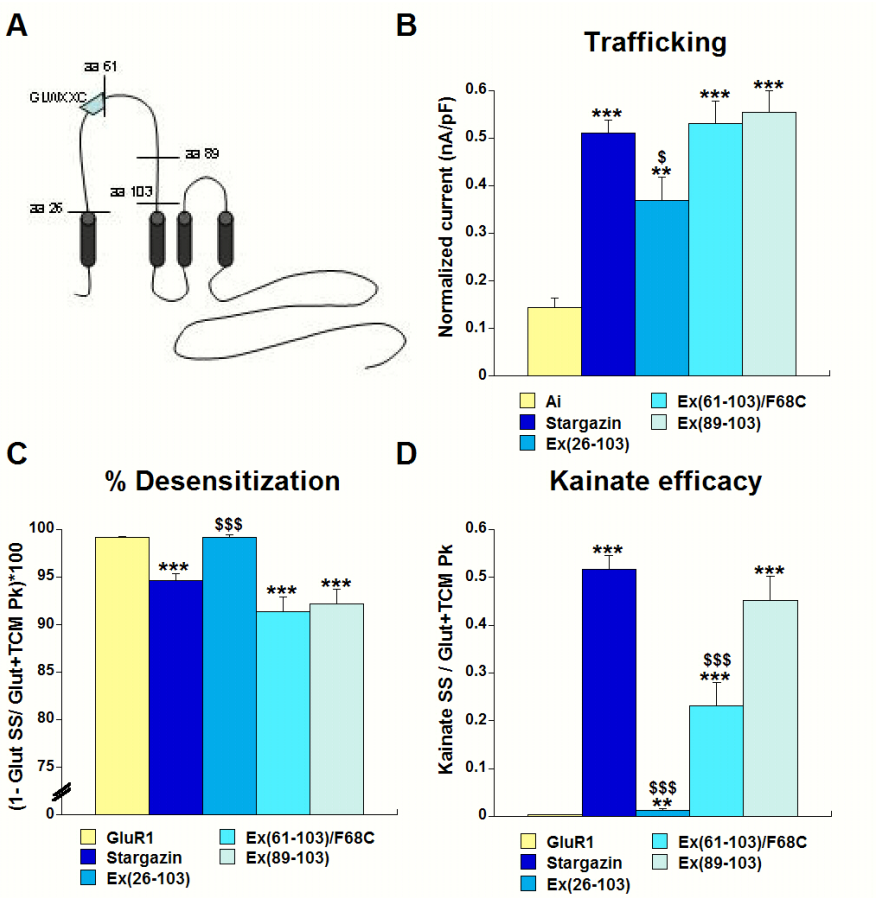

Figure 6.1: Chimeric exchanges between γ2 and γ5 identify areas of the first extracellular loop important for stargazin's effects on desensitization and kainate efficacy. Stargazin schematic, delineating residues bordering chimeric exchanges (A), Summary of the results of trafficking as measured by whole cell currents to application of Glutamate + TCM normalized to whole cell capacitance (B); Percent desensitization is measured relative to glutamate + TCM peak (C); and Kainate efficacy as measured by normalizing the kainate current to Glutamate + TCM peak (D) are represented by bar graphs illustrating means ± SEM, n = 12-18. * indicates statistical difference within each constructs, # indicates statistical difference compared to GluR1 expressed alone, $ indicates significance as compared to GluR1γ2. (** P<0.01; ***P<0.001).

Because the construct was functional after the introduction of the 4th cysteine, it suggested to us that disulfide bonding might play a role in the function of stargazin (Figure 6.1 B and C). These results further suggested that residues important for kainate efficacy are located between amino acids 26 and 89, while residues important for modulation of AMPA receptor desensitization are located between residues 26 and 61. To further address the functional effect of the extracellular portion of the protein, we turned to site-directed mutagenesis as a tool for identification of amino acids important for stargazin's effect on AMPA receptor function. Our lab is especially interested in the association sites between stargazin and AMPA receptors, therefore we initially focused on polar residues.

The loss of association on the extracellular portion of stargazin would most likely present with a phenotype similar to Ex(26-103): almost complete loss of stargazin's effect on desensitization and kainate efficacy with a small decrease in trafficking. It is also possible that some of the residues that we select for site-directed mutagenesis would affect conformational changes in stargazin, in which case only a partial loss of the functional effects of stargazin would be observed.

To select residues for site-directed mutagenesis we used homology between subunits in the γ (CACNG) family, which currently has 8 members. Initially it was thought that γ2 and γ3 were more important in their function on AMPA receptors, therefore we concentrated on residues that were conserved in γ2 and γ3, but different in γ5 (indicated in yellow in Figure 6.2). As the TARP field evolved, it became clear that both γ4 and γ8 also played important roles in AMPA receptor physiology, therefore γ4 and γ8 joined γ2 and γ3 to form class I TARPs.

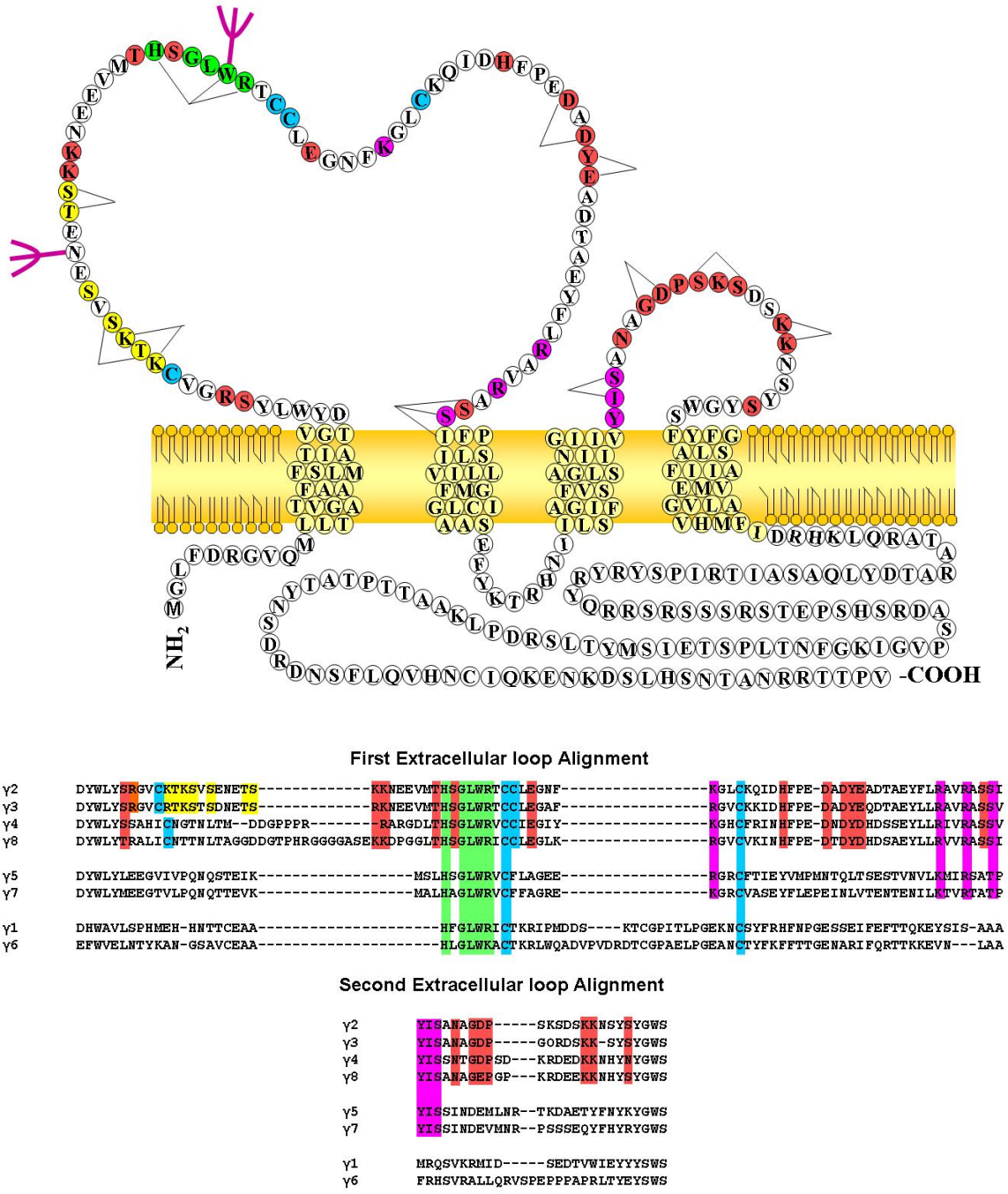

Figure 6.2: Stargazin schematic (top) and sequence alignment (bottom) indicating residues of interest in the extracellular domains of stargazin.

- polar residues conserved exclusively throughout class I TARPs.
- polar residues conserved only in γ2 and γ3.
- cysteines that may play a role in disulfide linkages.
- residues conserved in both classes of TARPs as well as γ1 and γ6.
- polar residues conserved in both classes of TARPs but not γ1 and γ6.

Thus, we selected residues that were conserved in all class I TARPS, but differed in γ5 (indicated in red in Figure 6.2).

Most recently, the class II TARPs, γ5 and γ7, were demonstrated to have small but significant, functional effects on AMPA receptors (Kato et al., 2007; Soto et al., 2007; Kato et al., 2008; Soto et al., 2009). This discovery led us to our final set of residues that were conserved in all TARPs but differed in voltage-gated calcium channel subunits γ1 and γ6 (illustrated in magenta in Figure 6.2). As discussed above, we knew that cysteines (indicated in blue on Figure 6.2) appear to be crucial for the function of stargazin; therefore we selected all 4 cysteine residues for site-directed mutagenesis (illustrated in blue in figure 6.2).

The role of glycosylation in AMPA receptors is controversial, where some reports indicate the importance of glycosylation in agonist binding (Kawamoto et al., 1995), while others indicate that AMPA receptors can function in the absence of glycosylation (Everts et al., 1997). Stargazin has consensus sites for N-linked glycosylation (NETS) (TS residues of the NETS motif are illustrated in yellow in Figure 6.2) and C-linked mannosylation (GLWRTC) (GLWR residues of the motif are illustrated in green in Figure 6.2). Although, the role of glycosylation in TARPs is unknown, deletion of N-linked glycosylation in γ1 does not alter its function (Arikkath et al., 2003), while deletion of C-mannosylation in MP-20 (a transmembrane protein distally related to TARPs) results in a construct that is unable to interact with other proteins (Ervin et al., 2005). Therefore we also selected these motifs for site-directed mutagenesis.

For completion, we selected residues in stargazin's extracellular loop 2 that were both conserved within class I TARPs and both classes of TARPs but not in γ1 and γ6.

Interestingly, earlier studies that examined the role of extracellular loop 2 in AMPA receptor function and concluded that it was not important also utilized chimeric exchanges between γ1 and γ5 (Tomita et al., 2005a). Recent insights into the role of γ5 on the function of AMPA receptor directed us to re-evaluate the role of second extracellular loop of stargazin.

6.2 Statement of purpose

We mutated a number of residues in the first and second extracellular loops of stargazin in order to identify amino acids that play a role in stargazin's effect on AMPA receptor desensitization and kainate efficacy.

6.3 Results and Discussion

Table 6.1 summarizes the constructs made and their effects on AMPA receptor trafficking, desensitization and kainate efficacy. Several of the constructs did not have a phenotype that was different from stargazin and thus will not be discussed in the data presentation below. One of the double mutations, Y89L/E90T, introduced a slight gain of function on AMPA receptor desensitization (Table 6.1), while 3 other mutations (T59A, E70A and D86N/D88Q) had significant, but modest effects on AMPA receptor desensitization and kainate efficacy (Table 6.1). Such changes are unlikely to be physiologically relevant and are not discussed in the data presentation below.

Table 6.1: Residues in stargazin that affect its desensitization and kainate effects on AMPA receptor

Mutation	N	% Desensitization	Kainate Efficacy	Trafficking
Control				
GluR1	61	**99.25**	**0.003**	**0.144**
GluR1 + stargazin	72	**94.27 *****	**0.536 *****	**0.509 *****
1st EC loop Cysteines				
C40I	12	94.72 ***	**0.453 $$ *****	0.615 ***
C67A	12	**99.61 $$**	**0.003 $$$**	**0.190 $$**
C68F	15	91.59 ***	0.557 ***	0.375 ***
C77A	12	**98.98 $$**	**0.0202 $$$**	0.423 ***
1st EC loop GLWXXC				
W64A	22	96.72 **	**0.339 $$$ *****	0.526 ***
H60F/W64A/R65L	16	**99.26 $$**	**0.007 $$$**	**0.246 $$**
1st EC loop NETS				
T50A/S51A	9	**83.51 $$ *****	**0.643 $$ *****	0.670 ***
1st EC loop residues				
S36A	17	95.68 ***	**0.269 $$$ *****	0.421 *
R37A	12	93.94 ***	0.507 ***	0.466 **
K41A/K43A	7	93.22 ***	0.497 ***	0.612 ***
T42A/S44A	5	95.13 ***	0.545 ***	0.531 ***
S46A	10	97.99	**0.26 $$$ *****	0.401 ***
K52A/K53A	6	92.75 ***	0.511 ***	0.451 **
T59A	9	97.36	0.453 ***	0.511 **
E70A	6	95.65 ***	**0.429 $ *****	**0.850 $$$*****
K74A	6	93.61 ***	0.543 ***	0.617 ***
H82Y	8	91.56 ***	0.568 ***	0.456 **
D86N/D88Q	6	95.15 **	**0.435 $ *****	0.437 *
Y89L/E90T	7	**85.68 $$$ *****	0.578	0.530 **
R99A	6	98.15	**0.371 $ *****	0.498 **
R102A	6	93.62 ***	0.537 ***	0.537 ***
S104A/S105T/I106P	7	95.19 ***	**0.358 $$ *****	0.613 ***
S36A/S104A/S105T/I106P	14	**98.42 $$**	**0.116 $$$ ***	0.584 *
S36A/S46A	9	94.06 **	**0.38 $$ *****	0.748 ***
2nd EC loop residues				
Y155M	11	**97.56 $**	**0.352 $ *****	0.459 ***
I156R/S157Q	11	95.6 *	**0.388 $ *****	0.421 ***
N159V	12	96.75	0.444 ***	0.527 ***
P163M	6	95.83 ***	0.619 ***	0.586 ***
K165A	5	96.98 ***	0.607 ***	0.734 ***
S174A	6	94.92***	0.543 ***	0.791 ***

Table 6.1: Average Desensitization, Kainate Efficacy and Trafficking for the above mutations are given (n=12-70). Yellow highlighting indicates mutations that had loss of stargazin function; magenta highlighting indicates gain of stargazin function. Statistics were performed with One-Way ANOVA and Student-Newman-Keuls post-hoc test compared to experimentally matched controls. $ indicates statistical difference compared to GluR1 co-expressed with stargazin, * indicates statistical difference compared to GluR1 alone (* P<0.05; ** P<0.01; *** P< 0.001)

6.3.1 Mutation of the cysteines in the first extracellular loop of stargazin result in constructs that have trafficking, desensitization and kainate efficacy deficits.

Based on the preliminary results from our laboratory indicating that cysteines in the first extracellular loop of stargazin are important for the protein's ability to function, we mutated two of the cysteines that were conserved (C40 and C68) only in class I TARPs to their corresponding residue in γ5 (resulting in C40I and C68F). We also mutated two cysteines that were conserved thoughout both classes of TARPs, as well as γ1 and γ6, (C67 and C77) to alanines (resulting in C67A and C77A). These constructs were co-expressed with homomeric GluR1 for electrophysiological analysis, and evaluated on their ability to affect AMPA receptor trafficking, desensitization and kainate efficacy.

γ2 (C67A) was unable to potentiate trafficking, or affect AMPA receptor desensitization or kainate efficacy, suggesting that it was non-functional (Figure 6.3 G, H, I and J). Other stargazin constructs γ2 (C40I), γ2 (C68F) and γ2 (C77A) were able to significantly increase the trafficking of homomeric GluR1 as compared to GluR1 alone (Figure 6.3D). Functional effects of stargazin on AMPA receptor desensitization and kainate efficacy were significantly impaired by the C77A point mutation, resulting in a construct that did not significantly reduce glutamate desensitization or increase kainate efficacy relative to GluR1 control (Figure 6.3 H, I and J). Mutant constructs γ2 (C40I) and γ2 (C68F) were comparable to wild-type stargazin co-expressed with GluR1 in their effect on % desensitization (Figure 6.3I) although γ2 (C40I) was slightly impaired in its effect on kainate efficacy (Figure 6.3 H). Consistent with the lack of effects on % desensitization construct γ2 (C67A) and γ2 (C77A) had no significant effect on the rate of recovery from desensitization (Figure 6.3 J).

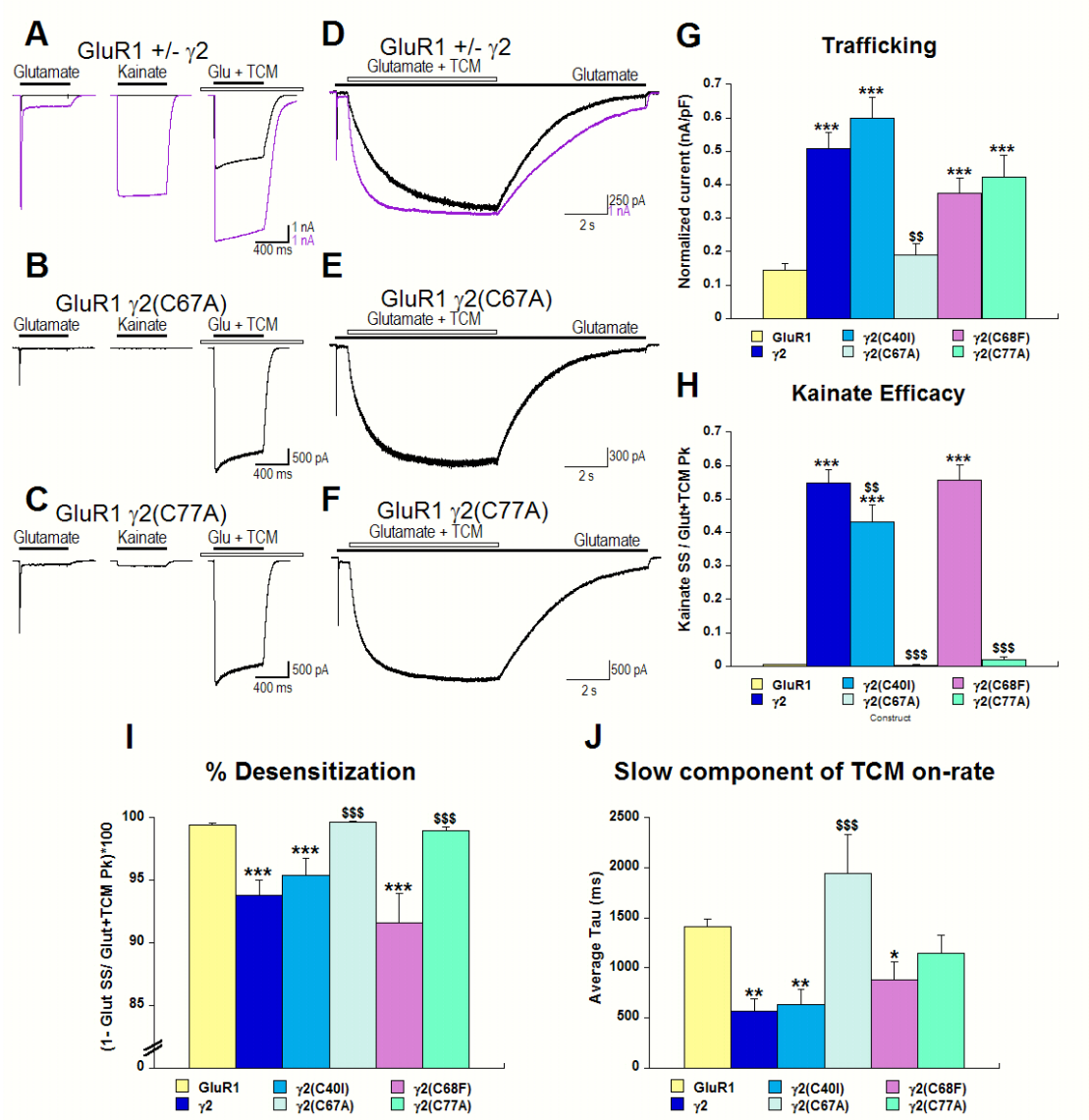

Figure 6.3: Mutation of cysteines in the first extracellular loop affect stargazin's function. Representative responses to glutamate in the presence and absence of TCM and kainate for GluR1 expressed alone (black) and co-expressed with stargazin (lavender) (A), GluR1 co-expressed with γ2 (C67A) (B) and GluR1 co-expressed with γ2 (C77A) (C). Representative responses to a 3 step protocol for GluR1 expressed alone (black) and with stargazin (lavender) (D), GluR1 co-expressed with γ2 (C67A) (E) and GluR1 co-expressed with γ2 (C77A) (F). Summary of the results of trafficking as measured by whole cell currents to application of Glutamate + TCM normalized to whole cell capacitance (G); Kainate efficacy as measured by normalizing the kainate current to Glutamate + TCM peak (H); Percent desensitization is measured relative to glutamate + TCM peak (I); The time constant of recovery from desensitization is represented by the slow component of a two exponential fit of the TCM on-rate in the presence of glutamate (J) are represented by bar graphs illustrating means ± SEM, n = 12-21. * indicates statistical difference compared to GluR1 alone, $ indicates significance compared to GluR1γ2. (* P<0.05; ** P<0.01; ***P<0.001).

Interestingly, γ2 (C77A), a single amino acid substitution, had almost as profound a phenotype as Ex(26-103), which exchanges the first extracellular loop. Because γ2 (C67A) also had a profound phenotype with complete loss of all function, while γ2 (C68F) and γ2 (C40I) phenotypes were almost indistinguishable from control γ2, we propose that disulfide bonding occurs between cysteine residues 67 and 77, thus maintaining the proper tertiary structure of the protein. Because C67 is a part of the mannosylation motif (see section 6.3.2) we cannot rule out that much of its phenotype is caused by the loss of the conserved motif for mannosylation.

6.3.2 Mutation of the consensus N-linked glycosylation motif enhances the effect of stargazin on desensitization and kainate efficacy.

TARPs are known to be glycosylated (Deng et al., 2006), but the location and type of glycosylation is unknown. A single consensus site for N-linked glycosylation exists in stargazin at residues 48-NETS-51. To elucidate the role of glycosylation on the function of stargazin we mutated residues T50 and S51 to alanines to alter this consensus site.

The resulting construct γ2 (T50A/S51A) had enhanced effects on AMPA receptor desensitization and kainate efficacy (Figure 6.4 D and E), while entirely preserving the trafficking function of stargazin (Figure 6.4 C). We are currently in the process of characterizing another mutant construct in the consensus site γ2 (N48Q). If the results of this mutation have a similar phenotype to γ2 (T50A/S51A), it would suggest that removing the consensus site for glycosylation allows for better association of stargazin with the AMPA receptor and/or increased function of stargazin. Loss of glycosylation in these constructs will have to be confirmed with protein biochemistry.

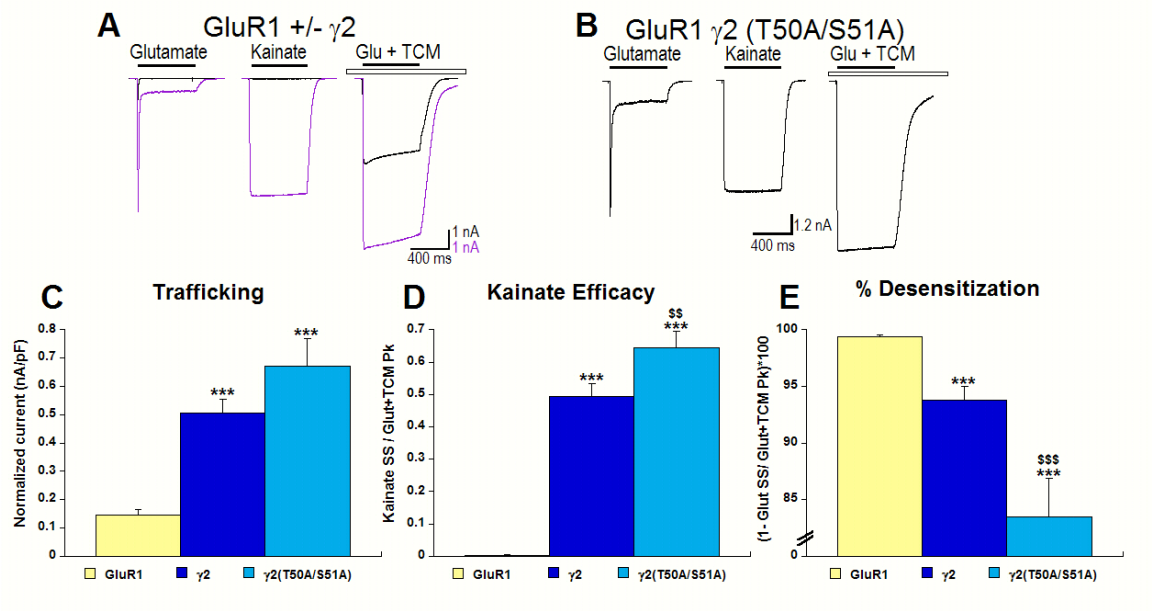

Figure 6.4: Mutation of residues in the conserved glycosylation motif NETS result in gain of function. Representative responses to glutamate +/- TCM and kainate for GluR1 expressed alone (black) and co-expressed with stargazin (lavender) (A) and GluR1 co-expressed with γ2 (T50A/S51A) (B). Summary of the results of trafficking as measured by whole cell currents to application of Glutamate + TCM normalized to whole cell capacitance (C); Kainate efficacy as measured by normalizing the kainate current to Glutamate + TCM peak (D); and Percent desensitization is measured relative to glutamate + TCM peak (E) are represented by bar graphs illustrating means ± SEM, n = 9-15. * indicates statistical difference compared to GluR1 alone, $ indicates significance compared to GluR1γ2. (* P<0.05; ** P<0.01; ***P<0.001).

6.3.3 Mutation of the conserved motif GLWXXC in the first extracellular loop of stargazin results in constructs with deficits in trafficking, desensitization and kainate efficacy.

All of the subunits in the CACNG family share a common motif GLWXXC (in γ2 residues 62-67). This motif is also present in claudins and the more distally related tetraspannins. These include the peripheral myelin protein 22 (PMP-22), mutations of which are implicated in inherited peripheral neuropathies and eye lens specific membrane protein 20 (MP20) of unknown function. This motif is a consensus site for C-linked mannosylation of the tryptophan (W) residue and is known to be mannosylated in PMP22 and MP20. In stargazin, this motif consists of GLWRTC and it is unknown whether this

motif is mannosylated or plays another role in the function of the protein. Using internet software (NetCGlyc available from www.expasy.org), we examined the sequence of the entire first extracellular loop of stargazin and scored the possibility of mannosylation at 0.422 (with 0.5 being mannosylated). To elucidate the role of this motif, we mutated residue W64 to alanine and also created a more extensive mutation that combined W64A mutation with residues H60 and R65 changed to their corresponding γ5 residues phenylalanine and leucine respectively.

Interestingly, the triple mutation of stargazin (H60F/W64A/R65L) was unable to potentiate trafficking, decrease the desensitization or increase kainate efficacy of homomeric GluR1. (Figure 6.5 G, H, I and J) The single amino acid substitution W64A in stargazin resulted in a construct that was able to increase trafficking and reduce desensitization of GluR1 comparable to a control GluR1 co-expressed with stargazin (Figure 6.5 G and I). Although kainate efficacy was significantly increased with γ2, (W64A), it was reduced compared to GluR1 co-expressed with stargazin (Figure 6.5 H). In contrast to its effect on steady-state desensitization, γ2 (W64A) was unable to speed the rate of recovery from desensitization (Figure 6.5 B and J).

Because the triple mutations H60F/W64A/R65L had no functional effects on glutamate desensitization, kainate efficacy or trafficking, we did not anticipate that it would have an effect on the rate of recovery from desensitization. Interestingly, γ2 (H60F/W64A/R65L) slowed the rate of recovery from desensitization as compared to control GluR1 expressed alone (Figure 6.5 C and F), in a direction opposing that of normal stargazin function.

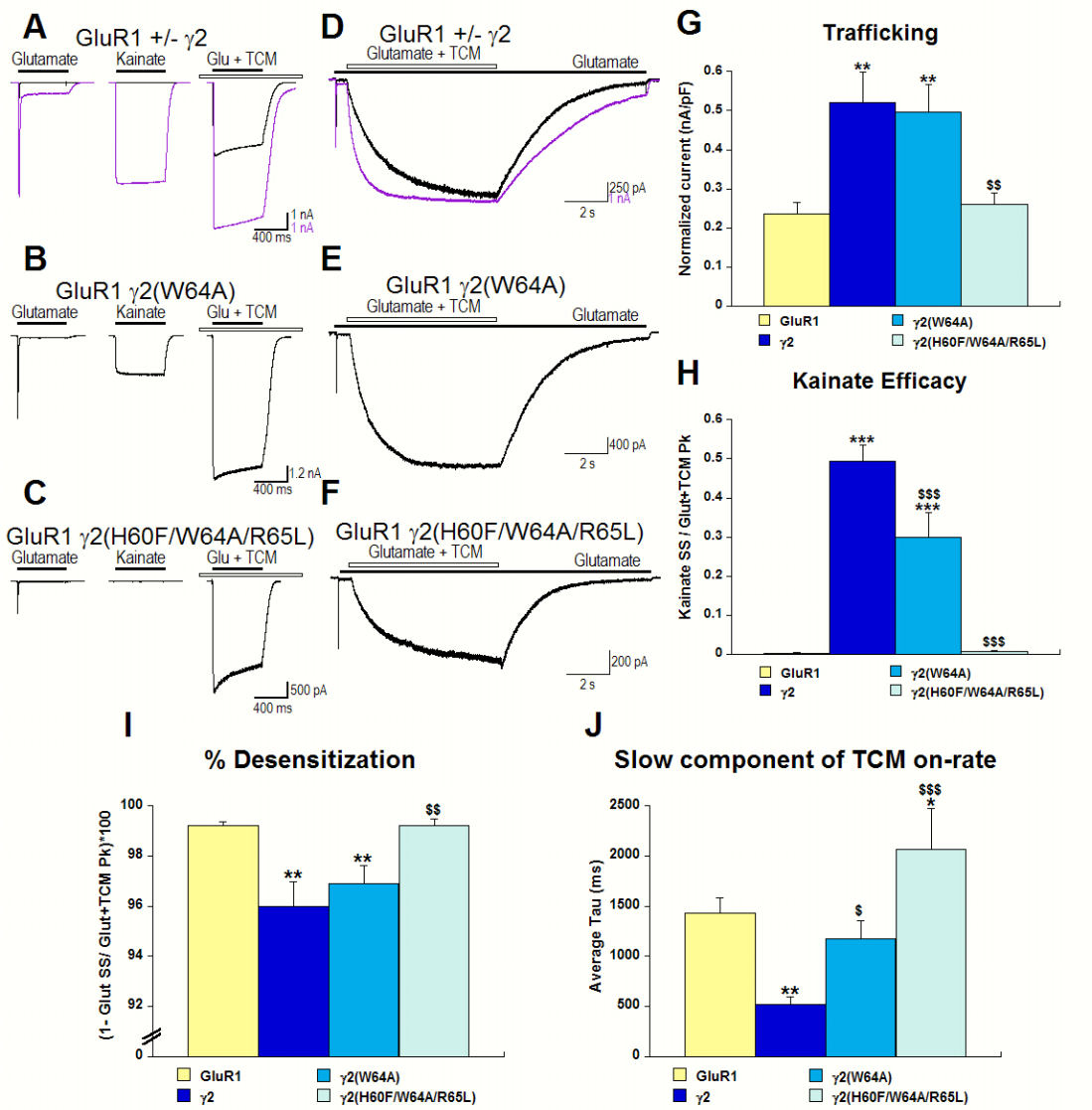

Figure 6.5: Mutation of residues in conserved motif GLWXXC affect stargazin's function. Representative responses to glutamate +/- TCM and kainate for GluR1 expressed alone (black) and co-expressed with stargazin (lavender) (A), GluR1 co-expressed with γ2 (W64A) (B) and GluR1 co-expressed with γ2 (H60F/W64A/R65L) (C). Representative responses to a 3 step protocol for GluR1 expressed alone (black) and with stargazin (lavender) (D), GluR1 co-expressed with γ2 (W64A) (E) and GluR1 co-expressed with γ2 (H60F/W64A/R65L) (F). Summary of the results of trafficking as measured by whole cell currents to application of Glutamate + TCM normalized to whole cell capacitance (G); Kainate efficacy as measured by normalizing the kainate current to Glutamate + TCM peak (H); Percent desensitization is measured relative to glutamate + TCM peak (I); The time constant of recovery from desensitization is represented by the slow component of a two exponential fit of the TCM on-rate in the presence of glutamate (J) are represented by bar graphs illustrating means ± SEM, n = 9-16. * indicates statistical difference compared to GluR1 alone, $ indicates significance compared to GluR1γ2. (* P<0.05; ** P<0.01; ***P<0.001).

Although γ2 (H60F/W64A/R65L) was seemingly non-functional, this result suggests that it was still able to associate with the AMPA receptor on the cell surface, and affect its function. Although it appears that at least some of these mutant constructs associate with the AMPA receptor, it is possible that mannosylation and/or the conserved motif might play a role in forward trafficking of the receptor. Therefore, it is possible that only a very small fraction of the receptors are associated with γ2 (H60F/W64A/R65L). Surface biotinylation studies will be needed to quantify the amount of GluR1 and γ2 (H60F/W64A/R65L) on the surface and further explore the role of this motif in forward trafficking.

Because the W64A mutation, which eliminates the tryptophan residue that supports C-linked mannosylation, had only a partially affected phenotype, while γ2 (H60F/W64A/R65L) and C67A were totally non-functional, we suspect that it is the GLWRTC motif itself, rather than mannosylation, that is necessary for proper tertiary structure.

6.3.4 Mutation of conserved polar residues proximal to the plasma membrane in the first extracellular loop of γ2 reduces effects of stargazin on AMPA receptor desensitization and kainate efficacy.

Stargazin shares multiple conserved polar residues and motifs with other proteins in the TARP family. To elucidate the role of these residues on the function of stargazin, we mutated the majority of the conserved residues in the first extracellular loop of stargazin (illustrated in Figure 6.2) to either alanines or their corresponding residues in γ5. The summary of resulting mutations is presented in Table 6.1.

Mutations that produced functional deficits in stargazin included: S36A, S46A, R99A and S104A/S105T/I106P. The trafficking function of all these mutant constructs was preserved (Figure 6.6 G). While all four of these mutations presented with decreased kainate efficacy (Figure 6.6 H), only S46A and R99A presented with decreased effect on steady-state desensitization (Figure 6.6 I). Consistent with this effect on % desensitization, γ2 (S46A) and γ2 (R99A) were also not able to significantly speed the rate of recovery from desensitization of GluR1 (Figure 6.6 J). We also combined mutations with partial phenotypes making constructs γ2 (S36A/S46A) and γ2 (S36/S104A/S105T/I106P) that were both able to significantly increase trafficking of GluR1 (Figure 6.6 G). The combination γ2 (S36A/S46A) presented with a phenotype similar to γ2 (S36A) with decreased kainate efficacy but normal effect on steady-state desensitization and partial effect on recovery from desensitization (Figure 6.6 H, I and J).

Combination of mutations S36A and S104A/S105T/I106P, γ2(S36/S104A/S105T/I106P), presented with a phenotype that exhibited further reduction in kainate efficacy (Figure 6.6 H) and an additive and possibly synergistic effect on steady-state desensitization (Figure 6.6 I). Consistent with this effect on % desensitization, this construct was unable to speed the recovery from desensitization (Figure 6.6 J). Overall, these results indicate that stargazin residues S36, S104, S105 and I106 located in the regions proximal to the plasma membrane of the first extracellular loop of stargazin play an important role in the function of stargazin.

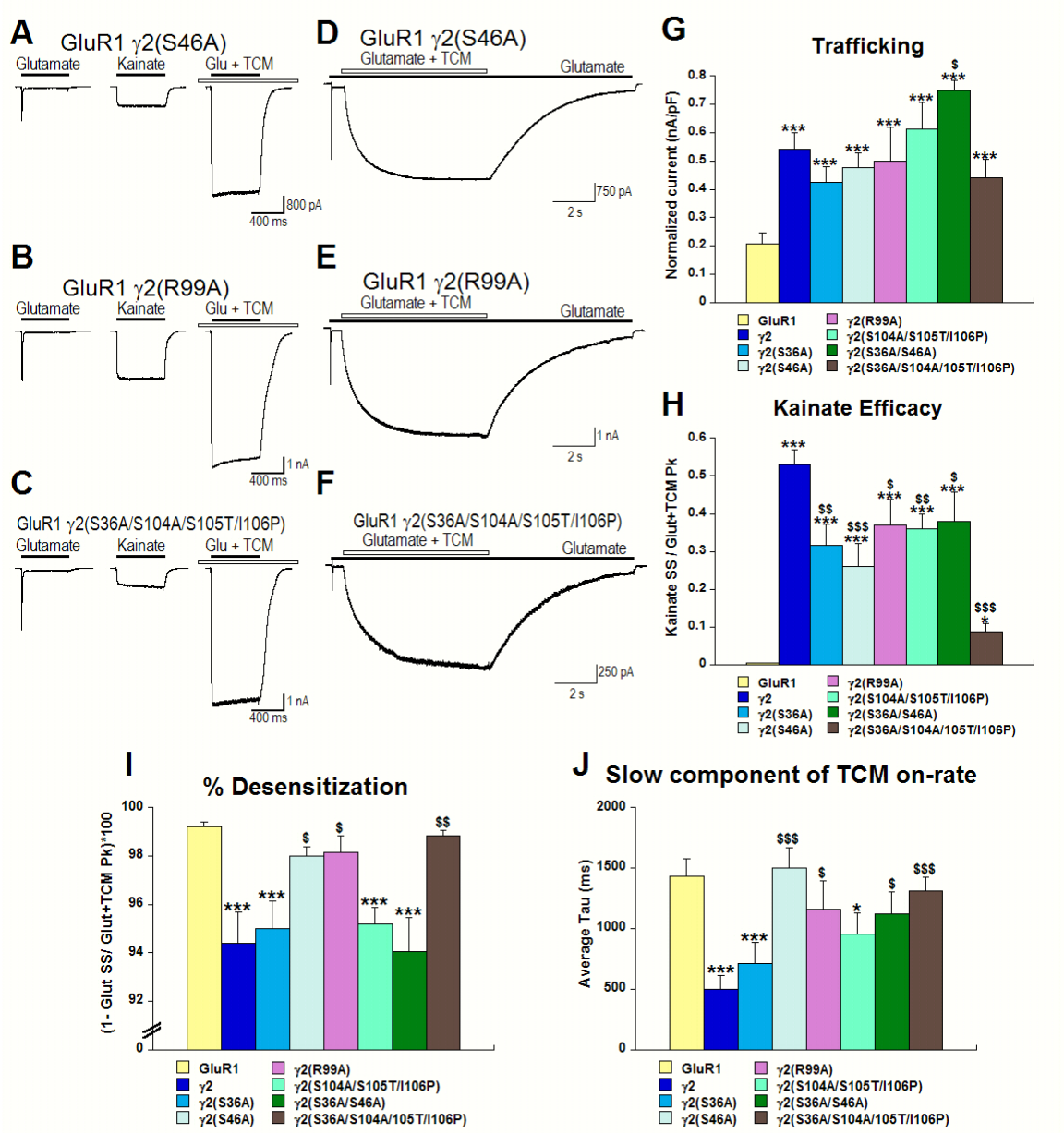

Figure 6.6: Mutation of residues proximal to the membrane in the 1st EC loop affect stargazin's function. Representative responses to glutamate +/- TCM and kainate for GluR1+γ2 (S46A) (A), GluR1+γ2 (R99A) (B), GluR1+γ2 (S36A/S104A/S105T/I106P) (C). Representative responses to a 3 step protocol for GluR1+γ2 (S46A) (D), GluR1+γ2 (R99A) (E), GluR1+γ2 (S36A/S104A/S105T/I106P) (F). Summary of the results of trafficking as measured by whole cell currents to application of Glutamate + TCM normalized to whole cell capacitance (G); Kainate efficacy as measured by normalizing the kainate current to Glutamate + TCM peak (H); Percent desensitization is measured relative to glutamate + TCM peak (I); The time constant of recovery from desensitization is represented by the slow component of a two exponential fit of the TCM on-rate in the presence of glutamate (J) are represented by bar graphs illustrating means ± SEM, n = 7-28. * indicates statistical difference compared to GluR1 alone, $ indicates significance compared to GluR1γ2. (* P<0.05; ** P<0.01; ***P<0.001).

6.3.5 Mutation of conserved polar residues proximal to the plasma membrane in the second extracellular loop of γ2 reduces effect of stargazin on AMPA receptor desensitization and kainate efficacy.

To be complete, we examined the second extracellular loop of stargazin and selected polar residues that were conserved within class I TARPs but not in class II TARPs (illustrated in red in Figure 6.2) as well as residues that were conserved among all TARPs but not in γ1 or γ6 (illustrated in magenta in Figure 6.2). Residues that were only conserved in class I TARPs did not have significantly different phenotype when compared to stargazin (see Table 6.1 for details), however, residues that were conserved in all TARPs (Y155, I156 and S157) did have a significantly different phenotype when mutated to their corresponding γ1 residues.

Two constructs carrying mutations in the conserved regions of both classes of TARPs γ2 (Y155M) and γ2 (I156R/S157Q) were able to increase trafficking of GluR1 2.5-3 fold comparable to wild-type stargazin (Figure 6.7 G). Both constructs presented with decreased kainate efficacy (Figure 6.7 H), while only γ2 (Y155M) was not able to decrease steady-state desensitization (Figure 6.7 I). Neither construct was able to speed the rate of recovery of GluR1 from desensitization (Figure 6.7 J).

Interestingly, γ2 (I156R/ S157Q) had an unexpected effect on kainate currents (Figure 6.7 C). The shape of the kainate response was affected, such that the onset of the response was significantly slowed. However, stargazin did not affect kainate binding, but instead increased its efficacy, suggesting that mutation I156R/ S157Q may introduce changes in gating properties of the channel that may slow the step-wise increases of conductance states (Rosenmund et al., 1998).

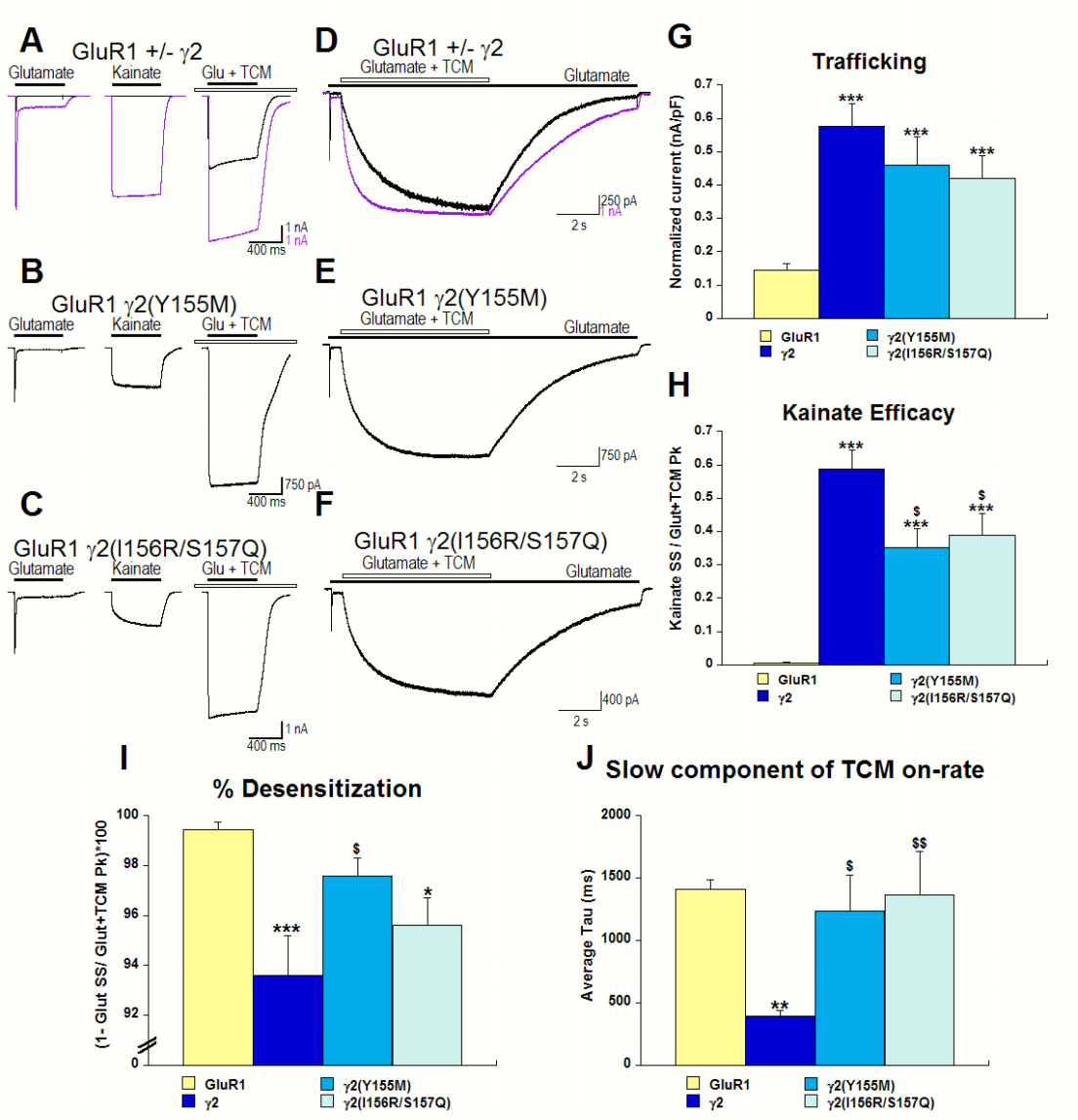

Figure 6.7: Mutation of residues proximal to the membrane in the 2nd EC loop affect stargazin's function. Representative responses to glutamate +/- TCM and kainate for GluR1 expressed alone (black) and co-expressed with stargazin (lavender) (A), GluR1+γ2 (Y155M) (B) and GluR1+γ2 (I156R/S157Q) (C). Representative responses to a 3 step protocol for GluR1 expressed alone (black) and with stargazin (lavender) (D), GluR1+γ2 (Y155M) (E) and GluR1+γ2 (I156R/S157Q) (F). Summary of the results of trafficking as measured by whole cell currents to application of Glutamate + TCM normalized to whole cell capacitance (G); Kainate efficacy as measured by normalizing the kainate current to Glutamate + TCM peak (H); Percent desensitization is measured relative to glutamate + TCM peak (I); The time constant of recovery from desensitization is represented by the slow component of a two exponential fit of the TCM on-rate in the presence of glutamate (J) are represented by bar graphs illustrating means ± SEM, n = 11-16. * indicates statistical difference compared to GluR1 alone, $ indicates significance compared to GluR1γ2. (* P<0.05; ** P<0.01; ***P<0.001).

The phenotypes of the mutant constructs γ2 (Y155M) and γ2 (I156R/S157Q) in the second extracellular loop of stargazin are similar to those of mutations in the regions proximal to the plasma membrane on the first extracellular loop of stargazin. This result indicates that residues close to the membrane in both loops of stargazin are important for its functional effects on the AMPA receptor.

6.4 Summary of the results

Our exploration of the stargazin molecule with site-directed mutagenesis and electrophysiology revealed a number of regions in stargazin that play a role in its effects on desensitization and kainate efficacy.

- Cysteines conserved among all members of the γ subunit family are crucial for the function or stability of stargazin.
- Destruction of the consensus motif for N-linked glycosylation results in a gain of function for kainate efficacy and desensitization.
- The conserved motif GLWXXC is essential for the function of stargazin.
- Polar residues located proximal to the membrane in the first and second extracellular loops of stargazin play an important role in stargazin's effects on AMPA receptor desensitization and kainate efficacy.

CHAPTER VII

DISCUSSION AND CONCLUSIONS

For these experiments we made 44 mutations on the AMPA receptor, only 9 of which have been previously reported, and 45 targeted mutations in stargazin. Previous research with stargazin always involved chimeric exchanges, making our study the most comprehensive mutagenesis on both the AMPA receptor and stargazin to date.

AMPA receptor desensitization is crucial for shaping the time course of synaptic transmission. Previous studies involving AMPA receptor desensitization primarily focused on the residues on the intra-dimer interface. These studies were able to elucidate the mechanism of desensitization onset, but did not further our knowledge of the mechanism of AMPA receptor recovery from desensitization. Examining mutations that we made in both the AMPA receptor and stargazin allowed us to suggest a novel mechanism for AMPA receptor recovery from desensitization and to identify candidate association sites between AMPA receptors and stargazin.

7.1 What we learned about stargazin.

In our attempt to understand the mechanism of stargazin's action on AMPA receptor function, as well as to identify association sites between the two proteins, we made multiple mutations in both the AMPA receptor and stargazin. The experiments confirmed that stargazin acts by speeding AMPA receptor recovery from desensitization and identified three possible sites in the AMPA receptor involved in association with stargazin, and refined the areas of stargazin important for efficacy.

7.1.1 Stargazin's mechanism of action is distinct from that of cyclothiazide and the L479Y mutation.

Previous studies by Sun and colleagues (2002) proposed a precise mechanism for the process of AMPA receptor desensitization based on observations from the crystal structure. Horning and Mayer (2004) confirmed this mechanism with their experiments concentrating on the stability of the protein interactions on the intra-dimer interface, yielding a clear explanation of how AMPA receptors enter the desensitized state. Introducing mutations that destabilized protein interactions on the intra-dimer interface resulted in receptors that entered the desensitized state more rapidly, while introducing mutations that stabilized protein interactions on the intra-dimer interface resulted in receptors that desensitized significantly slower. Priel and colleagues, 2005, suggested that TARPs may utilize a similar mechanism and decreases steady-state desensitization of AMPA receptors by stabilizing the intra-dimer interface.

In our attempt to understand the mechanism by which stargazin affects AMPA receptor desensitization, we prepared mutations on the intra-dimer interface of the AMPA receptor that produced moderate changes in onset of desensitization. Stargazin's effects on steady-state desensitization were additive, or possibly synergistic, with mutations that stabilized the dimer interface E482A and K748A, but were occluded in the mutation N743D that destabilized the dimer interface. Stargazin was able to speed the recovery from desensitization for all constructs on the dimer interface. These results support our hypothesis that stargazin does not act by stabilizing the dimer interface, but rather by speeding AMPA receptor's recovery from desensitization.

7.1.2 Sites of association and efficacy between the AMPA receptor and stargazin located on the AMPA receptor side.

In our attempt to identify areas important for association of stargazin and the AMPA receptor, we were guided by homology between AMPA receptors and kainate receptors as well as crystal structure of the ligand-binding domain. As a result of our experiments, we identified three areas on the AMPA receptor that include region downstream of helix H, region proximal to the membrane in the M4 linker and the intracellular loop 2 that are candidate association sites with stargazin.

The portion of the GluR1 crystal downstream of helix H that involves residues K693, G694 and K695 differs in structure from that of the kainate receptor, such that residues K693 and G694 are missing and residue K695 is substituted with aspartic acid (D) in GluR6. We mutated these lysine residues to alanines to preserve GluR1 spacing (K693A/K695A) and deleted them to preserve GluR6 spacing (del(K693/G694)/K695D) (residues illustrated on Figure 7.1). The mutant construct del(K693/G694)/K695D expressed alone had a significantly slower rate of recovery from desensitization, indicating that introducing GluR6 spacing into GluR1 made the desensitization profile of GluR1 more like that of GluR6. Such spacing difference between AMPA and kainate receptors may also be a part of what prevents kainate receptors from associating with TARPs.

When co-expressed with stargazin, both constructs presented with a striking lack of effect on AMPA receptor steady-state desensitization and recovery from desensitization, significantly decreased kainate efficacy but fully preserved trafficking. Results from del(K693/G694)/K695D construct, taken alone, are difficult to interpret because this

mutation introduces changes to the spacing and tertiary structure of the protein. The loss of effects of stargazin on AMPA receptor desensitization and decrease of effect on kainate efficacy, in the K693A/K695A construct that preserves GluR1 spacing suggests that this may be a site of extracellular association. However, because the effect of stargazin on receptor trafficking in this construct was preserved, we suggest that this mutant construct was still able to maintain the intracellular association responsible for trafficking. It is also possible that these mutations do not affect association of AMPA receptor pore-forming subunits with stargazin, but instead just alter the way the AMPA receptor transduces the effects of stargazin.

Co-expression of the mutant construct E674R/P675Q at the end of helix G with stargazin resulted in a similar desensitization and kainate phenotype as del(K693/G694)/K695D. The severe nature of this mutation, changing a negative charge to a positive at position 674 and removing a proline at position 675, would be expected to alter local tertiary structure of the protein. While it is possible that the E674R/P675Q actually forms an association with stargazin, it is more likely that this mutation affects the structure of the lower outer face of the AMPA receptor (by introducing tension at the end of helix G, therefore rearranging position of the residues downstream of helix H), an area identified by the K693A/K695A mutant as being important for stargazin function.

The mutant construct in the M4 linker S784G/A789G, that had no significantly different phenotype when expressed alone, also resulted in significantly less effect of stargazin on steady-state desensitization, rate of recovery from desensitization, kainate efficacy but fully preserved trafficking. These data indicate that residues S784 and A789 may also participate in the extracellular association with stargazin (Figure 7.1). However,

because the effects of stargazin on trafficking are fully preserved in S784G/A789G construct we suggest that intracellular association responsible for trafficking is still maintained. It is also possible that the resulting loss of stargazin's effects in this mutant is a result of diminished association located lower in the TM4 or decreased stargazin efficacy caused by the mutation.

Co-expression of constructs carrying mutations of residues in the second intracellular loop of GluR1 (S588M and S591A) resulted in significantly decreased effects of stargazin on steady-state desensitization and kainate efficacy and fully preserved trafficking. Recent data indicates that the intracellular loop and intracellular N-terminus of stargazin are important for stargazin's effects on AMPA receptor gating (Milstein and Nicoll, 2009). It is also possible that there are multiple intracellular association sites between the AMPA receptor pore-forming subunits and stargazin with one being exclusively important for trafficking. Therefore it is possible that mutations in the second intracellular loop of the AMPA receptor interfere with the one of the intracellular association sites with stargazin, consistent with stargazin's diminished effect on steady-state desensitization and kainate efficacy.

Mutations in helix K, K757M and D765G, on the lateral dimer interface/the lateral face of the receptor resulted in constructs with significantly slower rate of recovery from desensitization. Although the desensitization deficits caused by these mutations (significantly slowed rate of recovery from desensitization) were completely rescued by stargazin's effect on the recovery from desensitization, stargazin was unable to fully potentiate kainate currents in these constructs. Because we suspect that one of the association sites between stargazin and AMPA receptor is located in the M4 linker that

connects helix K with TM4, we suggest that residues in helix K do not directly associate with stargazin, but rather transduce its effects on the rest of AMPA receptor. It is possible that association with stargazin in the M4 linker causes a change in the positioning of helix K, therefore occluding the effects of these mutations on desensitization. We propose that stargazin alters protein conformation on the lateral dimer interface thus changing interactions between the two dimers.

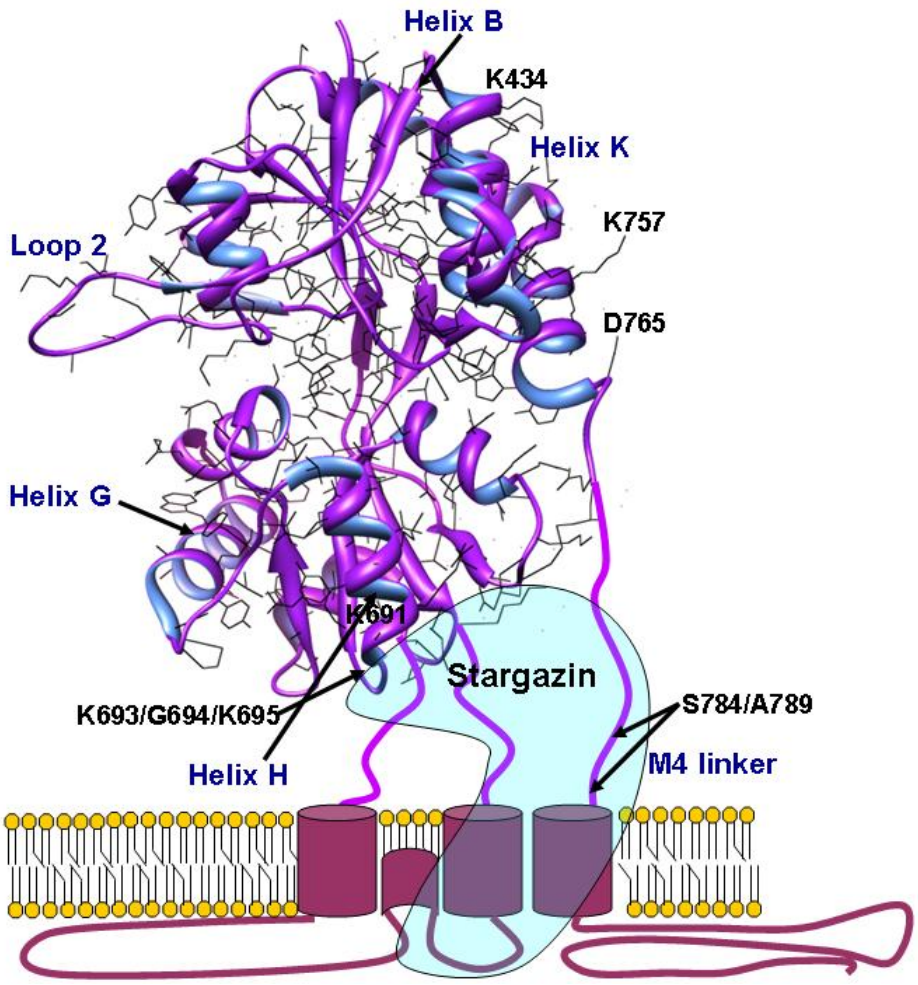

Figure 7.1: Possible sites of association with stargazin. Ribbon diagram illustrates a side view of the subunit, with the dimer interface pointing into the page and the outer face of the subunit pointing out of the page. Linkers connect the ligand-binding domain with TM regions. Stargazin is positioned in the lateral dimer interface where it could form contact with the M4 linker residues S784 and A789, area downstream of helix H, including residues K693 and K695, TM regions and the intracellular loop 2.

In summary, Figure 7.1 illustrates possible association sites between the AMPA receptor pore-forming subunit and stargazin. Our data suggests that stargazin is located on the lateral inter-dimer interface and forms a contact with residues S784 and A789 in the M4 linker, residues K693 and K695 downstream of helix H and possibly residues S588 and S591 in the second intracellular loop of AMPA receptor pore-forming subunit.

7.1.3 Sites of association and efficacy between the AMPA receptor and stargazin located on the stargazin protein.

Utilizing homology between class I TARPs and related proteins, we identified several residues in stargazin that are important for association with GluR1. These residues are concentrated near the plasma membrane in the first and second extracellular loops of stargazin and include S36 in the proximal portion of the first extracellular loop, R99, S104, S105 and I106 in the distal portion of the first extracellular loop and Y155, I156 and S157 in the proximal portion of the second extracellular loop of stargazin (illustrated in Figure 7.2). When mutated, these residues result in constructs that are unable to elicit stargazin's full effects on desensitization and kainate efficacy. Because of their location near the membrane and a phenotype similar to that of S784G/A789G in the M4 linker of the AMPA receptor, we suggest that they may play a role in association with this region in GluR1.

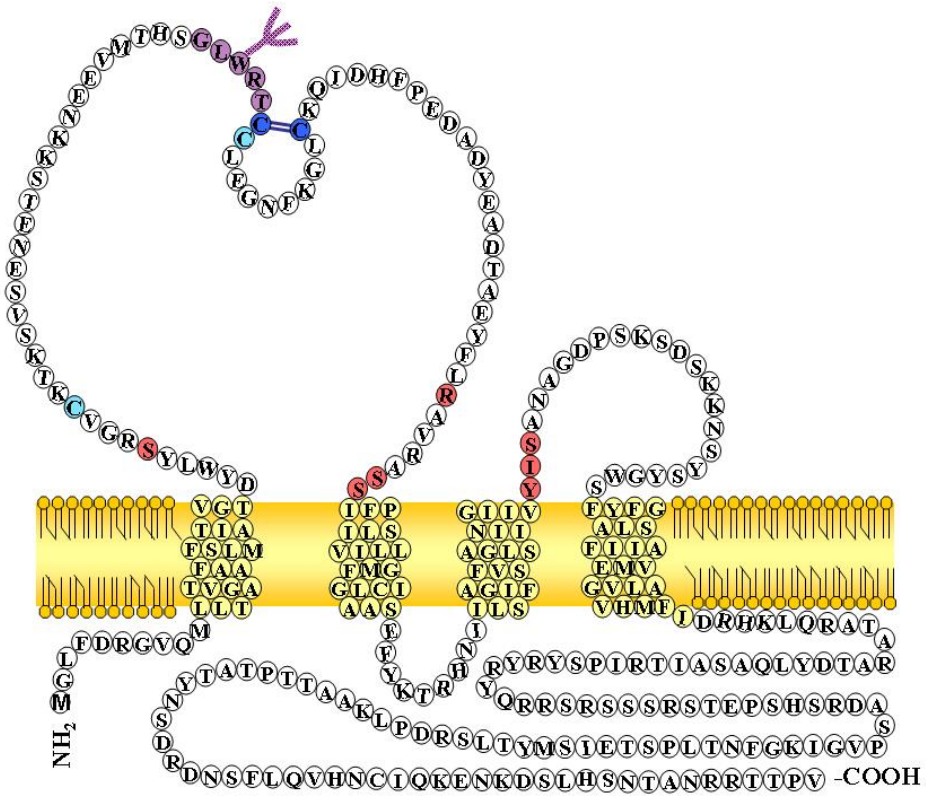

Figure 7.2: Stargazin schematic indicating residues of interest in the extracellular domains of stargazin.

- Polar residues important for stargazin's effect on AMPA receptor desensitization and kainate efficacy.
- Cysteine residues possibly participating in the mutual disulfide bond.
- Cysteine residues that do not play a role in disulfide linkages.
- Conserved mannosylation motif GLWXXC crucial for stargazin's function

All members of the γ subunit family have a conserved mannosylation motif GLWXXC (Figure 7.2), the function of which is unknown. Loss of this motif (and presumably mannosylation) in distally related PMP22 results in loss of association with other proteins (Ervin et al., 2005), while the loss of N-linked glycosylation in γ1 does not affect its association with voltage-gated calcium channels (Arikkath et al., 2003). In our attempt to understand the function of this motif, we prepared two mutants W64A and H60F/W64A/R65L. W64A, which removed the tryptophan that would be directly mannosylated, resulted in a deceased effect of stargazin on AMPA receptor kainate

efficacy and recovery from desensitization. The H60F/W64A/R65L mutation, however, resulted in the loss of all of stargazin's normal effects on the AMPA receptor, including a complete loss of trafficking. The only phenotype H60F/W64A/R65L demonstrated was a slight but significant slowing of the rate of recovery from desensitization in GluR1 (as opposed to stargazin's normal effect on speeding of recovery). This change in receptor kinetics suggests that H60F/W64A/R65L remains associated with GluR1 on the cell surface. It is, however, possible that interfering with the conserved GLWXXC motif does indeed alter the association of stargazin with AMPA receptors. Future experiments with surface biotinylation and western blots should be able to elucidate if the H60F/W64A/R65L construct is indeed associated with GluR1.

Two cysteine residues conserved throughout the γ subunit family (C67 and C77 in γ2) are crucial for stargazin's function and possibly participate in the mutual disulfide bond (Figure 7.2). Although the mutant construct C77A is unable to affect AMPA receptor desensitization or kainate efficacy, it is able to increase receptor trafficking, in contrast to C67A that appeared to be non-functional. It is possible that because C67 is also a part of the GLWXXC motif, the resulting loss of function is related to the motif rather than the loss of a disulfide bond. However, because both constructs lost all effects on AMPA receptor desensitization and kainate efficacy, we suggest that these residues participate in a disulfide bond that is necessary for the proper tertiary structure of the first extracellular loop and for stargazin function. As an alternative explanation, it is also possible that these cysteine residues participate in bonding with other proteins, as observed in immunoglobulins (Underdown et al., 1977) important for AMPA receptor function.

While examining all the stargazin mutations described in this dissertation, we identified only three with a profound loss of stargazin's effect on AMPA receptor steady-state desensitization, kainate efficacy and trafficking - C67A, H60F/W64A/R65L and Δ212 (described in chapter 1). Two of these mutant stargazin constructs (H60F/W64A/R65L and Δ212) slightly but significantly slowed the rate of recovery from desensitization in GluR1, in contrast to the normal effect of stargazin on speeding the rate of recovery from desensitization. These results suggest that although these constructs lost virtually all of the stargazin's function, they were still able to associate at the surface and it is possible that the opposite effect on the recovery from desensitization occurs because the non-functional stargazin construct sterically hinders normal AMPA receptor function.

7.1.4 Effects of stargazin on kainate efficacy.

Preliminary results from our laboratory suggest that the effects of stargazin on kainate efficacy consist of at least two components. Approximately 30% of the increase in kainate currents is due to stargazin's effect on kainate desensitization. The nature of the other effect is unclear. However, we suspect that it involves increased gating in the presence of kainate. It is of interest to note that, while performing the experiments to locate the association site between the AMPA receptors and stargazin, we observed that many mutations on the AMPA receptor were able to eliminate stargazin's effect on AMPA receptor glutamate desensitization, but not the effect on kainate efficacy. Even in GluR1 mutations that presented with loss of stargazin's effect on glutamate desensitization including K693A/K695A, S784G/A789G and mutations in the 2nd intracellular loop of GluR1, which was interpreted as the loss of an association, the effect on kainate efficacy was partially preserved. We do not have the data to determine

whether the partial loss of kainate effect in these mutations resulted from increased kainate desensitization or decreased gating. However, based on the loss of the stargazin's effects on glutamate desensitization in these mutations, we suspect that the partial loss of kainate efficacy results from a loss of stargazin's effect on kainate desensitization. These results therefore suggest that stargazin's effects on kainate gating is mostly preserved in all of these mutants. Because mutation of stargazin residues proximal to the membrane in the 2nd extracellular loop seems to affect kainate gating, we suggest that residues important for stargazin's effects on kainate gating are located in the transmembrane regions and are associated with the AMPA receptor ion channel.

7.2 What we learned about the AMPA receptor from our experiments.

7.2.1 Residues important for AMPA receptor recovery from desensitization are located in helices B and K as well as the M1 linker and intracellular loop 2

Previous experiments on the intra-dimer interface elucidated the mechanism involved in desensitization onset, but searches there or in loop 1 and helix G did not find any residues that affected the rate of recovery from desensitization (Horning and Mayer, 2004). Although the mechanism of desensitization onset has been elucidated, the mechanism of recovery from desensitization is still unknown. Here we present a series of mutations in the lateral dimer interface, M1 linker and first intracellular loop that affect the rate of recovery from desensitization.

In our search for residues important in association of stargazin and AMPA receptor, we identified several residues located on the lateral dimer interface/the lateral face of the receptor whose amino acid side chains were exposed and pointing out of the protein. When mutated to their corresponding residues in GluR6, these constructs in helix K

(K757M and D765G) presented with significantly slower rate of recovery from desensitization. Because these residues are located on the lateral dimer interface, it is possible that recovery from desensitization involves conformational rearrangements on the lateral dimer interface. Because stargazin's main effect is on the recovery from desensitization, the fact that it was able to fully rescue desensitization deficits in helix K mutants argues in support of this hypothesis.

Mutant construct K501A/K502A in the M1 linker also presented with a slower rate of recovery from desensitization. These residues are located in the lower portion of the crystal structure below the intra-dimer interface. However, because the artificial linker was introduced between the M1 and the M3 linkers, the position of these residues may be somewhat distorted in a crystal (illustrated in Figure 7.3). This mutation presented with a phenotype similar to helix B mutation K434T. Therefore we suggest that both of these residues at the very beginning of the M1 linker and the top of helix B participate in coordinating the recovery from desensitization, which must include the reconstitution of the dimer interface. The top of helix B, which sits immediately above helix J in the beginning of linker 1 (illustrated on Figure 7.3), which is low in the intra-dimer interface, would be logically placed to guide this reconstitution. One would predict that stargazin would have little effect on steady-state desensitization in AMPA receptors that had difficulty reconstituting their dimer interface, which is what we observed with both of these constructs. Interestingly, preliminary data from mutations in loop 2 (data not shown) of the AMPA receptor suggest that this region may also participate in the mechanism of recovery from desensitization.

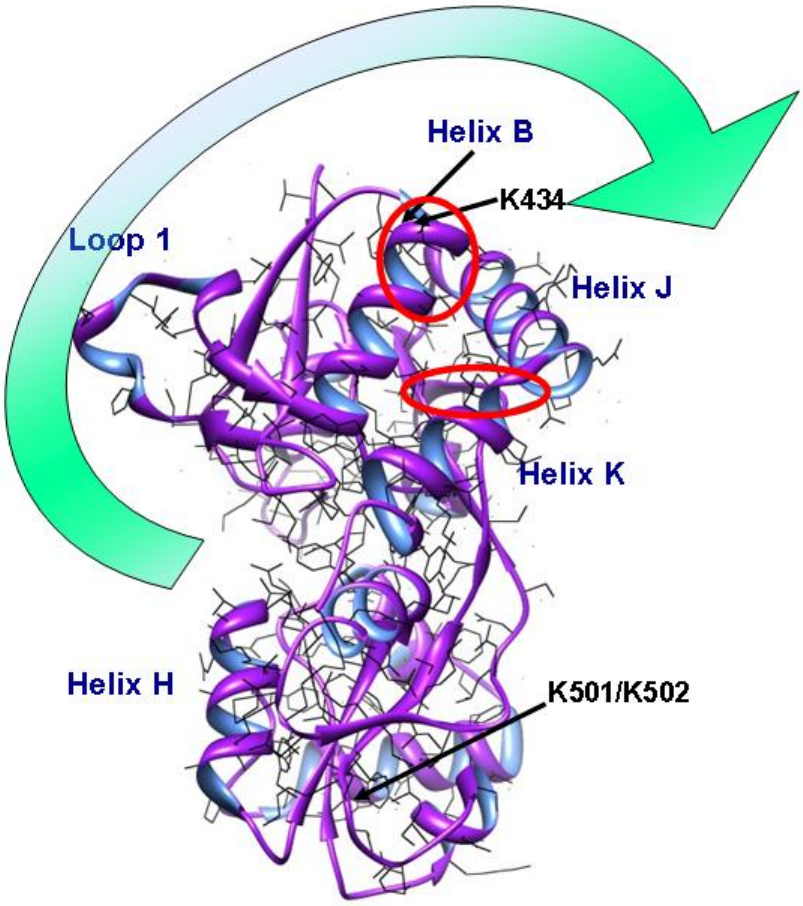

Figure 7.3: Areas of the AMPA receptor important for recovery from desensitization. Ribbon diagram represents a side view of the crystallized ligand-binding domain of GluR2 subunit, with the dimer interface pointing to the right of the page and the outer face of the subunit pointing to the left of the page. The arrow indicates the direction of the movement that the upper portion of the clamshell undergoes during recovery from desensitization and reconstitution of the intra-dimer interface.

The function of the intracellular loops of the AMPA receptor has received little attention in the literature. While trying to locate residues that might be important for association with stargazin, we identified three residues in the second intracellular loop of GluR1, S588, S591 and G594, that when mutated to their corresponding residues in GluR6, presented with slowed recovery from desensitization. Mutation of R595 to alanine or serine resulted in a non-functional construct, suggesting that this residue is

critical for ion channel function. It is therefore our interpretation that phenotypes observed with mutations at G594 most probably result from interference with R595. However, residue S588 in particular is important for recovery from desensitization. Because the recovery from desensitization must be coupled to opening of the ion pore, it is possible that S588, located 3 amino acids downstream from the re-entrant loop, is involved in this process.

7.2.2 Residues proximal to the membrane in the M1 and M4 linker regions control gating of AMPA receptor

AMPA receptor linkers are responsible for transducing the conformation of the ligand-binding core to the ion channel pore (Mathur et al., 1997). Because linkers are crucial for channel gating in voltage-gated ion channels, it is not surprising we identified two mutations that affected AMPA receptor gating.

A518S/Y519P and V788I mutant constructs in M1 and M4 linkers, respectively, presented with significantly decreased steady-state desensitization and significantly increased kainate efficacy, without any effect on the rate of desensitization onset or recovery. Because the kinetics of steady-state desensitization are shaped by the rates of desensitization onset and recovery, the change in steady-state desensitization in these constructs must have resulted from gating changes. These gating changes possibly resulted from either increased mean open time of the receptor or a shift to a higher conductance state. Because whole-cell recordings are limited in their ability to observe gating changes, single-channel recordings will be necessary to prove if these constructs indeed have higher conductance.

7.2.3 Mutations in helix D on the dimer interface of GluR1 present with different phenotypes compared to the same mutations in GluR2.

GluR1 and GluR2Q homomeric receptors differ in their desensitization profile, such that GluR2 desensitizes more slowly and to a lesser degree than GluR1 (99.5% for GluR1 and 98.5% for GluR2Q). While attempting to understand the effects of stargazin on desensitization of AMPA receptors, we prepared mutations that were previously described in GluR2 as affecting AMPA receptor steady-state desensitization and the rate of desensitization onset. Although most of the crystallographic work has been done in the GluR2 subunit, homomeric GluR2Q receptors do not occur endogenously, while homomeric GluR1*flip* subunits produce robust responses and are endogenously expressed.

Two of the four previously described mutations on the dimer interface presented with different phenotypes. The L479A mutation in GluR2 had decreased steady-state desensitization and slowed rate of desensitization onset (Horning and Mayer, 2004), while in GluR1 it had no distinguishable phenotype. Mutation E482A was previously shown to speed the rate of desensitization onset and increase steady-state desensitization of GluR2 (Horning and Mayer, 2004), while in GluR1 it had an opposite effect on desensitization properties with significantly slowed rate of desensitization onset and decreased steady-state desensitization. Such discrepancies are probably caused by the innate differences between two subunits.

These same two mutations on helix D, L479A and E482A, had an unexpected effect on negative cooperativity between glutamate and trichlormethiazide in GluR1, which was not observed in the GluR2 background. It appeared that, as more glutamate binds, the

ability of TCM to block desensitization in these mutants was reduced. A similar effect is seen in *flop* splice variants (the *flip/flop* cassette is known to contain part of the cyclothiazide binding site). However, these mutations are located in a region distinct from this alternative splice site. Because part of the binding site for TCM is located on the dimer interface and is coordinated by the residues on the β strand 7, downstream of helix D (Sun et al., 2002), it is possible that mutation of the residues in helix D alter the conformation or exert tension on β strand 7 during glutamate binding, thus decreasing the affinity for TCM in GluR1.

7.2.4 Existence of two desensitized states in AMPA receptors

While modeling AMPA receptor desensitization onset and recovery, it was previously observed that both rates are best fit with two exponentials in neurons (Patneau and Mayer, 1991; Raman and Trussell, 1992), suggesting that AMPA receptors transition between two desensitized states (Robert and Howe, 2003). While working on this project we made an observation that in any mutation with reduced steady-state desensitization (E482A, K748A, A518S/Y519P and V788I) effects of stargazin were always synergistic. However, in mutations that presented with more steady-state desensitization (N743D and K501A/K502A) effects of stargazin on steady-state desensitization were decreased or occluded. These results suggest two different desensitized states exist in the AMPA receptor. Because we suspect that N743D mutant construct is desensitized at rest, our data supports the hypothesis that one of these states is not agonist bound. Because stargazin is able to potentiate peak responses to glutamate even in the mutations with increased steady-state desensitization (N743D and K501A/K502A), we suggest that it is can influence both of these states.

7.3 Limitations of our studies

Although we were able to identify possible sites of association between AMPA receptors and stargazin, electrophysiological experiments cannot definitively prove that these are sites where stargazin and the pore-forming subunits of the AMPA receptor make contact with one another. We anticipated that the loss of extracellular association would present with a phenotype observed in the chimeric exchange between stargazin and γ5 Ex(26-103) (Figure 1.11), where most of the stargazin's effect on kainate efficacy and desensitization would be lost and trafficking effects would be only modestly decreased. However, none of the mutations we observed presented with this exact phenotype. Surprisingly, the effects of stargazin on kainate efficacy were always at least partially preserved with mutation in the AMPA receptor. We attribute the decreased effect of stargazin on kainate efficacy as the loss of the effect on kainate desensitization. Therefore, this result suggests that the effects of stargazin on kainate gating could be a result of interaction in the transmembrane regions rather than the purely extracellular association as we previously thought. Alternatively, it may be that multiple points of association in the extracellular domains are involved. The largest reduction in kainate efficacy was observed with the combined mutations proximal to the plasma membrane in the first extracellular loop of stargazin.

We also anticipated that the loss of intracellular association between the AMPA receptor and stargazin would present with a phenotype similar to the deletion of the C-terminal tail Δ212 (Figure 1.11), where the effects of stargazin on trafficking would be entirely lost, while the effects on desensitization and kainate efficacy would be only slightly decreased. However, none of the mutations on the AMPA receptor or stargazin

generated a similar phenotype. Therefore we suggest that there may be multiple intracellular associations, where one is exclusively important for trafficking, while the others are important for effects of stargazin on AMPA receptor desensitization, gating and kainate efficacy.

To answer the question if the effects of mutations were a result of association or efficacy, we will require further experiments with surface biotinylation and western blots. It is also possible that combining mutations that are candidate extracellular association sites (S784G/A789G with K693A/K695A) would result in a phenotype similar to that observed in Ex(26-103). If so, combing the extracellular association site mutations with intracellular loop 2 association site mutations could result in a protein that presents with complete loss of desensitization and kainate effects of stargazin on AMPA receptor. Such combinations of the extracellular and intracellular mutations might be able to completely break all association between the two proteins that we will be able to confirm electrophysiologically and with surface biotinylation.

In certain mutations outside-out patch and/or single-channel recordings will be necessary to prove suggested changes in gating. Patch recordings would also strengthen our findings regarding mechanism of recovery from desensitization. The standard protocol in the AMPA receptor field for measuring recovery from desensitization is to utilize twin-pulse recordings in patches. Instead we used a measurement that is proportional to the rate of recovery from desensitization, the on-rate of the TCM in the presence of glutamate. To definitively prove the effects of the mutations on the recovery from desensitization we may need to perform twin-pulse recordings in patches.

Several mutations (K693A/K695A, S588M and S591A) presented with decreased trafficking. We used current density as a proxy for trafficking, based on our previous demonstration that the levels of surface expression are correlated with changes in current density (Turetsky et al., 2005). However, the decreases in trafficking in mutations we made could have also resulted from decreased channel conductance. Whole-cell recording cannot distinguish between the actual decreases in receptor trafficking vs. the decrease in conductance. We also know that stargazin potentiates AMPA receptor trafficking; however, because stargazin potentiated trafficking of several mutants (K693A/K695A, S588M and S591A) several fold more than control GluR1, it is possible that in some of these mutations stargazin was also able to also elicit an effect on channel conductance. Therefore, to prove that trafficking of these mutants was a result of lower surface expression, we will need to perform single-channel recordings to make sure that the channel conductance in these mutants did not change, in conjunction with surface biotinylation experiments to show that the amount of AMPA receptors at the surface is decreased.

Although our studies were limited in understanding of all of the molecular mechanism underlying the effects of the mutations, we were still able to suggest areas of AMPA receptor important for recovery from desensitization and areas of association between AMPA receptor and stargazin.

7.4 Significance of our studies

Post-synaptic AMPA receptors play an important role in mediating fast excitatory neurotransmission in the mammalian CNS. Therefore AMPA receptor desensitization has a considerable effect on shaping the time course and amplitude of the synaptic

transmission. Current classes of drugs that are used for potentiation of synaptic transmission, AMPAkines, bind at the intra-dimer interface, therefore blocking the onset of desensitization (Lynch, 2006). Such a crude effect sometimes has an unwanted side effect of seizures.

Several non-competitive AMPA receptor antagonists (such as Talampanel) were suggested for use during the ischemic events to prevent the excitotoxicity (Tomillero and Moral, 2008; Luszczki, 2009). However, most of these drugs have the unwanted side effect of profound memory loss. Therefore, identifying areas of the AMPA receptor that mediate recovery from desensitization and a better understanding of the mechanism of recovery from desensitization could elucidate new targets for rational drug design. Such drugs could act on the lateral inter-dimer interface to either speed the rate of recovery from desensitization, therefore potentiating synaptic transmission, or to slow the rate of recovery from desensitization during ischemic events to ameliorate the neurotoxic effects of glutamate. Because stargazin has a large extracellular portion that plays such an important function in AMPA receptor physiology, it could also potentially be a candidate for rational drug design. Overall our studies provide a new insight into AMPA receptor physiology that is beneficial for scientific and medical fields.

REFERENCES

Abele R, Keinanen K, Madden DR (2000) Agonist-induced isomerization in a glutamate receptor ligand-binding domain. A kinetic and mutagenetic analysis. J Biol Chem 275:21355-21363.

Anderson P, Lomo T (1966) Mode of activation of hippocampal pyramidal cells by excitatory synapses on dendrites. Exp Brain Res 2:247-260.

Arai A, Kessler M, Ambros-Ingerson J, Quan A, Yigiter E, Rogers G, Lynch G (1996) Effects of a centrally active benzoylpyrrolidine drug on AMPA receptor kinetics. Neuroscience 75:573-585.

Arikkath J, Chen CC, Ahern C, Allamand V, Flanagan JD, Coronado R, Gregg RG, Campbell KP (2003) Gamma 1 subunit interactions within the skeletal muscle L-type voltage-gated calcium channels. J Biol Chem 278:1212-1219.

Armstrong DM, Ikonomovic MD, Sheffield R, Wenthold RJ (1994) AMPA-selective glutamate receptor subtype immunoreactivity in the entorhinal cortex of non-demented elderly and patients with Alzheimer's disease. Brain Res 639:207-216.

Armstrong N, Gouaux E (2000) Mechanisms for activation and antagonism of an AMPA-sensitive glutamate receptor: crystal structures of the GluR2 ligand binding core. Neuron 28:165-181.

Armstrong N, Jasti J, Beich-Frandsen M, Gouaux E (2006) Measurement of conformational changes accompanying desensitization in an ionotropic glutamate receptor. Cell 127:85-97.

Armstrong N, Mayer M, Gouaux E (2003) Tuning activation of the AMPA-sensitive GluR2 ion channel by genetic adjustment of agonist-induced conformational changes. Proc Natl Acad Sci U S A 100:5736-5741.

Armstrong N, Sun Y, Chen GQ, Gouaux E (1998) Structure of a glutamate-receptor ligand-binding core in complex with kainate. Nature 395:913-917.

Arvola M, Keinanen K (1996) Characterization of the ligand-binding domains of glutamate receptor (GluR)-B and GluR-D subunits expressed in Escherichia coli as periplasmic proteins. J Biol Chem 271:15527-15532.

Arikkath J, Chen CC, Ahern C, Allamand V, Flanagan JD, Coronado R, Gregg RG, Campbell KP (2003) Gamma 1 subunit interactions within the skeletal muscle L-type voltage-gated calcium channels. J Biol Chem 278:1212-1219.

Ayalon G, Segev E, Elgavish S, Stern-Bach Y (2005) Two regions in the N-terminal domain of ionotropic glutamate receptor 3 form the subunit oligomerization interfaces that control subtype-specific receptor assembly. J Biol Chem 280:15053-15060.

Ayalon G, Stern-Bach Y (2001) Functional assembly of AMPA and kainate receptors is mediated by several discrete protein-protein interactions. Neuron 31:103-113.

Balannik V, Menniti FS, Paternain AV, Lerma J, Stern-Bach Y (2005) Molecular mechanism of AMPA receptor noncompetitive antagonism. Neuron 48:279-288.

Barrionuevo G, Schottler F, Lynch G (1980) The effects of repetitive low frequency stimulation on control and "potentiated" synaptic responses in the hippocampus. Life Sci 27:2385-2391.

Barry MF, Ziff EB (2002) Receptor trafficking and the plasticity of excitatory synapses. Curr Opin Neurobiol 12:279-286.

Bats C, Groc L, Choquet D (2007) The interaction between Stargazin and PSD-95 regulates AMPA receptor surface trafficking. Neuron 53:719-734.

Bedoukian MA, Whitesell JD, Peterson EJ, Clay CM, Partin KM (2008) The stargazin C terminus encodes an intrinsic and transferable membrane sorting signal. J Biol Chem 283:1597-1600.

Behe P, Stern P, Wyllie DJ, Nassar M, Schoepfer R, Colquhoun D (1995) Determination of NMDA NR1 subunit copy number in recombinant NMDA receptors. Proc Biol Sci 262:205-213.

Bennett JA, Dingledine R (1995) Topology profile for a glutamate receptor: three transmembrane domains and a channel-lining reentrant membrane loop. Neuron 14:373-384.

Bigge CF, Malone TC, Boxer PA, Nelson CB, Ortwine DF, Schelkun RM, Retz DM, Lescosky LJ, Borosky SA, Vartanian MG, et al. (1995) Synthesis of 1,4,7,8,9,10-hexahydro-9-methyl-6-nitropyrido[3,4-f]- quinoxaline-2,3-dione and related quinoxalinediones: characterization of alpha-amino-3-hydroxy-5-methyl-4-isoxazolepropionic acid (and N-methyl-D-aspartate) receptor and anticonvulsant activity. J Med Chem 38:3720-3740.

Bjerrum EJ, Biggin PC (2008) Rigid body essential X-ray crystallography: distinguishing the bend and twist of glutamate receptor ligand binding domains. Proteins 72:434-446.

Bokel C, Dass S, Wilsch-Brauninger M, Roth S (2006) Drosophila Cornichon acts as cargo receptor for ER export of the TGFalpha-like growth factor Gurken. Development 133:459-470.

Boulter J, Hollmann M, O'Shea-Greenfield A, Hartley M, Deneris E, Maron C, Heinemann S (1990) Molecular cloning and functional expression of glutamate receptor subunit genes. Science 249:1033-1037.

Bredt DS, Nicoll RA (2003) AMPA receptor trafficking at excitatory synapses. Neuron 40:361-379.

Brorson JR, Li D, Suzuki T (2004) Selective expression of heteromeric AMPA receptors driven by flip-flop differences. J Neurosci 24:3461-3470.

Brose N, Huntley GW, Stern-Bach Y, Sharma G, Morrison JH, Heinemann SF (1994) Differential assembly of coexpressed glutamate receptor subunits in neurons of rat cerebral cortex. J Biol Chem 269:16780-16784.

Buchan AM, Lesiuk H, Barnes KA, Li H, Huang ZG, Smith KE, Xue D (1993) AMPA antagonists: do they hold more promise for clinical stroke trials than NMDA antagonists? Stroke 24:I148-152.

Burgess DL, Gefrides LA, Foreman PJ, Noebels JL (2001) A cluster of three novel Ca2+ channel gamma subunit genes on chromosome 19q13.4: evolution and expression profile of the gamma subunit gene family. Genomics 71:339-350.

Carlton SM, Coggeshall RE (1999) Inflammation-induced changes in peripheral glutamate receptor populations. Brain Res 820:63-70.

Castillon GA, Watanabe R, Taylor M, Schwabe TM, Riezman H (2009) Concentration of GPI-anchored proteins upon ER exit in yeast. Traffic 10:186-200.

Catarzi D, Colotta V, Varano F (2007) Competitive AMPA receptor antagonists. Med Res Rev 27:239-278.

Catterall WA, Dib-Hajj S, Meisler MH, Pietrobon D (2008) Inherited neuronal ion channelopathies: new windows on complex neurological diseases. J Neurosci 28:11768-11777.

Chen GQ, Sun Y, Jin R, Gouaux E (1998) Probing the ligand binding domain of the GluR2 receptor by proteolysis and deletion mutagenesis defines domain boundaries and yields a crystallizable construct. Protein Sci 7:2623-2630.

Chen L, Chetkovich DM, Petralia RS, Sweeney NT, Kawasaki Y, Wenthold RJ, Bredt DS, Nicoll RA (2000) Stargazin regulates synaptic targeting of AMPA receptors by two distinct mechanisms. Nature 408:936-943.

Chen L, El-Husseini A, Tomita S, Bredt DS, Nicoll RA (2003) Stargazin differentially controls the trafficking of alpha-amino-3-hydroxyl-5-methyl-4-isoxazolepropionate and kainate receptors. Mol Pharmacol 64:703-706.

Chenu C, Serre CM, Raynal C, Burt-Pichat B, Delmas PD (1998) Glutamate receptors are expressed by bone cells and are involved in bone resorption. Bone 22:295-299.

Chetkovich DM, Chen L, Stocker TJ, Nicoll RA, Bredt DS (2002) Phosphorylation of the postsynaptic density-95 (PSD-95)/discs large/zona occludens-1 binding site of stargazin regulates binding to PSD-95 and synaptic targeting of AMPA receptors. J Neurosci 22:5791-5796.

Cho CH, St-Gelais F, Zhang W, Tomita S, Howe JR (2007) Two families of TARP isoforms that have distinct effects on the kinetic properties of AMPA receptors and synaptic currents. Neuron 55:890-904.

Choi DW (1988) Glutamate neurotoxicity and diseases of the nervous system. Neuron 1:623-634.

Choi J, Ko J, Park E, Lee JR, Yoon J, Lim S, Kim E (2002) Phosphorylation of stargazin by protein kinase A regulates its interaction with PSD-95. J Biol Chem 277:12359-12363.

Christofi G, Nowicky AV, Bolsover SR, Bindman LJ (1993) The postsynaptic induction of nonassociative long-term depression of excitatory synaptic transmission in rat hippocampal slices. J Neurophysiol 69:219-229.

Cokic B, Stein V (2008) Stargazin modulates AMPA receptor antagonism. Neuropharmacology 54:1062-1070.

Collingridge GL, Isaac JT, Wang YT (2004) Receptor trafficking and synaptic plasticity. Nat Rev Neurosci 5:952-962.

Cotton JL, Partin KM (2000) The contributions of GluR2 to allosteric modulation of AMPA receptors. Neuropharmacology 39:21-31.

Curtis DR, Duggan AW, Felix D, Johnston GA, Teb ecis AK, Watkins JC (1972) Excitation of mammalian central neurones by acidic amino acids. Brain Res 41:283-301.

Curtis DR, Phillis JW, Watkins JC (1959) Chemical excitation of spinal neurones. Nature 183:611-612.

Deng F, Price MG, Davis CF, Mori M, Burgess DL (2006) Stargazin and other transmembrane AMPA receptor regulating proteins interact with synaptic scaffolding protein MAGI-2 in brain. J Neurosci 26:7875-7884.

Desai MA, Valli MJ, Monn JA, Schoepp DD (1995) 1-BCP, a memory-enhancing agent, selectively potentiates AMPA-induced [3H]norepinephrine release in rat hippocampal slices. Neuropharmacology 34:141-147.

Dingledine R, Borges K, Bowie D, Traynelis SF (1999) The glutamate receptor ion channels. Pharmacol Rev 51:7-61.

Donevan SD, Rogawski MA (1993) GYKI 52466, a 2,3-benzodiazepine, is a highly selective, noncompetitive antagonist of AMPA/kainate receptor responses. Neuron 10:51-59.

Dong H, O'Brien RJ, Fung ET, Lanahan AA, Worley PF, Huganir RL (1997) GRIP: a synaptic PDZ domain-containing protein that interacts with AMPA receptors. Nature 386:279-284.

Duggan AW, Johnston GA (1970) Glutamate and related amino acids in cat spinal roots, dorsal root ganglia and peripheral nerves. J Neurochem 17:1205-1208.

Egebjerg J, Bettler B, Hermans-Borgmeyer I, Heinemann S (1991) Cloning of a cDNA for a glutamate receptor subunit activated by kainate but not AMPA. Nature 351:745-748.

Egebjerg J, Heinemann SF (1993) Ca2+ permeability of unedited and edited versions of the kainate selective glutamate receptor GluR6. Proc Natl Acad Sci U S A 90:755-759.

Ervin LA, Ball LE, Crouch RK, Schey KL (2005) Phosphorylation and glycosylation of bovine lens MP20. Invest Ophthalmol Vis Sci 46:627-635.

Everts I, Villmann C, Hollmann M (1997) N-Glycosylation is not a prerequisite for glutamate receptor function but Is essential for lectin modulation. Mol Pharmacol 52:861-873.

Fletcher EJ, Lodge D (1996) New developments in the molecular pharmacology of alpha-amino-3-hydroxy-5-methyl-4-isoxazole propionate and kainate receptors. Pharmacol Ther 70:65-89.

Fukata Y, Tzingounis AV, Trinidad JC, Fukata M, Burlingame AL, Nicoll RA, Bredt DS (2005) Molecular constituents of neuronal AMPA receptors. J Cell Biol 169:399-404.

Fukaya M, Tsujita M, Yamazaki M, Kushiya E, Abe M, Akashi K, Natsume R, Kano M, Kamiya H, Watanabe M, Sakimura K (2006) Abundant distribution of TARP gamma-8 in synaptic and extrasynaptic surface of hippocampal neurons and its major role in AMPA receptor expression on spines and dendrites. Eur J Neurosci 24:2177-2190.

Gallo V, Upson LM, Hayes WP, Vyklicky L, Jr., Winters CA, Buonanno A (1992) Molecular cloning and development analysis of a new glutamate receptor subunit isoform in cerebellum. J Neurosci 12:1010-1023.

Gardner SM, Trussell LO, Oertel D (2001) Correlation of AMPA receptor subunit composition with synaptic input in the mammalian cochlear nuclei. J Neurosci 21:7428-7437.

Greger IH, Khatri L, Kong X, Ziff EB (2003) AMPA receptor tetramerization is mediated by Q/R editing. Neuron 40:763-774.

Hayashi T (1952) A physiological study of epileptic seizures following cortical stimulation in animals and its application to human clinics. Jpn J Physiol 3:46-64.

Hollmann M, Maron C, Heinemann S (1994) N-glycosylation site tagging suggests a three transmembrane domain topology for the glutamate receptor GluR1. Neuron 13:1331-1343.

Hollmann M, O'Shea-Greenfield A, Rogers SW, Heinemann S (1989) Cloning by functional expression of a member of the glutamate receptor family. Nature 342:643-648.

Honore T, Davies SN, Drejer J, Fletcher EJ, Jacobsen P, Lodge D, Nielsen FE (1988) Quinoxalinediones: potent competitive non-NMDA glutamate receptor antagonists. Science 241:701-703.

Horning MS, Mayer ML (2004) Regulation of AMPA receptor gating by ligand binding core dimers. Neuron 41:379-388.

Huettner JE (1990) Glutamate receptor channels in rat DRG neurons: activation by kainate and quisqualate and blockade of desensitization by Con A. Neuron 5:255-266.

Hume RI, Dingledine R, Heinemann SF (1991) Identification of a site in glutamate receptor subunits that controls calcium permeability. Science 253:1028-1031.

Hunter JC, Singh L (1994) Role of excitatory amino acid receptors in the mediation of the nociceptive response to formalin in the rat. Neurosci Lett 174:217-221.

Iino M, Ozawa S, Tsuzuki K (1990) Permeation of calcium through excitatory amino acid receptor channels in cultured rat hippocampal neurones. J Physiol 424:151-165.

Inagaki N, Kuromi H, Gonoi T, Okamoto Y, Ishida H, Seino Y, Kaneko T, Iwanaga T, Seino S (1995) Expression and role of ionotropic glutamate receptors in pancreatic islet cells. FASEB J 9:686-691.

Isaacson JS, Nicoll RA (1991) Aniracetam reduces glutamate receptor desensitization and slows the decay of fast excitatory synaptic currents in the hippocampus. Proc Natl Acad Sci U S A 88:10936-10940.

Ito I, Tanabe S, Kohda A, Sugiyama H (1990) Allosteric potentiation of quisqualate receptors by a nootropic drug aniracetam. J Physiol 424:533-543.

Ives JH, Fung S, Tiwari P, Payne HL, Thompson CL (2004) Microtubule-associated protein light chain 2 is a stargazin-AMPA receptor complex-interacting protein in vivo. J Biol Chem 279:31002-31009.

Jin R, Clark S, Weeks AM, Dudman JT, Gouaux E, Partin KM (2005) Mechanism of positive allosteric modulators acting on AMPA receptors. J Neurosci 25:9027-9036.

Jin R, Gouaux E (2003) Probing the function, conformational plasticity, and dimer-dimer contacts of the GluR2 ligand-binding core: studies of 5-substituted willardiines and GluR2 S1S2 in the crystal. Biochemistry 42:5201-5213.

Jin R, Singh SK, Gu S, Furukawa H, Sobolevsky AI, Zhou J, Jin Y, Gouaux E (2009) Crystal structure and association behaviour of the GluR2 amino-terminal domain. EMBO J 28:1812-1823.

Kato AS, Siuda ER, Nisenbaum ES, Bredt DS (2008) AMPA receptor subunit-specific regulation by a distinct family of type II TARPs. Neuron 59:986-996.

Kato AS, Zhou W, Milstein AD, Knierman MD, Siuda ER, Dotzlaf JE, Yu H, Hale JE, Nisenbaum ES, Nicoll RA, Bredt DS (2007) New transmembrane AMPA receptor regulatory protein isoform, gamma-7, differentially regulates AMPA receptors. J Neurosci 27:4969-4977.

Kawai N, Niwa A, Abe T (1982) Spider venom contains specific receptor blocker of glutaminergic synapses. Brain Res 247:169-171.

Kawamoto S, Hattori S, Sakimura K, Mishina M, Okuda K (1995) N-linked glycosylation of the alpha-amino-3-hydroxy-5-methylisoxazole-4-propionate (AMPA)-selective glutamate receptor channel alpha 2 subunit is essential for the acquisition of ligand-binding activity. J Neurochem 64:1258-1266.

Keinanen K, Jouppila A, Kuusinen A (1998) Characterization of the kainate-binding domain of the glutamate receptor GluR-6 subunit. Biochem J 330 (Pt 3):1461-1467.

Keinanen K, Wisden W, Sommer B, Werner P, Herb A, Verdoorn TA, Sakmann B, Seeburg PH (1990) A family of AMPA-selective glutamate receptors. Science 249:556-560.

Kirkwood A, Lee HK, Bear MF (1995) Co-regulation of long-term potentiation and experience-dependent synaptic plasticity in visual cortex by age and experience. Nature 375:328-331.

Klein RM, Howe JR (2004) Effects of the lurcher mutation on GluR1 desensitization and activation kinetics. J Neurosci 24:4941-4951.

Klugbauer N, Dai S, Specht V, Lacinova L, Marais E, Bohn G, Hofmann F (2000) A family of gamma-like calcium channel subunits. FEBS Lett 470:189-197.

Kohler M, Burnashev N, Sakmann B, Seeburg PH (1993) Determinants of Ca2+ permeability in both TM1 and TM2 of high affinity kainate receptor channels: diversity by RNA editing. Neuron 10:491-500.

Korber C, Werner M, Kott S, Ma ZL, Hollmann M (2007) The transmembrane AMPA receptor regulatory protein gamma 4 is a more effective modulator of AMPA receptor function than stargazin (gamma 2). J Neurosci 27:8442-8447.

Koshland DE (1958) Application of a Theory of Enzyme Specificity to Protein Synthesis. Proc Natl Acad Sci U S A 44:98-104.

Koshland DE, Jr., Nemethy G, Filmer D (1966) Comparison of experimental binding data and theoretical models in proteins containing subunits. Biochemistry 5:365-385.

Krnjevic K (1970) Glutamate and gamma-aminobutyric acid in brain. Nature 228:119-124.

Kubalek E, Ralston S, Lindstrom J, Unwin N (1987) Location of subunits within the acetylcholine receptor by electron image analysis of tubular crystals from Torpedo marmorata. J Cell Biol 105:9-18.

Letts VA (2005) Stargazer-a mouse to seize! Epilepsy Curr 5:161-165.

Letts VA, Felix R, Biddlecome GH, Arikkath J, Mahaffey CL, Valenzuela A, Bartlett FS, 2nd, Mori Y, Campbell KP, Frankel WN (1998) The mouse stargazer gene encodes a neuronal Ca2+-channel gamma subunit. Nat Genet 19:340-347.

Leuschner WD, Hoch W (1999) Subtype-specific assembly of alpha-amino-3-hydroxy-5-methyl-4-isoxazole propionic acid receptor subunits is mediated by their n-terminal domains. J Biol Chem 274:16907-16916.

Lomeli H, Sprengel R, Laurie DJ, Kohr G, Herb A, Seeburg PH, Wisden W (1993) The rat delta-1 and delta-2 subunits extend the excitatory amino acid receptor family. FEBS Lett 315:318-322.

Magazanik LG, Samoilova MV, Buldakova SL, Esin KV, Gmiro VE (1997) Selective block of AMPA/kainate receptors of hippocampal interneurons as a new approach to the investigation of inhibitory system. Ross Fiziol Zh Im I M Sechenova 83:19-39.

Malenka RC, Bear MF (2004) LTP and LTD: an embarrassment of riches. Neuron 44:5-21.

Malinow R (2003) AMPA receptor trafficking and long-term potentiation. Philos Trans R Soc Lond B Biol Sci 358:707-714.

Mammen AL, Kameyama K, Roche KW, Huganir RL (1997) Phosphorylation of the alpha-amino-3-hydroxy-5-methylisoxazole4-propionic acid receptor GluR1 subunit by calcium/calmodulin-dependent kinase II. J Biol Chem 272:32528-32533.

Mamonova T, Speranskiy K, Kurnikova M (2008) Interplay between structural rigidity and electrostatic interactions in the ligand binding domain of GluR2. Proteins 73:656-671.

Man HY, Sekine-Aizawa Y, Huganir RL (2007) Regulation of (Arikkath et al.)-amino-3-hydroxy-5-methyl-4-isoxazolepropionic acid receptor trafficking through PKA phosphorylation of the Glu receptor 1 subunit. Proc Natl Acad Sci U S A 104:3579-3584.

Mano I, Teichberg VI (1998) A tetrameric subunit stoichiometry for a glutamate receptor-channel complex. Neuroreport 9:327-331.

Mansour M, Nagarajan N, Nehring RB, Clements JD, Rosenmund C (2001) Heteromeric AMPA receptors assemble with a preferred subunit stoichiometry and spatial arrangement. Neuron 32:841-853.

Martin AR, Wickelgren WO, Ber1anek R (1970) Effects of iontophoretically applied drugs on spinal interneurons of the lamprey. J Physiol 207:653-665.

Mathur R, Zheng J, Yan Y, Sigworth FJ (1997) Role of the S3-S4 linker in Shaker potassium channel activation. J Gen Physiol 109:191-199.

May PC, Robison PM (1993) GYKI 52466 protects against non-NMDA receptor-mediated excitotoxicity in primary rat hippocampal cultures. Neurosci Lett 152:169-172.

Mayer ML (2005) Glutamate receptor ion channels. Curr Opin Neurobiol 15:282-288.

Mayer ML, Vyklicky L, Jr. (1989) Concanavalin A selectively reduces desensitization of mammalian neuronal quisqualate receptors. Proc Natl Acad Sci U S A 86:1411-1415.

Menuz K, Stroud RM, Nicoll RA, Hays FA (2007) TARP auxiliary subunits switch AMPA receptor antagonists into partial agonists. Science 318:815-817.

Meyer T, Lenk U, Kuther G, Weindl A, Speer A, Ludolph AC (1995) Studies of the coding region of the neuronal glutamate transporter gene in amyotrophic lateral sclerosis. Ann Neurol 37:817-819.

Milstein AD, Nicoll RA (2009) TARP modulation of synaptic AMPA receptor trafficking and gating depends on multiple intracellular domains. Proc Natl Acad Sci U S A.

Monod J, Wyman J, Changeux JP (1965) On the Nature of Allosteric Transitions: A Plausible Model. J Mol Biol 12:88-118.

Morita K, Furuse M, Fujimoto K, Tsukita S (1999) Claudin multigene family encoding four-transmembrane domain protein components of tight junction strands. Proc Natl Acad Sci U S A 96:511-516.

Moss FJ, Viard P, Davies A, Bertaso F, Page KM, Graham A, Canti C, Plumpton M, Plumpton C, Clare JJ, Dolphin AC (2002) The novel product of a five-exon stargazin-related gene abolishes Ca(V)2.2 calcium channel expression. Embo J 21:1514-1523.

Nakanishi N, Shneider NA, Axel R (1990) A family of glutamate receptor genes: evidence for the formation of heteromultimeric receptors with distinct channel properties. Neuron 5:569-581.

Olsen RW, Szamraj O, Houser CR (1987) [3H]AMPA binding to glutamate receptor subpopulations in rat brain. Brain Res 402:243-254.

Partin KM (2001) Domain interactions regulating ampa receptor desensitization. J Neurosci 21:1939-1948.

Partin KM, Patneau DK, Mayer ML (1994) Cyclothiazide differentially modulates desensitization of alpha-amino-3-hydroxy-5-methyl-4-isoxazolepropionic acid receptor splice variants. Mol Pharmacol 46:129-138.

Patneau DK, Mayer ML (1990) Structure-activity relationships for amino acid transmitter candidates acting at N-methyl-D-aspartate and quisqualate receptors. J Neurosci 10:2385-2399.

Patneau DK, Mayer ML (1991) Kinetic analysis of interactions between kainate and AMPA: evidence for activation of a single receptor in mouse hippocampal neurons. Neuron 6:785-798.

Patneau DK, Vyklicky L, Jr., Mayer ML (1993) Hippocampal neurons exhibit cyclothiazide-sensitive rapidly desensitizing responses to kainate. J Neurosci 13:3496-3509.

Patneau DK, Wright PW, Winters C, Mayer ML, Gallo V (1994) Glial cells of the oligodendrocyte lineage express both kainate- and AMPA-preferring subtypes of glutamate receptor. Neuron 12:357-371.

Patton AJ, Genever PG, Birch MA, Suva LJ, Skerry TM (1998) Expression of an N-methyl-D-aspartate-type receptor by human and rat osteoblasts and osteoclasts suggests a novel glutamate signaling pathway in bone. Bone 22:645-649.

Pollard H, Heron A, Moreau J, Ben-Ari Y, Khrestchatisky M (1993) Alterations of the GluR-B AMPA receptor subunit flip/flop expression in kainate-induced epilepsy and ischemia. Neuroscience 57:545-554.

Priel A, Kolleker A, Ayalon G, Gillor M, Osten P, Stern-Bach Y (2005) Stargazin reduces desensitization and slows deactivation of the AMPA-type glutamate receptors. J Neurosci 25:2682-2686.

Raman IM, Trussell LO (1992) The kinetics of the response to glutamate and kainate in neurons of the avian cochlear nucleus. Neuron 9:173-186.

Robert A, Howe JR (2003) How AMPA receptor desensitization depends on receptor occupancy. J Neurosci 23:847-858.

Roche KW, O'Brien RJ, Mammen AL, Bernhardt J, Huganir RL (1996) Characterization of multiple phosphorylation sites on the AMPA receptor GluR1 subunit. Neuron 16:1179-1188.

Roche KW, Tingley WG, Huganir RL (1994) Glutamate receptor phosphorylation and synaptic plasticity. Curr Opin Neurobiol 4:383-388.

Rogawski MA (1993) Therapeutic potential of excitatory amino acid antagonists: channel blockers and 2,3-benzodiazepines. Trends Pharmacol Sci 14:325-331.

Rosen DR, Siddique T, Patterson D, Figlewicz DA, Sapp P, Hentati A, Donaldson D, Goto J, O'Regan JP, Deng HX, et al. (1993) Mutations in Cu/Zn superoxide dismutase gene are associated with familial amyotrophic lateral sclerosis. Nature 362:59-62.

Rosenmund C, Stern-Bach Y, Stevens CF (1998) The tetrameric structure of a glutamate receptor channel. Science 280:1596-1599.

Rothstein JD, Van Kammen M, Levey AI, Martin LJ, Kuncl RW (1995) Selective loss of glial glutamate transporter GLT-1 in amyotrophic lateral sclerosis. Ann Neurol 38:73-84.

Schmid SM, Korber C, Herrmann S, Werner M, Hollmann M (2007) A domain linking the AMPA receptor agonist binding site to the ion pore controls gating and causes lurcher properties when mutated. J Neurosci 27:12230-12241.

Schnell E, Sizemore M, Karimzadegan S, Chen L, Bredt DS, Nicoll RA (2002) Direct interactions between PSD-95 and stargazin control synaptic AMPA receptor number. Proc Natl Acad Sci U S A 99:13902-13907.

Schwenk J, Harmel N, Zolles G, Bildl W, Kulik A, Heimrich B, Chisaka O, Jonas P, Schulte U, Fakler B, Klocker N (2009) Functional proteomics identify cornichon proteins as auxiliary subunits of AMPA receptors. Science 323:1313-1319.

Seal AJ, Collingridge GL, Henley JM (1995) An investigation of the membrane topology of the ionotropic glutamate receptor subunit GluR1 in a cell-free system. Biochem J 312 (Pt 2):451-456.

Seeburg PH, Single F, Kuner T, Higuchi M, Sprengel R (2001) Genetic manipulation of key determinants of ion flow in glutamate receptor channels in the mouse. Brain Res 907:233-243.

Selkoe DJ (2002) Alzheimer's disease is a synaptic failure. Science 298:789-791.

Sheardown MJ, Nielsen EO, Hansen AJ, Jacobsen P, Honore T (1990) 2,3-Dihydroxy-6-nitro-7-sulfamoyl-benzo(F)quinoxaline: a neuroprotectant for cerebral ischemia. Science 247:571-574.

Shi SH, Hayashi Y, Petralia RS, Zaman SH, Wenthold RJ, Svoboda K, Malinow R (1999) Rapid spine delivery and redistribution of AMPA receptors after synaptic NMDA receptor activation. Science 284:1811-1816.

Silverman JB, Restituito S, Lu W, Lee-Edwards L, Khatri L, Ziff EB (2007) Synaptic anchorage of AMPA receptors by cadherins through neural plakophilin-related arm protein AMPA receptor-binding protein complexes. J Neurosci 27:8505-8516.

Sobolevsky AI, Yelshansky MV, Wollmuth LP (2004) The outer pore of the glutamate receptor channel has 2-fold rotational symmetry. Neuron 41:367-378.

Sommer B, Keinanen K, Verdoorn TA, Wisden W, Burnashev N, Herb A, Kohler M, Takagi T, Sakmann B, Seeburg PH (1990) Flip and flop: a cell-specific functional switch in glutamate-operated channels of the CNS. Science 249:1580-1585.

Song I, Kamboj S, Xia J, Dong H, Liao D, Huganir RL (1998) Interaction of the N-ethylmaleimide-sensitive factor with AMPA receptors. Neuron 21:393-400.

Soto D, Coombs ID, Kelly L, Farrant M, Cull-Candy SG (2007) Stargazin attenuates intracellular polyamine block of calcium-permeable AMPA receptors. Nat Neurosci 10:1260-1267.

Soto D, Coombs ID, Renzi M, Zonouzi M, Farrant M, Cull-Candy SG (2009) Selective regulation of long-form calcium-permeable AMPA receptors by an atypical TARP, gamma-5. Nat Neurosci 12:277-285.

Srivastava S, Osten P, Vilim FS, Khatri L, Inman G, States B, Daly C, DeSouza S, Abagyan R, Valtschanoff JG, Weinberg RJ, Ziff EB (1998) Novel anchorage of GluR2/3 to the postsynaptic density by the AMPA receptor-binding protein ABP. Neuron 21:581-591.

Stern-Bach Y, Bettler B, Hartley M, Sheppard PO, O'Hara PJ, Heinemann SF (1994) Agonist selectivity of glutamate receptors is specified by two domains structurally related to bacterial amino acid-binding proteins. Neuron 13:1345-1357.

Stern-Bach Y, Russo S, Neuman M, Rosenmund C (1998) A point mutation in the glutamate binding site blocks desensitization of AMPA receptors. Neuron 21:907-918.

Sun Y, Olson R, Horning M, Armstrong N, Mayer M, Gouaux E (2002) Mechanism of glutamate receptor desensitization. Nature 417:245-253.

Swanson GT, Feldmeyer D, Kaneda M, Cull-Candy SG (1996) Effect of RNA editing and subunit co-assembly single-channel properties of recombinant kainate receptors. J Physiol 492 (Pt 1):129-142.

Tarnawa I, Farkas S, Berzsenyi P, Patfalusi M, Andrasi F (1990) Reflex inhibitory action of a non-NMDA type excitatory amino acid antagonist, GYKI 52466. Acta Physiol Hung 75 Suppl:277-278.

Taverna F, Xiong ZG, Brandes L, Roder JC, Salter MW, MacDonald JF (2000) The Lurcher mutation of an alpha-amino-3-hydroxy-5-methyl- 4-isoxazolepropionic acid receptor subunit enhances potency of glutamate and converts an antagonist to an agonist. J Biol Chem 275:8475-8479.

Thompson DM, Guidotti A, DiBella M, Costa E (1995) 7-Chloro-3-methyl-3,4-dihydro-2H-1,2,4-benzothiadiazine S,S-dioxide (IDRA 21), a congener of aniracetam, potently abates pharmacologically induced cognitive impairments in patas monkeys. Proc Natl Acad Sci U S A 92:7667-7671.

Tomita S, Adesnik H, Sekiguchi M, Zhang W, Wada K, Howe JR, Nicoll RA, Bredt DS (2005a) Stargazin modulates AMPA receptor gating and trafficking by distinct domains. Nature 435:1052-1058.

Tomita S, Chen L, Kawasaki Y, Petralia RS, Wenthold RJ, Nicoll RA, Bredt DS (2003) Functional studies and distribution define a family of transmembrane AMPA receptor regulatory proteins. J Cell Biol 161:805-816.

Tomita S, Fukata M, Nicoll RA, Bredt DS (2004) Dynamic interaction of stargazin-like TARPs with cycling AMPA receptors at synapses. Science 303:1508-1511.

Tomita S, Sekiguchi M, Wada K, Nicoll RA, Bredt DS (2006) Stargazin controls the pharmacology of AMPA receptor potentiators. Proc Natl Acad Sci U S A 103:10064-10067.

Tomita S, Stein V, Stocker TJ, Nicoll RA, Bredt DS (2005b) Bidirectional synaptic plasticity regulated by phosphorylation of stargazin-like TARPs. Neuron 45:269-277.

Trussell LO, Thio LL, Zorumski CF, Fischbach GD (1988) Rapid desensitization of glutamate receptors in vertebrate central neurons. Proc Natl Acad Sci U S A 85:2834-2838.

Turetsky D, Garringer E, Patneau DK (2005) Stargazin modulates native AMPA receptor functional properties by two distinct mechanisms. J Neurosci 25:7438-7448.

Underdown BJ, De Rose J, Plaut A (1977) Disulfide bonding of secretory component to a single monomer subunit in human secretory IgA. J Immunol 118:1816-1821.

Vandenberghe W, Ihle EC, Patneau DK, Robberecht W, Brorson JR (2000) AMPA receptor current density, not desensitization, predicts selective motoneuron vulnerability. J Neurosci 20:7158-7166.

Vandenberghe W, Nicoll RA, Bredt DS (2005a) Interaction with the unfolded protein response reveals a role for stargazin in biosynthetic AMPA receptor transport. J Neurosci 25:1095-1102.

Vandenberghe W, Nicoll RA, Bredt DS (2005b) Stargazin is an AMPA receptor auxiliary subunit. Proc Natl Acad Sci U S A 102:485-490.

Verdoorn TA, Burnashev N, Monyer H, Seeburg PH, Sakmann B (1991) Structural determinants of ion flow through recombinant glutamate receptor channels. Science 252:1715-1718.

Vyklicky L, Jr., Patneau DK, Mayer ML (1991) Modulation of excitatory synaptic transmission by drugs that reduce desensitization at AMPA/kainate receptors. Neuron 7:971-984.

Wallace RH, Wang DW, Singh R, Scheffer IE, George AL, Jr., Phillips HA, Saar K, Reis A, Johnson EW, Sutherland GR, Berkovic SF, Mulley JC (1998) Febrile seizures and generalized epilepsy associated with a mutation in the Na+-channel beta1 subunit gene SCN1B. Nat Genet 19:366-370.

Weaver CD, Yao TL, Powers AC, Verdoorn TA (1996) Differential expression of glutamate receptor subtypes in rat pancreatic islets. J Biol Chem 271:12977-12984.

Williams K (1997) Modulation and block of ion channels: a new biology of polyamines. Cell Signal 9:1-13.

Wu Y et al. (2007) Mutations in ionotropic AMPA receptor 3 alter channel properties and are associated with moderate cognitive impairment in humans. Proc Natl Acad Sci U S A 104:18163-18168.

Xia J, Zhang X, Staudinger J, Huganir RL (1999) Clustering of AMPA receptors by the synaptic PDZ domain-containing protein PICK1. Neuron 22:179-187.

Yamada KA, Rothman SM (1992) Diazoxide blocks glutamate desensitization and prolongs excitatory postsynaptic currents in rat hippocampal neurons. J Physiol 458:409-423.

Yamada KA, Tang CM (1993) Benzothiadiazides inhibit rapid glutamate receptor desensitization and enhance glutamatergic synaptic currents. J Neurosci 13:3904-3915.

Yamakawa K, Mitchell S, Hubert R, Chen XN, Colbern S, Huo YK, Gadomski C, Kim UJ, Korenberg JR (1995) Isolation and characterization of a candidate gene for progressive myoclonus epilepsy on 21q22.3. Hum Mol Genet 4:709-716.

Yasuda H, Barth AL, Stellwagen D, Malenka RC (2003) A developmental switch in the signaling cascades for LTP induction. Nat Neurosci 6:15-16.

Yelshansky MV, Sobolevsky AI, Jatzke C, Wollmuth LP (2004) Block of AMPA receptor desensitization by a point mutation outside the ligand-binding domain. J Neurosci 24:4728-4736.

Yin HZ, Park DD, Lindsay AD, Weiss JH (1995) Spinal cord neurons are vulnerable to rapidly triggered kainate neurotoxicity in vitro. Brain Res 689:265-270.

Zappala M, Grasso S, Micale N, Polimeni S, De Micheli C (2001) Synthesis and structure-activity relationships of 2,3-benzodiazepines as AMPA receptor antagonists. Mini Rev Med Chem 1:243-253.

Zhang W, Robert A, Vogensen SB, Howe JR (2006) The relationship between agonist potency and AMPA receptor kinetics. Biophys J 91:1336-1346.

Zhu JJ, Esteban JA, Hayashi Y, Malinow R (2000) Postnatal synaptic potentiation: delivery of GluR4-containing AMPA receptors by spontaneous activity. Nat Neurosci 3:1098-1106.

Zivkovic I, Thompson DM, Bertolino M, Uzunov D, DiBella M, Costa E, Guidotti A (1995) 7-Chloro-3-methyl-3-4-dihydro-2H-1,2,4 benzothiadiazine S,S-dioxide (IDRA 21): a benzothiadiazine derivative that enhances cognition by attenuating DL-alpha-amino-2,3-dihydro-5-methyl-3-oxo-4-isoxazolepropanoic acid (AMPA) receptor desensitization. J Pharmacol Exp Ther 272:300-309.

Zorumski CF, Yamada KA, Price MT, Olney JW (1993) A benzodiazepine recognition site associated with the non-NMDA glutamate receptor. Neuron 10:61-67.

VITA

Yanina Levchenko-Lambert

Candidate for the Degree of

Doctor of Philosophy

Dissertation: STRUCTURE-FUNCTION RELATIONSHIPS OF THE PORE-FORMING SUBUNITS OF AMPA RECEPTOR AND THE AUXILIARY SUBUNIT STARGAZIN

Major Field: Neuroscience

Biographical:

Personal Data: Born in Poltava, Ukraine. A single daughter of Nikolay and Oleksandra Levchenko. Married James Lambert on March 12, 2005 in Jenks, OK

Education: Graduated from Poltava High School # 29 in May 2000, moved to USA to attend Oral Roberts University. Graduated in May of 2004 with BS degree in Biomedical Engineering. Completed the requirements for the Doctor of Philosophy in Neuroscience at Oklahoma State University, Tulsa, Oklahoma in July, 2009.

Name: Yanina Levchenko-Lambert Date of Degree: July, 2009

Institution: Oklahoma State University Location: Tulsa, OK

Title of Study: STRUCTURE-FUNCTION RELATIONSHIPS OF THE PORE-FORMING SUBUNITS OF AMPA RECEPTOR AND THE AUXILIARY SUBUNIT STARGAZIN

Pages in Study: 141 Candidate for the Degree of Doctor of Philosophy

Major Field: Neuroscience

ABSTRACT: AMPA receptors mediate the majority of neurotransmission in the CNS. One of the most important properties of AMPA receptors is their quick and profound desensitization in the presence of glutamate. Although, the mechanism of AMPA receptor desensitization onset has been elucidated and involves breaking of the protein interactions on the dimer interface in response to agonist binding, the mechanism of recovery from desensitization remains unknown. When co-expressed with the auxiliary subunit stargazin AMPA receptor functional properties are affected: steady-state desensitization is decreased, recovery from desensitization is faster, kainate efficacy is increased and deactivation is slowed. The mechanism of stargazin's action on AMPA receptor and their sites of association remain unknown. Previous studies suggested that stargazin decreases AMPA receptor steady-state desensitization by stabilizing the dimer interface. However, in our studies we were able to demonstrate that stargazin's effect on steady-state desensitization in mutations that stabilize the dimer interface is additive, while its effects on steady-state desensitization in a mutant that destabilized the dimer interface is occluded, indicating that stargazin does not act by stabilizing the intra-dimer interface, but instead destabilizes the desensitized state and speeds the recovery from desensitization. To identify residues that may be part of association between the AMPA pore-forming subunits and stargazin we were guided by the homology between AMPA and kainate receptors and the crystal structure of the LBD. We identified residues downstream of helix H (K693 and K695) and in the M4 linker (S784 and A789) that when co-expressed with stargazin presented with loss of it effects, suggesting that these residues may participate in the association with stargazin. Based on our data we were also able to propose a mechanism for recovery from desensitization that includes residues in helix B (K434) and the M1 linker (K501 and K502). Utilizing a similar approach in stargazin we were able to identify areas that are necessary for its association with the AMPA receptors, including polar residues proximal to the plasma membrane in the 1st and 2nd extracellular loops and others that are crucial for its function, the conserved motif GLWXXC and conserved cysteine residues at positions 67 and 77.

ADVISER'S APPROVAL: Doris K. Patneau